PNL-8451
UC-510

SPENT NUCLEAR FUEL STORAGE - PERFORMANCE TESTS AND DEMONSTRATIONS

M. A. McKinnon
V. A. DeLoach

April 1993

Prepared for
the U.S. Department of Energy
under Contract DE-AC06-76RLO 1830

Pacific Northwest Laboratory
Richland, Washington 99352

ABSTRACT

This report summarizes the results of heat transfer and shielding performance tests and demonstrations conducted from 1983 through 1992 by or in cooperation with the U. S. Department of Energy (DOE), Office of Commercial Radioactive Waste Management (OCRWM). The performance tests consisted of 6 to 14 runs involving one or two loadings, usually three backfill environments (helium, nitrogen, and vacuum backfills), and one or two storage system orientations. A description of the test plan, spent fuel load patterns, results from temperature and dose rate measurements, and fuel integrity evaluations are contained within the report. Supporting cask demonstrations have included the licensing and operation of an Independent Spent Fuel Storage Installation (ISFSI) at Virginia Power's (VP) Surry Reactor site. A CASTOR V/21, a MC-10, and a Nuclear Assurance NAC-I28 have been loaded and placed at the VP ISFSI as part of the demonstration program. The demonstration program will be concluded with the placement of a CASTOR X cask on the VP ISFSI.

From both heat transfer and shielding perspectives, dry storage systems (with minor refinements) can be effectively implemented at reactor sites and central storage facilities for safe storage of unconsolidated and consolidated spent fuel. Pretest temperature predictions computed with the COBRA-SFS and HYDRA-II heat transfer computer codes are in good agreement with test data. Consolidation of spent fuel reduces the non-fuel-bearing components that are major contributors to the fuel's gamma radiation. Peak gamma dose rates from consolidated pressurized water reactor (PWR) fuel were about 1/4 of those for unconsolidated fuel assemblies. Dry rod consolidation resulted in development of a small number of leaks in fuel rods. The size of the cladding penetrations was estimated to be extremely small, and has had no adverse effect on testing efforts.

ACRONYMS AND INITIALISMS

BWR	boiling water reactor
CCP	Chemical Processing Plant at INEL
CCT	concrete cask testing
COBRA-SFS	thermal hydraulics computer code; spent fuel storage
CP&L	Carolina Power and Light
CSFM	Commercial Spent Fuel Management Program
DAS	data acquisition system
DOE	U.S. Department of Energy
DOE-HQ	U.S. Department of Energy-Headquarters
DOE-RL	U.S. Department of Energy-Richland Field Office
DSC	dry shield canister
EPRI	Electric Power Research Institute
FRDS	Fuel Rod Detection System
FTT	Fuel Temperature Test
GE	General Electric Company
GNSI	General Nuclear System, Inc.
HSM	horizontal storage module
HYDRA	steady-state thermal hydraulics computer code
INEL	Idaho National Engineering Laboratory
ISFSI	Independent Spent Fuel Storage Installation
LANL	Los Alamos National Laboratory
LCSS	lid closure and seal system
LLNL	Lawrence Livermore National Laboratory
MRS	monitored retrievable storage

MSB	Multi-Assembly Sealed Basket
NRC	U.S. Nuclear Regulatory Commission
NUHOMS	NUTECH horizontal modular storage
NWPA	Nuclear Waste Policy Act of 1982
OCRWM	Office of Commercial Radioactive Waste Management
PCDP	Prototypical Consolidation Demonstration Project
PNL	Pacific Northwest Laboratory
PSN	Pacific Sierra Nuclear Associates (currently, SNC)
PWR	pressurized water reactor
R&D	research and development
R&H	receiving and handling
SCAP	solicitation for Cooperative Agreement Proposal
SFS	Spent Fuel Storage
SNC	Sierra Nuclear Corporation (formerly, PSN)
TAD	Thermocouple Attachment Device
TAN	Test Area North
TCs	thermocouples
TEDs	track etch dosimeters
TLDs	thermoluminescent dosimeters
UT	ultrasonic
VCC	Ventilated Concrete Cask
VP	Virginia Power
WEPC	Wisconsin Electric Power Company

CONTENTS

FIGURES

TABLES

1.0 INTRODUCTION

The need for additional storage capacity for spent fuel from commercial nuclear power reactors is near term for some utilities. The consequences of failure to provide additional storage capacity are significant if reactors are forced to terminate operations until required storage expansions can be provided. Storage capacity requirements can be expected to increase in the foreseeable future until monitored retrievable storage (MRS) sites and/or repositories are established. Therefore, a proven method of interim dry storage of spent fuel is needed in the near term to avoid reactor shutdowns and, in the long term, to provide contingency storage capability in the event that implementation of an MRS or a repository is delayed.

The Nuclear Waste Policy Act of 1982 (NWPA) assigns the U.S. Department of Energy (DOE) the responsibility for assisting utilities with their spent fuel storage problems. Other participants in the various programs included General Electric (GE), Virginia Power (VP), Sierra Nuclear Corporation (SNC), the Electric Power Research Institute (EPRI), Carolina Power & Light Co. (CP&L), Wisconsin Electric Power Company (WEPC), Transnuclear, Inc., Lawrence Livermore National Laboratory (LLNL), EG&G Idaho Inc., the Pacific Northwest Laboratory (PNL), and Los Alamos National Laboratory (LANL). Spent fuel storage (SFS) systems included in the performance testing included a Ridihalgh, Eggers & Associates REA 2023 cask (currently available from Mitsubishi of Japan as an MSF-IV), a Gesellschaft fur Nuklear Service CASTOR-V/21 cask, a Transnuclear, Inc. TN-24P cask, a Westinghouse MC-10 cask, a NUTECH horizontal modular storage system (NUHOMS), and an SNC-ventilated vertical concrete storage cask.

An additional provision of the NWPA is that DOE, in cooperation with the private sector, enter into demonstration programs of spent fuel dry storage systems at nuclear power reactor sites. The DOE Commercial Spent Fuel Management (CSFM) Program[a] and operators of commercial nuclear power reactors

---

(a) The CSFM Program was managed by the Pacific Northwest Laboratory, which is operated for the U.S. Department of Energy by Battelle Memorial Institute under contract number DE-AC06-76RLO 1830.

identified concrete and metal storage systems as candidates among available dry storage concepts for interim spent fuel storage. The number of casks needed could be very large, representing a substantial investment. Economics is, therefore, an important consideration, and every effort should be made to ensure that the chosen interim storage system provides the minimum cost commensurate with environmental and safety considerations. Therefore, performance tests were performed to 1) provide experimental data to support licensing efforts, 2) determine cask operating limits, 3) gain cask handling and decontamination experience, 4) identify candidate cask design improvements, and 5) evaluate computer codes that could perform future design and licensing analyses.

The objective of the cooperative demonstrations was to establish one or more storage technologies that the U.S. Nuclear Regulatory Commission (NRC) could, by rule, approve for use at civilian reactor sites without the need for additional site-specific approvals by the NRC. In addition, the NWPA authorized DOE to establish a research and development (R&D) program at federally owned facilities as part of the cooperative demonstrations to collect data necessary to assist utilities in their licensing activities.

In May 1983, a solicitation for Cooperative Agreement Proposal (SCAP) was issued to the private sector by DOE-Richland Field Office (DOE-RL) and proposals were received in August 1983. VP proposed that pressurized water reactor (PWR) spent fuel storage (SFS) cask performance testing be conducted at a federal site in support of their at-reactor licensed demonstration. The performance test was to be followed by a demonstration at the Surry reactor site. VP and DOE signed a Cooperative Agreement in March 1984, and VP signed a separate agreement with EPRI, essentially establishing a three-party cooperative agreement. CP&L proposed a demonstration of the NUHOMS concept at their H. B. Robinson site. The Cooperative Agreement between DOE and CP&L was also signed in 1984.

A preliminary assessment of candidate federal sites capable of performing dry storage system tests was undertaken by PNL in parallel with the issuance and response to the SCAP. The three sites evaluated were Idaho, Nevada, and Hanford. In July 1984, DOE selected the Test Area North (TAN) facility

located at the Idaho National Engineering Laboratory (INEL) operated by EG&G Idaho, Inc., as the federal cask testing facility, and the VP/DOE cask performance testing effort was initiated.

Dry rod consolidation and cask testing with consolidated fuel at INEL were removed from the VP/DOE cooperative agreement. In March 1986, a decision was reached to continue the design, checkout, and operation of the dry rod consolidation at INEL as a DOE-only funded project. Later, in August 1987, after the cask performance testing with unconsolidated fuel was completed, a decision was made to close out the VP/DOE cask-testing activity at INEL. At the time the decision was made, the TN-24P cask was in the final stages of being loaded with consolidated fuel. Given the relatively small incremental cost involved in testing the TN-24P cask once it was filled with consolidated fuel, DOE and EPRI elected to extend the performance testing to include consolidated fuel in the TN-24P cask. Transnuclear, Inc. arranged to have an additional partially insulated run added to the end of the test matrix. At the conclusion of the metal cask testing, a cooperative agreement was established between DOE and Pacific Sierra Nuclear (PSN)[a] to test a ventilated concrete cask at INEL. The VSC-17 cask was tested at INEL in 1990.

The primary objective of PWR spent fuel storage cask performance testing was to obtain heat transfer and shielding data and limited spent fuel integrity data needed to support VP's at-reactor licensing efforts at its twin Surry reactors. Spent fuel with decay heat generation rates near cask design limits were used when practical. Other objectives of the testing effort were to provide data to other utilities; gain cask-handling experience; identify candidate cask design improvements; and obtain heat transfer and shielding data for computer code evaluations.

Dry (cold) runs with a nonirradiated dummy fuel assembly were performed to gain operating experience and finalize handling and test procedures. The PWR spent fuel assemblies were ultrasonically examined and videotaped to

---

(a) Pacific Sierra Nuclear Associates (PSN) is currently known as Sierra Nuclear Corporation (SNC).

ensure integrity. The exterior cask surface was instrumented with thermocouples and radiation dose rate sensors. Thermocouples were inserted into selected fuel assembly guide tubes after the cask was loaded with fuel assemblies to monitor temperatures throughout the test. The backfill environments used were vacuum, nitrogen, and helium, and they were sampled and analyzed to detect leaking fuel rods. Where possible, vertical and horizontal orientations were investigated and test runs were performed inside under controlled conditions. At the conclusion of testing, selected fuel assemblies were videotaped and photographed, and smear samples were collected and analyzed.

Conceptual designs and analyses for interim or lag storage indicate that concrete spent fuel storage casks are economically and technically competitive with metal casks. Therefore, a Concrete Cask Testing (CCT) Program was conducted to evaluate the benefits of concrete as a storage cask material and to provide assistance in licensing activities if appropriate. DOE-Idaho through EG&G Idaho, Inc., anticipated conducting a spent fuel Prototypical Consolidation Demonstration Project (PCDP) at INEL to develop and demonstrate candidate Federal receiving and handling (R&H) facility production scale rod consolidation equipment. The CCT project could provide an additional cask for storage in support of the PCDP program.

In response to this need for storage, DOE-HQ provided guidance to DOE-RL and PNL to obtain concrete storage modules for testing that could be used at utility sites or at R&H facilities of Federal interim storage or disposal sites. The guidance resulted in the establishment of a cooperative agreement between DOE and PSN. In the agreement, signed in September 1988, PSN agreed to provide a ventilated concrete storage cask to DOE for performance testing of the cask by DOE at INEL. Six runs involving a combination of cover gases and vent blockage conditions were performed during the test. Vent blockage conditions were used to simulate accident conditions.

2.0 CONCLUSIONS

Dry storage systems can be satisfactorily handled in many reactor facilities with only minor modifications to the supplied handling equipment and procedures. Performance testing of a CASTOR-V/21, TN-24P, MC-10, and VSC-17 PWR SFS casks were successfully completed at TAN. A similar performance test of NUHOMS was conducted at the H.B Robinson reactor site.

The tests demonstrated that the storage systems could be satisfactorily handled and loaded dry, and demonstrated the heat transfer and shielding performance of the system when loaded with intact or consolidated PWR spent fuel. The heat transfer performance of the storage systems was good and in most cases exceeded design expectations. Peak cladding temperatures with helium backfill gas in the casks with the casks in vertical orientations were below the allowable of 340°C for design heat loads. In general, shielding performance met design expectations. Some of the casks had dose rate peaks associated with parting planes or discontinuities in shielding structure that could be removed with minor changes to the designs. From both heat transfer and shielding perspectives, the systems can, with minor refinements, be effectively implemented at reactor sites and central storage facilities for safe storage of spent fuel.

The following are significant findings and conclusions.

Cask Handling and Decontamination

- Cask-handling procedures are site-specific, and procedures should be developed for each site. Cask design drawings and specifications, operating and maintenance manuals, procedures, and spare parts are helpful in developing cask-handling procedures. Dry runs of the cask and associated equipment should be performed for all phases of cask handling and loading, including backfilling the cask with a cover gas and gas sampling. Dry (cold) runs with a nonirradiated dummy assembly were valuable in familiarizing personnel with cask-handling characteristics and in finalizing test procedures. Operational tests of project-specific equipment, especially that equipment used for remote operations, allowed problems to be resolved before the equipment was used with irradiated fuel.

- Approximately 1 hour was required to pump the cask down to 1 mbar and backfill with gas to 600 mbar. During a double pumpdown backfill operation, measured guide tube temperatures increased by <20°C during a 2-hour period. It is anticipated that evacuating and backfilling the cask after loading in a water basin will require a longer period and result in higher temperature increases.

- The cover gas system used to evacuate, backfill, monitor, and obtain gas samples should be carefully designed. The difficulty associated with backfilling the cask with a pure (>99%) cover gas and obtaining gas samples without introducing air should not be underestimated. The cask should be pumped down and backfilled a minimum of two times to ensure purity (>99%) of the final cover gas.

- When loading dry, sealing surface protectors were used by INEL to ensure that crud or particles did not lodge on these surfaces and result in blemishes or scratches that could compromise the finish of the sealing surfaces.

- The method required to rotate the cask from a horizontal to a vertical orientation or vice versa using a center trunion is awkward; the standard method of using a shipping cradle as a pivot base is recommended.

- Contamination was not a major problem during fuel transfers in air between shipping and storage casks. About 4 total hours of decontamination were required to remove contamination on the personnel work platform between the storage and shipping casks.

- The REA 2023 cask interior was decontaminated to below Class A licensing limits by flushing it with water, even when a small leak was present in a fuel rod. Significant amounts of crud were not found in the cask after the fuel was unloaded. The cask exterior can be decontaminated using soap and water in a manner similar to that used for transportation casks.

- Total personnel exposures during cask testing effort were less than 1.8 man-rem. The exposure at a reactor or storage facility will be even lower because casks will not be incrementally loaded or continuously worked around.

- The dual elastomer/metallic O-ring sealing technique used in the CASTOR-V/21 cask performed exceptionally well during many repetitive on/off lid operations. Similar high quality lid gaskets that can withstand repetitive use are desirable if incremental loading is to be performed.

- The cask's basket fuel storage cell openings size and wall smoothness should be designed for removal of fuel assemblies or canisters after extended storage. Allowances should be made for possible

warpage and bowing of the fuel. Consideration should be given to prevent the formation of ledges or discontinuities that could hold/restrain fuel assemblies or canisters. (Difficulty was encountered in removing consolidated fuel from the TN-24P cask. One of the canisters of fuel could not be removed.)

- If shielding material is used in cask lids, it should be completely isolated from the internal cask environment to prevent contamination of cask cover gas through off-gassing of the shielding material.

Fuel Characterization and Integrity

- Results of pretest in-basin sipping of each Cooper spent fuel assembly indicated that no failed fuel was loaded in the REA-2023 cask. Results of pretest and in-test fuel integrity activities (pretest ultrasonic, photographic, and video examinations) resulted in the conclusion that no failed fuel rods were loaded in the CASTOR-V/21, TN-24P or MC-10 casks.

- Pre- and post-test inspections of selected assemblies revealed that no noticeable changes occurred during the testing. Expected uneven rod growth during irradiations and slight rod bowing was observed in some fuel assemblies during video scans and photography before and after cask performance testing. Video scans and photography indicated the presence of an intermittent crud layer on the fuel assemblies.

- Only two leaking fuel rods have been detected during cask performance testing with unconsolidated fuel, one in the REA-2023 cask and one in the TN-24P cask. Several (about 10) fuel rods began to leak after the fuel was consolidated. No leaking fuel rods were detected during the consolidation process at INEL. The leaks were detected through determination of the concentration of Krypton-85 in gas samples. The size of the cladding penetration was estimated to be extremely small, and it had no adverse effects on the testing effort.

- Post-test gas sampling of casks at INEL containing unconsolidated fuel and casks containing consolidated fuel are recommended to determine the long-term impact of consolidation on fuel integrity.

- Smear samples from selected fuel assemblies indicated that large quantities of ^{60}Co were present, but no fission product species were detected.

Heat Transfer Performance

- The thermal performance section of the report should be consulted for peak fuel temperatures found in each of the SFS systems.

- Effects of fill gas on the thermal performance of the cask were apparent. The increased convection in a vertical cask filled with nitrogen shifted peak cladding temperatures upward in the cask. Peak cladding temperatures showed some upward shift because of helium convection in a vertical cask. Temperature profiles in vertical vacuum runs showed that peak cladding temperatures occurred at an axial location where the axial decay heat rate peaked, indicating the absence of convection.

- Replacing the intact fuel in a cask with consolidated fuel canisters reduced the effects of convection for the vertical nitrogen run and almost eliminated any noticeable effect of convection for the vertical helium run in the TN-24P and VSC-17 casks.

- Rotating the cask from a vertical to a horizontal orientation resulted in higher temperature differences between the peak cladding and ambient, i.e., the additional contact between fuel assemblies and the cask basket in the horizontal orientation was not sufficient to overcome the convection present in a vertical orientation. The axial location of the peak cladding temperatures corresponded to the location of the peak axial decay heat rate, indicating the absence of convection.

- Comparisons of temperature profiles across the diameter of the REA-2023 cask for vertical and horizontal orientations indicated a change in contact resistance between the basket and the cask because of the effects of gravity. This change in contact resistance resulted in higher temperatures in the upper quadrants and lower temperatures in the lower quadrants of a horizontal cask.

- The metal spent fuel storage casks had thermal time constants of approximately 22 hours.

- From data obtained in conjunction with the REA-2023 cask performance test, solar insolation does not appear to add to the total cask heat load in a significant or correlatable manner.

- Temperature transients in the casks were not excessive. They were generally less than 30°C/h on heatup and on cooldown.

- Critical basket gaps should be controlled. Backfill gas affects the temperature drop in gaps. The temperature drop between the basket and cask wall accounts for most of the change in magnitude of the radial temperature profile because of different backfill gases. Basket designs can minimize fuel temperatures by maximizing thermal conductance between the basket and cask wall.

- Eight indications of cracks were observed in the CASTOR V/21 basket in a post-test inspection. It was concluded that the relatively tight fit between the test basket and cask inner wall, along with substantial axial temperature gradients, were the potential causes

of cracking. A tight fit was used to align the basket with the lid and permit thermocouple lances to be inserted through the cask lid into selected fuel assembly guide tubes.

Shielding Performance

- Except for parting planes, end of neutron shields, and outlet vents, total dose rates on the cask surface were less than expected for each of the loaded dry storage systems. Minor modifications in the shielding design could eliminate dose rate peaks. The peaks are usually associated with parting planes.

- Shielding designs for consolidated fuel storage should consider the effect of the absence of nonfuel-bearing components on the gamma shielding requirements. Casks containing only consolidated fuel require less gamma shielding than casks that contain unconsolidated fuel or the nonfuel-bearing components. Peak gamma dose rates from the consolidated fuel PWR used in the tests performed at INEL were approximately 1/4 of those for unconsolidated fuel assemblies. The dose reduction comes from removal of the ^{60}Co containing, nonfuel-bearing components during the consolidation process.

Heat Transfer Analysis

- COBRA-SFS and HYDRA are effective codes that can be used to accurately predict temperatures in spent fuel dry storage systems.

- Code predictions of dry storage system temperatures within 25°C can be obtained. Further, if it is desirable to improve this agreement, the following, in order of importance, should be pursued:

  - System geometries, especially gap widths and characteristics of contacting surfaces, must be better known.

  - Emissivities of important basket/cask components should be measured.

  - The effects of free-stream turbulence and mixed convection (free and forced) adjacent to the exterior surface of the cask should be modeled.

  - Velocity fields should be measured in simulated casks, and HYDRA predictions should be evaluated with the measured distributions.

  - The accuracy of the correlation used to represent heat transfer to and from the cask exterior wall should be improved.

  - Use sufficient detail for a representative model of the fuel canister.

3.0 SPENT FUEL

Three types of spent fuel have been used during the cask performance testing and demonstration program. BWR 7x7 spent fuel assemblies were used for the performance test of the REA-2023 cask. Westinghouse 15x15 PWR was used in the CASTOR V/21, TN-24P, MC-10 and NUHOMS performance tests. A portion of this fuel was consolidated at INEL and used in performance tests of the TN-24P and VSC-17 casks, also at INEL. Table 3.1 gives a summary of the fuel used in each of the performance tests. A description of the spent fuel and the results of spent fuel monitoring during the performance test follows.

3.1 BWR 7x7 FUEL ASSEMBLIES

The BWR assemblies used during the REA 2023 cask performance test were of a General Electric 7x7 design and were taken from the Nebraska Power Cooper Reactor. The 7x7 design specifications are given in Table 3.2. The upper and lower tie plates are 304 stainless steel castings.

The lower tie plate has a nose-piece that supports the fuel assembly in the reactor. The upper tie plate has a handle for transferring the fuel assembly.

TABLE 3.1. Spent Fuel Assembly Characteristics

Cask	REA-2023	CASTOR V/21	TN-24P	TN-24P[a]	MC-10	VSC-17[a]	NUHOMS
Fuel Type	BWR	PWR	PWR	PWR	PWR	PWR	PWR
Assembly Type	7 x 7	15 x 15	15 x 15	Consolidated 15 x 15	15 x 15	Consolidated 15 x 15	15 x 15
Burnup, GWd/MTU	24-28	24-35	29-32	24-35	24-35	26-35	31-34
Cooling Time, years	2.3-3.4	2.2-3.8	4.2	6.2-12.2	4.6-10.1	8.8-14.3	5
Enrichment, wt%	2.5	2.9-3.1	2.9-3.2	1.9-3.2	1.9-3.2	2.56-3.2	2.9
Assembly Decay Heat, W	235-370	1000-1800	832-919	701-1185	400-700	700-1050	692-834
Average, W	290	1350	860	970	530	877	766
Cask, kW	15.2	28.4	20.6	23.3	12.6	14.9	5.3

(a) Performance test utilizing consolidated fuel in the cask.

TABLE 3.2. Design Characteristics of Cooper BWR Fuel Rods and Assemblies

Fuel Assembly Data		
Overall length	4.47 m	(175.83 in.)
Nominal active fuel length	3.71 m	(144 in.)
Fuel rod pitch	1.87 cm	(0.738 in.)
Space between fuel rods	0.445 cm	(0.175 in.)
Fuel bundle heat transfer area	8.04 m^2	(86.52 ft2)
Fuel rod array, 7 x 7	--	--
Zr-2 weight	48.000 kg/ass.	(105.8 lb/ass.)
304 stainless steel	8.600 kg/ass.	(18.96 lb/ass.)
Fuel Rod Data		
Average linear rod power	23.2 kW/m	(7.079 kW/ft)
Outside diameter	1.43 cm	(0.563 in.)
Cladding thickness	0.081 cm	(0.032 in.)
Pellet outside diameter	1.24 cm	(0.487 in.)
Fission gas plenum length	40.6 cm	(16 in.)
Pellet immersion density	10.42 g/cc	--
Cladding material	Zircaloy-2	--
Helium fill gas pressure	1 atm	--
Fuel	UO_2	--

In addition to having standard BWR fuel rods, each assembly has eight tie rods that thread into the lower tie plate casting. The upper ends of the tie rods extend through and are fastened to the upper tie plate with stainless steel hexagonal nuts and locking tabs. These tie rods support the weight of the assembly during fuel-handling operations when the assembly hangs by the handle. The center rod of each fuel assembly has been designed to maintain the position of the fuel rod spacers. It is inserted into the fuel assembly and rotated to lock the spacers into their respective locations. The spacers have Inconel-X springs to maintain rod-to-rod spacing. The fuel rods are pressurized with helium and sealed by welding end plugs on each end.

Additional information on the Cooper fuel assemblies is found within the REA 2023 performance report (McKinnon 1986). Information contained in that report includes burnup and burnup history. Each assembly was initially enriched to 2.5 wt% ^{235}U averaged over all rods in the assembly.

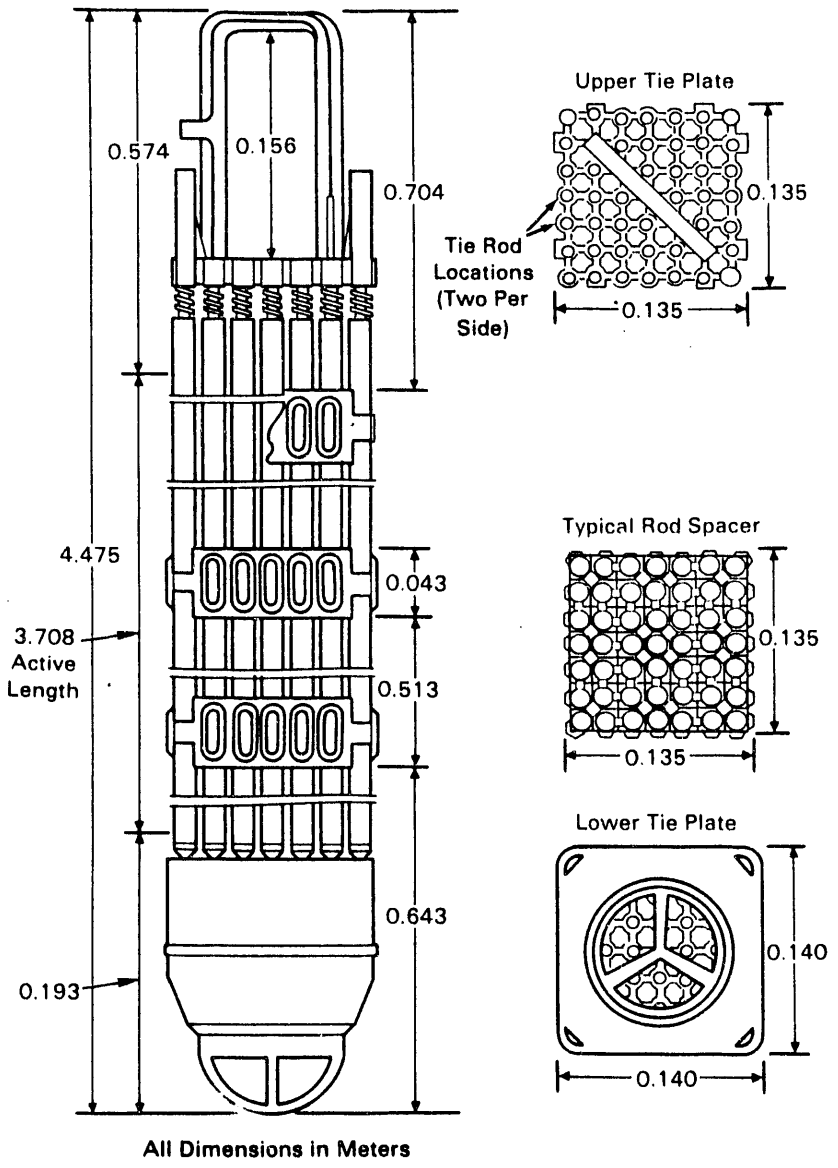

FIGURE 3.1. Cooper Spent Fuel Assembly

3.2 PWR 15x15 FUEL ASSEMBLIES

The fuel assemblies are square in cross section, nominally 214 mm (8.426 in.) on a side, and have a total length of 4058 mm (159.765 in.). The fuel column is 3658-mm (144-in.) long. The overall configuration is shown in Figure 3.2.

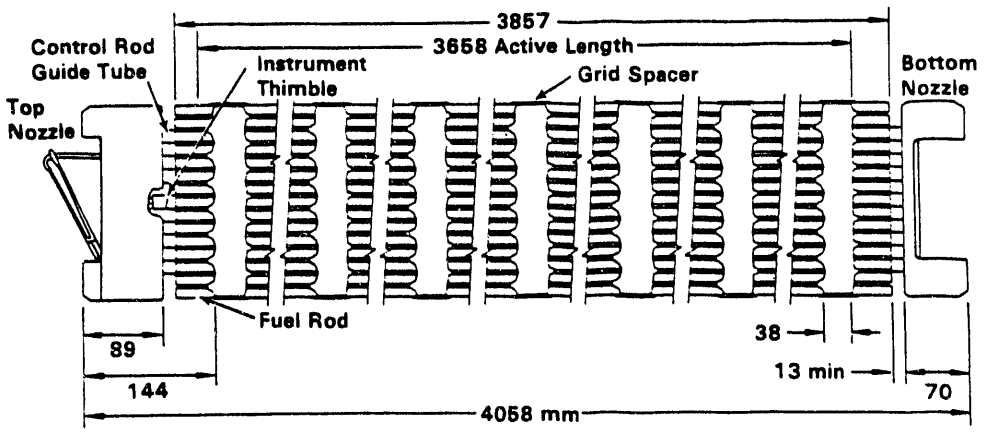

FIGURE 3.2. 15 x 15 PWR Fuel Assembly

The fuel rods in a fuel assembly are arranged in a square array with 15 rod locations per side and a nominal rod-to-rod centerline pitch of 14.3 mm (0.563 in.) as shown in Figure 3.3. Of the total possible 225 rod locations per assembly, 20 were occupied by guide tubes for the control rods and burnable poison rods, and one central thimble was reserved for in-core instrumentation. The remaining 204 locations contained fuel rods. In addition, a fuel

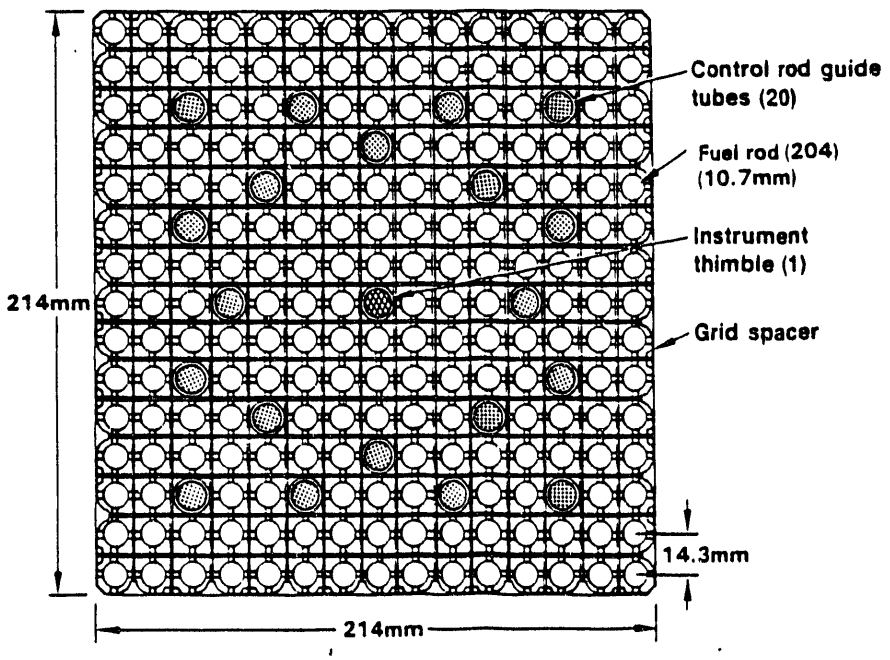

FIGURE 3.3. 15 x 15 PWR Fuel Assembly Cross Section

assembly also included a top nozzle, a bottom nozzle, and seven grid assemblies. The guide tubes, central thimble, grid assemblies, and the top and bottom nozzles provide the basic structure for the fuel assembly.

The fuel rods consist of UO_2 ceramic pellets contained in slightly cold-worked and partially annealed Zircaloy 4™ tubing, which is plugged and seal-welded at the ends to clad the fuel. Nominal dimensions include a 9.29-mm (0.3659-in.) pellet diameter, 10.71-mm (0.422-in.) tube outside diameter, 0.62-mm (0.0243-in.) tube thickness, and 3860-mm (152-in.) length.

Sufficient void volume and clearances are provided within the rod to accommodate fission gases released from the fuel, differential thermal expansion between the cladding and the fuel, and fuel swelling due to accumulated fission products without overstressing of the cladding or seal welds. Shifting of the fuel within the cladding is prevented during handling or shipping before core loading by a carbon-steel helical compression spring that bears on the top of the fuel pellet column. The holddown force to prevent fuel shifting is obtained by compression of the spring between the top end plug and the top fuel pellet of the stack.

During assembly, the pellets are stacked in the cladding to the required fuel height. The compression spring is then inserted into the top end of the fuel, and the end plugs are pressed into the ends of the tube and welded. During the welding process, the fuel rods are internally pressurized with helium to between 20.7 and 27.6 bar (300 and 400 psia).

The fuel rod void space is sized to ensure adherence to the pressure criterion. The end-of-life pressure is evaluated for the worst rod under expected conditions of fuel operation and at the peak steady-state power. The model used to predict the quantity of fission gas in the gap at end-of-life is based on an extensive comparison to published performance of fuel rods under a variety of conditions. The composition of the gas in the gap at end-of-life is a maximum of approximately 50% fission.

The fuel pellets are right circular cylinders consisting of slightly enriched UO_2 powder, which is compacted by cold pressing and sintering to the required density. The ends of each pellet are dished slightly to allow the

greater axial expansion at the center of the pellets to be taken up within the pellets themselves and not in the overall fuel length. The nominal design enrichment ranged from 1.86 wt% to 3.20 wt%. Information on burnup history and enrichment for each fuel assembly used during testing is found within the individual performance reports (Creer 1986; McKinnon 1986, 1987a, 1987b, 1989, 1992; Strope 1990). The nominal density is 95% of theoretical density for all of the fuel pellets.

3.3 CONSOLIDATED FUEL CANISTERS (PWR 15x15 FUEL)

During the consolidation process the fuel rods were removed from 48 of the PWR fuel assemblies described in the previous subsection and placed into 24 canisters. Two-to-one consolidation was consistently achieved, because each canister was able to hold 410 fuel rods and two fuel assemblies provided 408 rods. This left two extra fuel rod storage locations per canister. Simulated guide tubes with funnel-shaped tops were placed in seven canisters to provide locations for inserting TC lances during performance testing. The simulated guide tubes displaced three fuel rod locations. The overflow fuel rod caused by inserting a guide tube in a canister was placed in the next canister of fuel.

A stainless steel fuel canister, Figure 3.4, consists of a base and a top-locking cover. A series of spacers, support bars, and tines is attached to the base of the canister to align and hold the fuel rods during consolidation. Once the fuel has been placed on the base, the top cover is placed over the fuel and locked into place. The design of the top cover, the sliding fit between the top cover and base, and the canister locking mechanism do not seal the canister but do limit gas flow into and out of the canister. The loaded canister is 216-mm (8.5-in.) square by 4053-mm (159.57-in.) long. The lower end plate and support angles attached to the top cover raise the fuel 41.5 mm (1.635 in.) off the bottom of the cask.

3.4 SPENT FUEL INTEGRITY

This section of the report contains gas sampling information from the spent fuel dry storage metal cask performance tests. It documents the

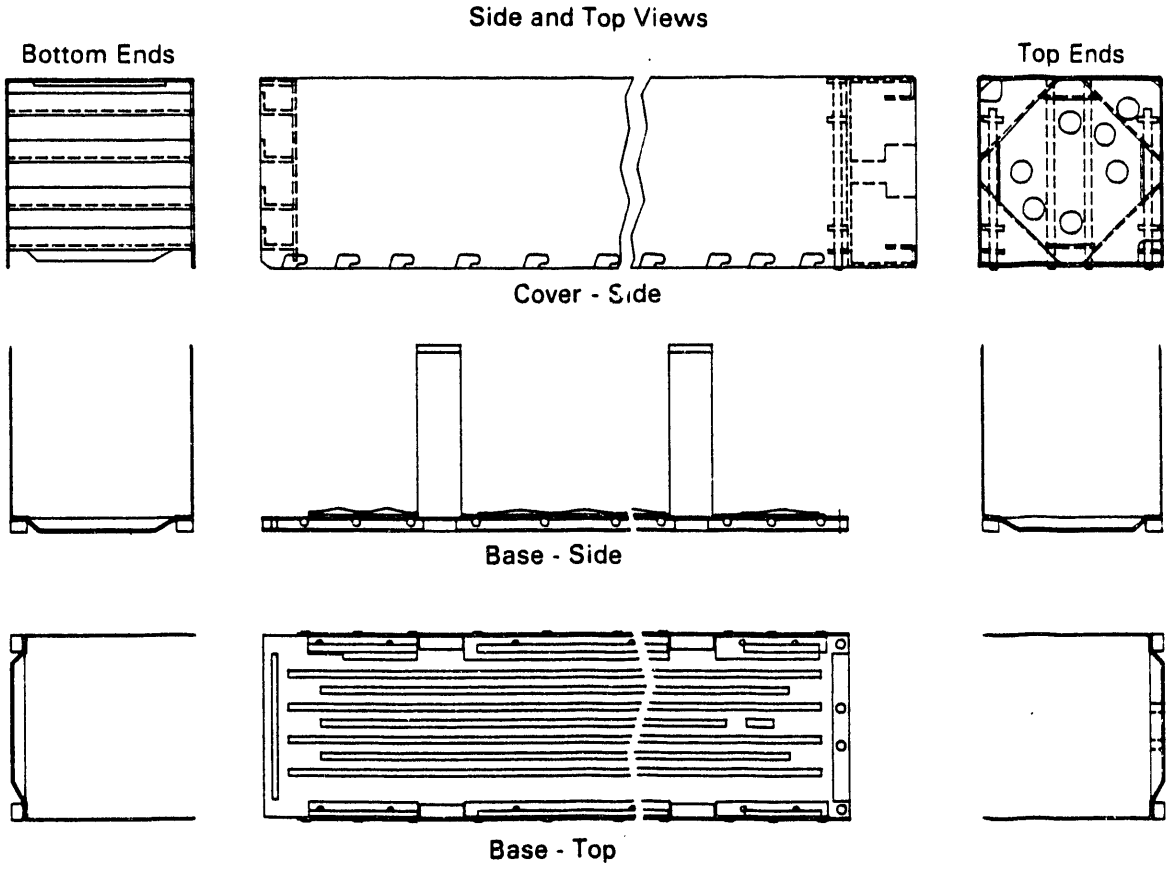

FIGURE 3.4. Consolidated Fuel Canister

condition of the BWR fuel from Nebraska Power's Cooper Station and PWR fuel from the VP's Surry reactor before testing and the effect of testing on fuel integrity as ascertained through gas sampling during cask performance tests at GE, Morris, Illinois, and INEL, and subsequent surveillance at INEL. Results are presented for tests using both intact and consolidated PWR spent fuel.

Fuel integrity was addressed in individual cask reports for each of the performance tests. That data have been consolidated in this report. This report also contains surveillance data taken after the conclusion of each performance test not previously reported.

The results of the gas sampling done during testing and after test surveillance indicates that dry storage of unconsolidated fuel does not seem to have an adverse affect on fuel integrity. However, consolidation of spent

fuel rods appeared to produce pin holes or hair line cracks in the fuel cladding and resulted in more leaking rods during dry storage.

Before testing, the Surry PWR spent fuel assemblies used in the cask performance tests were characterized using in-basin ultrasonic examinations and video scans. The BWR fuel was characterized using in-basin sipping and video scans. Cask internal cover gas samples were taken during testing. After testing, selected fuel assemblies were videotaped and photographed. Then fuel assemblies used in the TN-24P and MC-10 cask performance tests along with a few Turkey Point reactor spent fuel assemblies were consolidated and loaded into the TN-24P cask for another performance test.

Performance test runs involved a combination of cover gases and cask orientations. The backfill environments used were vacuum, nitrogen, and helium; nitrogen and helium were sampled and analyzed to detect leaking spent fuel rods. The integrity of the fuel assemblies was determined from cover gas sampling (Creer 1986; McKinnon 1986, 1987a, 1987b, 1989). At the conclusion of each performance test, periodic gas sampling was conducted on each cask as part of a cask surveillance and monitoring activity.

Information on spent fuel integrity is of interest in evaluating the impact of dry storage and fuel-handling operations associated with dry storage on the behavior of spent fuel rods during long-term dry storage. The main areas of interest include the integrity of the fuel cladding, condition of the spent fuel assembly hardware, and the character and condition of the crud. Specific information obtained through the cask performance tests included visual observation and ultrasonic examination of the condition of the cladding, fuel rods, and fuel assembly hardware before dry storage and consolidation of the fuel; and a qualitative determination of the effect of dry storage and fuel consolidation on fission gas release from the spent fuel rods.

This section is divided into two subsections: the first subsection describes the condition of the fuel before testing based on ultrasonic evaluations, in-basin sipping, and visual examinations. The second subsection presents results of gas sampling during and after cask performance testing.

3.4.1 In-Pool Ultrasonic Inspections

In-pool ultrasonic inspections were performed on the PWR fuel at VP's Surry Reactor using the Babcock & Wilcox Failed Fuel Rod Detection System (FRDS). This system is a portable system designed to be used underwater in spent fuel pools. The system consists of an underwater manipulator, an ultrasonic probe, electronic controls, recording equipment, and a support plate. The FRDS system uses ultrasonic techniques to differentiate between non-leaking and leaking rods by detecting the presence of moisture in the latter.

Numerous factors must be considered when interpreting the X-Y plots of each fuel assembly examined. These factors include pulse height, crud deposits on the fuel rods, fuel assembly, and fuel rod bowing. Because the proximity of the UT probe to the fuel rods may vary with fuel rod bowing, pulse amplitudes would also tend to vary in height. Fuel assemblies that had SUSPECT traces were re-examined from all four faces. In each case, fuel rods that were SUSPECT during the initial examination were found to be either CLEAR or INDICATION (failed) during re-examination. Only fuel assemblies with CLEAR examinations were used in the cask testing.

3.4.2 In-Basin Sipping

The 52 BWR fuel assemblies from the Cooper Reactor used in the REA 2023 cask performance test were sipped "in-basin" and "in-vessel" to investigate fuel rod integrity before dry storage and to determine whether any of the fuel rods developed leaks during testing. In-basin sipping was conducted in the fuel storage basin, while in-vessel sipping was conducted in the calorimetry vessel located in the smaller unloading basin. The assemblies were sipped both before and after testing, and assembly CZ205 was resipped each time fuel assemblies from a new basket were sipped, to ensure appropriate consistency. In-basin sipping consisted of placing a hood over the selected assembly and analyzing the water that was drawn off the top of the assembly. All the sipping data was compared to background readings to assess fuel integrity.

Detailed results for the in-basin sipping are given in McKinnon (1986). Data are provided on the date, time, basin temperature, and background radiation levels for both ^{137}Cs and ^{60}Co. The ^{137}Cs levels detected during pretest

and post-test sipping are summarized in that report. Although there is some variation in the differences between the pretest and post-test radionuclide concentrations, the values were lower than would exist if the assembly contained leaking fuel rods. The sipping results did not indicate any leaking fuel rods in any of the fuel assemblies used in the cask either before or after cask testing.

3.4.3 Visual, Video, and Photographic Examinations

The PWR fuel assemblies were examined visually to establish their general condition after shipment from VP, after handling at the INEL hot shop, after cask performance testing, and during consolidation. Similar exams were made of the Cooper BWR fuel during the REA 2023 performance tests at GE-Morris. Two kinds of visual examinations were used: black-and-white videos and color photography of selected fuel assemblies.

The black-and-white videos taken at GE-Morris, VP and INEL did not provide sufficient detail to characterize the crud or very small features on the fuel rods. They did not reveal any indication of significant variations in the fuel rods after shipment, handling, and performance testing. The resolution of the videotapes did not provide enough information to adequately determine the integrity and condition of the fuel and fuel cladding. Examination of the video scans showed that all the fuel assemblies and fuel rods look basically the same when viewed from outside the assemblies. There was some discoloration of the fuel rod cladding in the area of the grid spacers, which was expected.

Color photographs showed that a typical orange/reddish crud (probably Fe_2O_3) was evenly deposited on all of the Zircaloy 2 cladding and fuel assembly hardware. There were no noticeable changes in the characteristics or adherence of the crud during handling operations involving the spent fuel assemblies at GE-Morris or INEL. Some scratches and worn spots were apparent on the spacer grids and some fuel rods, but these features did not change as a result of examination or handling operations. In general, the fuel rods were in excellent condition with a very adherent crud layer.

Additional visual examinations of the fuel were conducted during the dry rod consolidation program. According to Vinjamuri (1988a,b):

> No noticeable cladding defects in the rod surfaces were observed for any of the fuel processed. The oxide layer on the surface of the fuel rods appears to be intact and firmly attached to the cladding. The oxide layer does not appear to be loose, thick, soft, or powdery. However, the oxide layer and some of the zirconium cladding was scraped from the rod surface by the spacer grids as the rod was pulled during fuel consolidation. Very little crud buildup on the surfaces of the rods was observed. The surfaces of the rods displayed only a thin oxide layer, which had the appearance of surface discoloration rather than any rough or loose material. The rod surfaces are discolored near the spacer grids. The discoloration has an appearance of a dark mottling of the surface and is progressively more predominant from the middle of the rod length toward the rod bottom. The rods are generally clean, with limited amounts of clad discoloration and oxidation . . . The evidence of fuel rod growth since fabrication was visually obvious during the consolidation process . . . Length variation between rods appears to be as much as 2 cm (0.8 inch). The rods that grew longer than others appeared to be randomly located within the fuel assembly. (Ellipses by McKinnon.)

3.4.4 Cask Cover Gas Sampling

The cask cover gas was sampled several times during each cask performance test to evaluate the integrity of the spent fuel rods. Each sample was collected in a separate 500-cc stainless steel cylinder. The cylinders were checked for leaks before sampling. Initially, during the CASTOR-V/21 cask performance test, the cylinders were equipped only with quick disconnect-fittings and no bellows-sealed valves as part of the closure. During the early sampling efforts with the CASTOR-V/21 cask, the cover gas samples in the cylinders were diluted with ambient air from the vicinity of the sampling apparatus, air that leaked into the cylinder during shipment, and argon introduced at LLNL. In many cases, this dilution was made more severe by the collection of small amounts of cask cover gas, presumably due to short equilibration times between the cask and the sample bottle during the actual cask cover gas collection procedure. The end effect of small, diluted samples on the cask cover gas analyses was to increase detection limits, increase measurement

uncertainties, and introduce questions of sample validity. Once bellows-sealed valves were added to the sampling cylinders, the problem of air leakage into the sampling cylinders was eliminated.

The gas sample analysis was performed at LLNL and INEL. Initially, at LLNL and later, as upgrades were made in INEL's gas analysis capabilities, the gas sampling analysis was shifted from LLNL to INEL. The results of the gas analyses are presented in Tables 3.3, 3.4, 3.5, and 3.6. Mass spectra were analyzed for all common fixed gases with masses less than 100 to verify backfill gas composition. Only N_2, O_2, He, Ar, and CO_2 concentrations above 0.01% are detected in any of the samples. It is obvious from values in the table that significant amounts of air were introduced into many of the CASTOR V/21 gas samples as previously discussed. TN-24P sample 4C-PT (Table 3.5) shows the effect of leaving a valve open; some 85Kr gas was detected shortly after the sample was taken, but by the time the gas was analyzed, the cylinder content had reverted to air.

The integrity of the fuel rods was assessed from the radionuclide concentration. Initial indications of the presence of radionuclides (screening analysis) was determined at the test site using a multichannel analyzer before

TABLE 3.3. REA-2023 Cask Gas Sample Identification (BWR fuel)

Sample		Cover	Volume Percent[a]			Radionuclide Concentration pCi/ml[(STP)] (1/1/85)[b]			
Number	Date	Gas	N_2	O_2	He	Screening Analysis	^{85}Kr	$^{14}CO_2$	^{14}CO
1A	11/27/84	N2	99.96	0.018	--	<1	0.11 ± 0.02	--	--
2A	12/08/84	N2	99.98	--	--	<1	0.19 ± 0.01	<0.08	--
3A	12/08/84	He	0.25	0.06	99.68	<1	<0.06	0.08 ± 0.01	--
4A	01/02/85	He	0.20	0.04	99.75	<1	<0.02	<0.02	--
5A	01/21/85	N2	99.98	--	--	20.1 ± 0.3	18.70 ± 0.2	<0.02	--
6A	02/05/85	N2	99.99	--	--	14680 ± 160	14680 ± 170	0.28 ± 0.01	0.110 ± 0.03
7A	02/05/85	He	0.31	0.07	99.61	17.0 ± 0.2	12.90 ± 0.2	0.20 ± 0.01	--
8A	03/12/85	He	0.02	--	99.98	35600 ± 400	34600 ± 400	<0.02	0.031 ± 0.005
13A	03/12/85	N2	99.99	--	--	19.6 ± 0.2	15.8 ± 0.1	--	--
13C	03/15/85	N2	99.98	0.01	--	3360 ± 40	3220 ± 60	0.06 ± 0.01	--
14A	04/11/85	He	0.05	--	99.93	36040 ± 630	35670 ± 390	<0.03	0.736 ± 0.004

(a) Species present in mass spectra at 0.01% or more. Accuracy of these measurements is ±0.2% or ±1 unit in the least significant digit.

(b) Picocuries per milliliter of sample at 760 torr, 0°C decay corrected to 1/1/85. Indicated errors are one standard deviation of the mean of replicate measurements.

TABLE 3.4. Gas Samples from the CASTOR-V/21 Cask

Sample Number	Collection Time/Date	Cover Gas	Volume Percent						Radionuclide	
			He	N_2	O_2	Ar	CO_2	H_2	Screening Analysis	^{85}Kr
1A	1400/9-06-85	He	69.30	21.90	5.967	2.798	0.029	<0.01	4.78 ± 0.39	0.09 ± 0.05b
1B	1330/9-11-85	He	62.51	25.57	6.692	5.148	0.033	<0.01	4.60 ± 0.57	--
1D	1300/9-11-85	He	59.59	17.59	4.110	18.66	0.048	<0.01	15.9 ± 3.5	0.37 ± 0.13b
2A	1920/9-11-85	N2	<0.01	95.34	1.180	3.457	0.017	<0.01	<0.13	<0.05
2B	1930/9-11-85	N2	<0.01	90.58	6.81	2.581	0.024	<0.01	0.22 ± 0.08b	--
2C	1345/9-13-85	N2	0.031	68.79	3.134	27.95	0.059	<0.01	7.15 ± 0.69	0.26 ± 0.09b
2D	1430/9-13-85	N2	0.042	70.08	8.43	21.29	0.153	<0.01	5.98 ± 0.36	--
4B	1410/9-16-85	He	70.59	14.23	5.95	9.09	0.060	0.018	5.77 ± 0.58	--
4A	1419/9-16-85	He	32.38	50.55	13.31	3.700	0.053	<0.01	0.23 ± 0.16b	0.07 ± 0.04b
4C	1045/9-20-85	He	65.69	1.560	0.156	32.58	<0.01	<0.01	1.92 ± 0.16	0.05 ± 0.01b
4D	1050/9-20-85	He	<0.01	76.94	20.26	2.746	0.054	<0.01	<0.08	--
5A	NA/9-20-85	N2	0.050	74.92	11.441	13.43	0.120	0.016	1.38 ± 0.46	<0.17
5B	NA/9-20-85	N2	<0.01	73.95	18.77	7.217	0.060	<0.01	<0.08	--
5C	1300/9-23-85	N2	0.048	85.63	5.559	8.533	0.065	0.159	4.01 ± 0.41	0.18 ± 0.07b
5D	1300/9-23-85	N2	0.068	91.06	0.158	8.462	0.044	0.207	8.28 ± 0.75	0.19 ± 0.11b
Post Cask Performance Test Gas Sampling										
GN-3A	3-05-86	He	99.0	0.82	0.2	≤0.01	≤0.01	--	--	--
GN-3B	3-05-86	He	99.7	0.27	0.06	≤0.01	≤0.01	--	--	--
GN-4A	3-17-86	He	99.86	0.11	0.03	≤0.01	≤0.01	--	--	--
GN-4B	3-17-86	He	99.81	0.15	0.04	≤0.01	≤0.01	--	--	--
GN-5A	3-24-86	He	99.84	0.13	0.03	≤0.01	≤0.01	--	--	--
GN-5B	3-24-86	He	99.83	0.14	0.03	≤0.01	≤0.01	--	--	--
GN-8A	6-27-86	He	65.3	29.1	4.2	0.36	1.1	--	--	--
GN-9A	8-15-86	He	99.8	0.05	0.002	0.001	0.001	0.15	--	<0.0274
GN-9B	8-15-86	He	99.78	0.05	0.006	0.001	0.002	0.16	--	<0.0289
GN-10A	9-26-86	He	99.8	0.03	<0.01	<0.01	<0.01	0.17	--	<0.024
GN-11A	12-08-86	He	99.8	0.06	0.01	≤0.01	≤0.01	0.10	--	<0.057

shipment of the gas samples to the measurement laboratory. The differences between the screening analysis and the more exact laboratory measurements is apparent from Table 3.5. It was generally expected that the screening analysis would agree with the laboratory measured 85Kr result. However, for these samples the screening counts were significantly greater than the laboratory measured krypton results. The disparity between screening and laboratory measured concentrations remains unexplained. However, the relatively low amounts of 85Kr detected indicate that no leaking fuel rods were present in the GNS CASTOR-V/21 and MC-10 casks during performance testing with unconsolidated fuel and up to about a year after testing had been completed. This is

TABLE 3.5. Gas Samples from the Transnuclear TN-24P Cask

Sample Number	Collection Time/Date	Cover Gas	Volume Percent						Radionuclide Concentration, pCi/ml	
			He	N_2	O_2	Ar	CO_2	H_2	Screening Analysis	^{85}Kr
1A-PR	1815/1-10-86	He	99.97	<0.01	0.020	<0.01	<0.01	<0.01	≤0.08	--
1B-PR	1830/1-10-86	He	99.96	0.037	<0.01	<0.01	<0.01	<0.01	≤0.06	≤0.01
1C-PT	0945/1-14-86	He	99.92	0.056	0.017	<0.01	<0.01	<0.01	0.44 ± 0.06	≤0.02
1D-PT	0955/1-14-86	He	99.93	0.057	<0.01	<0.01	<0.01	<0.01	0.65 ± 0.24	≤0.02
2A-PR	1600/1-14-86	N2	<0.01	99.99	<0.01	<0.01	<0.01	<0.01	≤0.07	--
2B-PR	1605/1-14-86	N2	<0.01	99.99	<0.01	<0.01	<0.01	<0.01	≤0.07	≤0.02
2C-PT	1030/1-17-86	N2	<0 01	99.94	<0.01	<0.01	<0.01	<0.01	2.05 ± 0.29	--
2D-PT	1020/1-17-86	N2	<0.01	99.98	<0.01	<0.01	<0.01	0.011	2.65 ± 0.13	≤0.02
4A-PR	1258/1-24-86	He	99.99	<0.01	<0.01	<0.01	<0.01	<0.01	≤0.07	--
4B-PR	1303/1-24-86	He	99.93	0.077	<0.01	<0.01	<0.01	<0.01	≤0.07	≤0.02
4C-PT[a]	1245/1-27-86	He	0.379	77.73	20.83	0.931	0.058	<0.01	2657 ± 37	--
4D-PT	1255/1-27-86	He	87.42	9.792	2.592	0.118	0.014	<0.01	7269 ± 166	7506 ± 82
5A-PR	1939/1-27-86	N2	0.063	98.93	0.937	0.063	<0.01	<0.01	277 ± 7	--
5B-PR	1947/1-27-86	N2	0.058	98.68	1.162	0.074	<0.01	<0.01	251 ± 6	252 ± 3
5C-PT	1115/1-31-86	N2	<0.01	99.95	<0.01	0.028	0.012	<0.01	2132 ± 30	--
5D-PT	1125/1-31-86	N2	<0.01	99.93	<0.01	0.029	<0.01	<0.01	2110 ± 24	2077 ± 38
Post Cask Performance Test Gas Sampling										
TN-1A	1300/2-28-86	He	99.99	<0.01	<0.01	<0.01	<0.01	<0.01	7.31 ± 0.10	--
TN-1B	1310/2-28-86	He	99.99	<0.01	<0.01	<0.01	<0.01	<0.01	7.09 ± 0.1	7.24 ± 0.54
TN-1C	2-28-86	He	99.9	<0.03	<0.01	<0.001	<0.005	--	--	--
TN-1D	2-28-86	He	99.9	<0.02	<0.01	<0.001	<0.006	--	--	--
TN-2A	8-13-86	He	99.77	0.16	0.04	0.001	0.020	--	--	ND[b]
TN-2B	8-13-86	He	99.82	0.12	0.03	0.001	0.018	--	--	ND
TN-3A	12-11-86	He	99.35	0.49	0.13	0.007	0.016	0.009	--	12.9 ± 0.6
TN-31A	5-07-87	He	99.83	0.11	0.03	<0.01	0.03	<0.01	--	20.7
Dry Rod Consolidation Started May 1987. Finished Loading Cask With Consolidated Fuel September 28, 1987										
Pretest	12-18-87	He							86,320	
B1-P	1505/1-07-88	He	99.9	0.03	<0.01	<0.01	<0.01	<0.01		
A1-PT	1000/1-12-88	He	99.9	0.03	<0.01	<0.01	<0.01	<0.01	24,530	21,300 ± 1700
A2-PR	1700/1-13-88	N2	0.08	99.86	0.01	0.04	<0.01	<0.01		
A2-PT	1000/1-18-88	N2	0.10	99.82	<0.01	0.04	0.04	<0.01	7,680	6000 ± 500
A4-PR	1330/1-27-88	He	99.95	0.04	0.01	<0.01	<0.01	<0.01		
A4-PT	0930/2-01-88	He	99.98	0.02	<0.01	<0.01	<0.01	<0.01	2,100	1300 ± 140
A5-PR	0900/2-03-88	N2	0.10	99.84	0.01	<0.01	<0.01	<0.01		
A5-PT	0900/2-08-88	N2	0.02	99.95	0.02	<0.01	0.01	<0.01	7,160	4500 ± 400
A7-PT	1540/2-29-88	He	99.97	0.02	<0.01	<0.01	<0.01	<0.01	17,130	14,100 ± 1000
Post Test	8-11-88	He	99.77	0.15	0.04	<0.01	0.04	ND	118,000	69,890 ± 5170

(a) Bottles received with one open valve on each sample.
(b) Not Detected.

TABLE 3.6. Gas Samples from the Westinghouse MC-10 Cask

Sample Number	Collection Time/Date	Cover Gas	Volume Percent						Radionuclide Concentration, pCi/ml	
			He	N_2	O_2	Ar	CO_2	H_2	Screening Analysis	^{85}Kr
1A-PR	5/29/86	He	99.96	0.03	0.003	--	<0.01	<0.01		
1B-PR	1600-5/29/86	He	99.89	0.092	0.019	<0.01	<0.01	<0.01	≤0.09	--
1C-PR	1605-5/29/86	He	99.95	0.039	<0.01	<0.01	<0.01	<0.01	≤0.10	≤0.02
1A-PT	6/02/86	He	99.85	0.09	0.02	--	0.004	0.03		
1B-PT	1400-6/02/86	He	99.93	0.040	<0.01	<0.01	<0.01	0.016	≤0.09	--
1C-PT	1410-6/02/86	He	99.94	0.034	<0.01	<0.01	<0.01	0.018	≤0.09	≤0.01
2A-PR	6/03/86	N2	--	99.97	<0.01	0.016	--	<0.01		
2B-PR	1450-6/03/86	N2	0.370	99.60	<0.01	0.015	<0.01	0.018	≤0.08	--
2C-PR	1500-6/03/86	N2	<0.01	99.97	<0.01	0.015	<0.01	0.018	≤0.08	≤0.02
2A-PT	6/06/86	N2	0.07	99.87	0.01	0.015	0.009	0.02		
2B-PT	0915-6/06/86	N2	0.033	99.92	<0.01	0.015	<0.01	0.032	0.24 ± 0.16b	--
2C-PT	0930-6/06/86	N2	<0.01	99.95	<0.01	0.015	<0.01	0.033	0.30 ± 0.11b	≤0.02
4A-PR	6/13/86	He	99.96	0.03	<0.01	--	--	<0.01		
4B-PR	1320-6/13/86	He	99.99	<0.01	<0.01	<0.01	<0.01	<0.01	≤0.07	--
4C-PR	1325-6/13/86	He	99.99	<0.01	<0.01	<0.01	<0.01	<0.01	≤0.08	<0.01
4B-PT	1420-6/16/86	He	99.99	<0.01	<0.01	<0.01	<0.01	0.01	≤0.06	--
4C-PT	1540-6/16/86	He	99.99	<0.01	<0.01	<0.01	<0.01	<0.01	≤0.08	≤0.02
5A-PR	6/18/86	N2	0.8	99.2	<0.01	0.02	--	--		
5B-PR	1545-6/18/86	N2	0.707	99.25	<0.01	0.019	<0.01	0.011	≤0.08	--
5C-PR	1550-6/18/86	N2	0.051	99.92	<0.01	0.019	<0.01	<0.01	≤0.08	≤0.02
5A-PT	6/23/86	N2	0.05	99.89	<0.01	0.02	--	0.03		
5B-PT	0920-6/23/86	N2	0.687	99.22	<0.01	0.018	0.010	0.033	≤0.07	--
5C-PT	0930-6/23/86	N2	0.386	99.55	<0.01	0.019	<0.01	0.030	≤0.07	≤0.02
Post Cask Performance Test Gas Sampling										
MC-1A	1330-8/06/86	He	99.67	0.195	<0.01	<0.01	<0.01	0.119	≤0.08	--
MC-1B	1345-8/06/86	He	99.71	0.156	<0.01	<0.01	<0.01	0.119	≤0.08	≤0.02
MC-3A	9-30-86	He	99.6	0.18	0.01	<0.01	0.01	0.24	--	<0.031
MC-4A	12-16-86	He	99.97	0.17	0.004	0.001	ND(a)	0.005	--	<0.02
MC-31A	5-21-87	He	95.88	3.09	0.80	0.04	0.02	0.18	--	--
Dry Rod Consolidation from May 1987 to September 1987										
	3-03-88	He	98.7	1.0	0.24	0.01	0.02	≤0.01	--	--
	8-10-88	He	99.0	0.82	0.02	0.01	0.12	ND	--	ND

(a) Not Detected.

particularly significant because the first few assemblies loaded in the CASTOR-V/21 cask were exposed to air for approximately 200 h during incremental loading of the cask and fuel assembly/basket inspections at a reduced

temperature. In addition, after testing was completed and long-term surveillance started, all the fuel assemblies were in a 70% He and 30% air environment for approximately four months because a quick disconnect fitting on the CASTOR-V/21 cask lid had not sealed shut.

Krypton gas was found in samples 6A, 6B, 8A, 8B, 14A, and 14B for the REA 2023 cask (Table 3.3). The estimated amount of 85Kr released to the cask during each sample period was determined. These amounts were accumulated and plotted as a function of total cask storage time, as shown in Figure 3.5. The release of 85Kr to the cask was essentially linear during the 2.5 months of testing and indicates that the defect in the cladding was very small.

The krypton releases during the REA 2023 cask test are compared in Figure 3.6 with the 85Kr releases observed in assembly B02 in the Fuel Temperature Test (FTT) (Johnson and Gilbert 1983) that was conducted to assess dry storage of spent fuel. The background level (3.086 x 10-8 Ci) in the FTT, 1% release of the 85Kr produced in a single fuel rod, and 20% release of the 85Kr produced in a single fuel rod are plotted in Figure 3.6 for comparison with

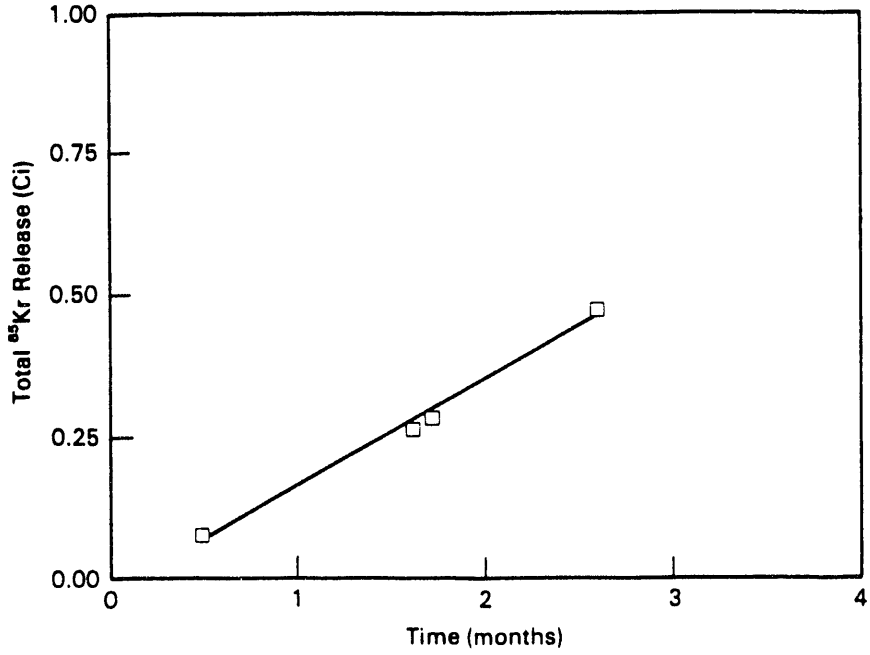

FIGURE 3.5. Release of Krypton-85 Fission Gas During the REA-2023 BWR Cask Performance Test

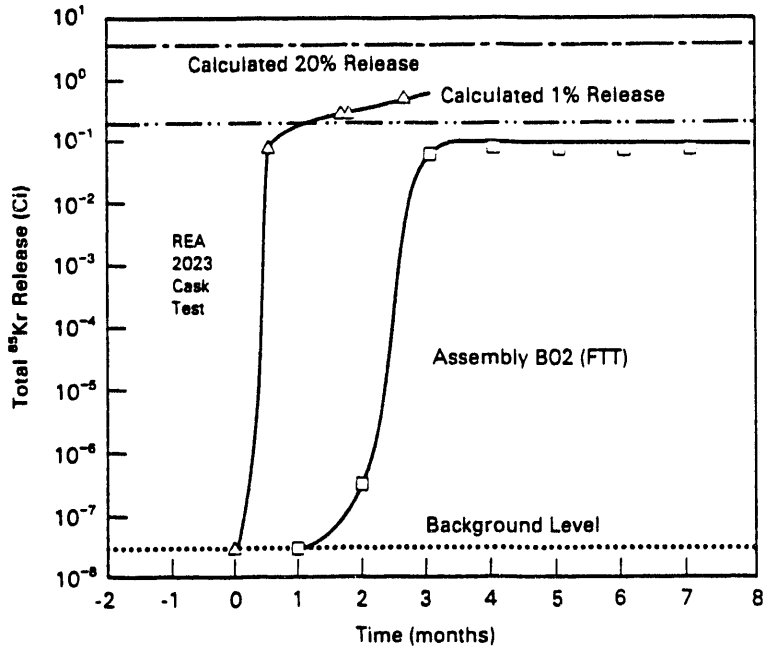

FIGURE 3.6. Comparison of Krypton-85 Fission Gas Release During the REA-2023 BWR Cask Performance Test and the Fuel Temperature Test

the release observed in the cask test. The krypton levels observed in the cask test are less than that expected for a single fuel rod with 20% release of 85Kr from the fuel. The krypton levels in the FTT were less than that from a fuel rod with 1% release. The higher release of 85Kr during the cask test would be consistant with that expected from failure of a corner rod that probably experienced higher power during reactor operation. If the background level from the FTT is also used with the cask test data, it appears that the release of fission gas from both tests would have similar behaviors. With increasing time, the release of krypton in the cask would probably have decreased as indicated by the curve for the FTT data. The difference in release rates during the first few months of testing in the REA cask and the FTT may have resulted from difference in the size of the defects or in the number of failed rods.

There was no confirmation of a leaking fuel rod either by visual inspection or sipping of the fuel assemblies after the cask test. An extremely small defect may have opened up, perhaps at a previous cladding crack. The LLNL gas analyses provided the only indication of a leaking fuel rod. In any

event, leaking fuel rods had no impact on the basin operation or handling of the fuel assemblies subsequent to the cask test.

During the performance test with the TN-24P cask loaded with unconsolidated fuel, the amount of 85Kr detected during test runs 4 and 5 (samples 4D-PT and 5D-PT, Table 3.5) indicated a leaking fuel rod was present during this portion of the test. The relatively low amounts of 85Kr in the other samples are what would be expected to result from crud, not a leaking fuel rod. The increase in 85Kr content coincides with the cask being rotated from vertical to horizontal, which suggests that a fuel rod(s) may have started leaking because of the change in position. The decay in the leak rate, sample 5D-PT being less than sample 4D-PT and sample TN-1B being less than the previous two samples, indicates that the leak was small (or most of the gas had already been lost) and took several days to vent the gas from the fuel rod(s).

In May 1987, 36 of the 48 intact fuel assemblies in the TN-24P and MC-10 casks (see Table 3.3) plus 12 intact assemblies that had been in the Turkey Point Reactor were consolidated into 24 consolidated fuel canisters as part of INEL's Dry Rod Consolidation Technology Project. The consolidated fuel canisters were placed in the TN-24P cask. The remaining 12 intact assemblies from the TN-24P and MC-10 cask were placed in the MC-10 cask. Gas samples taken from the MC-10 cask after dry rod consolidation suggest that there were no leaking fuel rods in the MC-10 cask.

During the fuel rod consolidation process, the exhaust gases from the consolidation area were monitored to detect the release of radioactive gases from the fuel that would indicate a cladding failure. One of the conclusions reached was that all fuel rods from the 48 assemblies were pulled and canisterized without rod failures. Pulling forces and rod profiles were recorded during the consolidation process. The minimum and maximum breakaway forces were 80 and 350 Newtons (8.2 and 35.8 kgf), respectively. The average X- and Y-diameters were 10.669 and 10.668 mm. The as-fabricated fuel rod diameter was 10.719 $\pm$ 0.0025 mm, indicating there was fuel rod cladding creep-down (Vinjamuria 1988b).

As can be seen from Table 3.6, significant amounts of 85Kr were released from the consolidated fuel in the TN-24P cask. Additional test data that permitted calculations of the cumulative release of 85Kr are given in Table 3.7. The cumulative release of 85Kr is shown in Figure 3.7. The single-rod release of 85Kr for a PWR rod is based on a combination of ORIGEN2 predictions of total 85Kr gas available and experimental measurements. The experimental measurements indicated that no more than 0.5% of the available 85Kr gas was

TABLE 3.7. Release of 85Kr in the TN-24P Cask Loaded with Consolidated Fuel

Sample Number	Estimated Cask Gas Temperature°C	Cask Gas Volume m^3	Cask Pressure mBar	Kr-85 Concentration				Gas Residence Time, days
				Sample, nCi/cc		Cask, Ci		
				Screen	CPP	Screen	CPP	
Pretest	150	2.61	1500	86.32		0.231	0.000	80.00
A1-PT	150	2.61	1500	24.53	21.30	0.066	0.057	4.79
A2-PT	190	2.61	1500	7.68	6.00	0.019	0.015	4.65
A4-PT	150	2.61	1500	2.10	1.30	0.006	0.003	4.69
A5-PT	200	2.61	1500	7.17	4.50	0.017	0.011	5.75
A7-PT	150	2.61	1500	17.13	14.10	0.046	0.038	6.05
Post Test	150	2.61	1500	118.00	69.89	0.316	0.187	161.00
Pre VSC-17	140	2.61	1500	139.00	100.80	0.381	0.276	1288.00

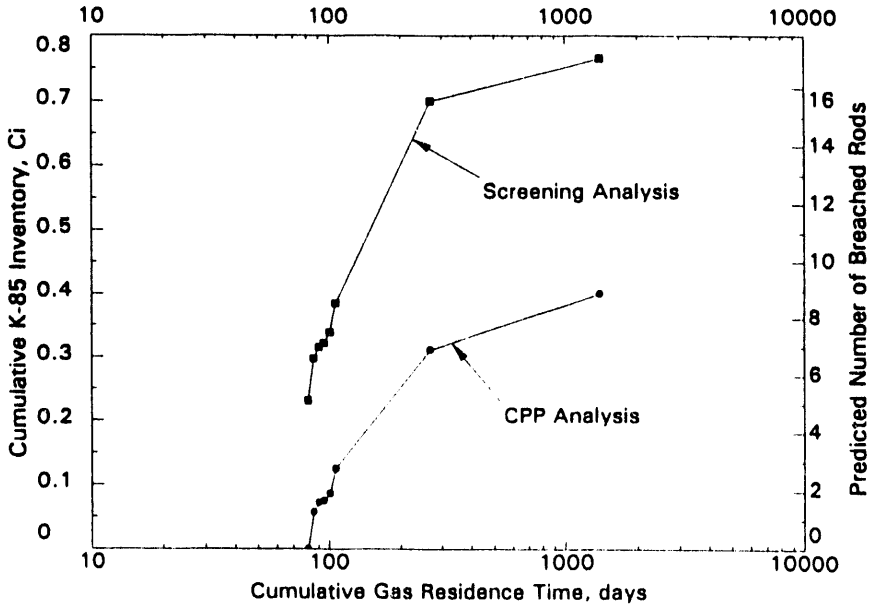

FIGURE 3.7. Cumulative Release of 85Kr Gas from the TN-24P Cask Loaded with Consolidated Fuel

released. The rest of the gas was captured in the fuel (Barner 1985, Guenther 1988). For the fuel used in the testing, the expected single rod release of 85Kr would be between 0.034 and 0.056 Ci. An average value of 0.045 Ci has been used for determining the number of breached rods in Figure 3.7. Figure 3.7 accounts for most of the time helium or nitrogen backfills were in the cask, from the time the cask was fully loaded with consolidated fuel until 6 months after the TC lances were removed at the end of testing. The 85Kr release shown in Figure 3.7 does not include any 85Kr that may have been released during the vacuum runs. The data indicates that four or more rods may have developed leaks before TC lance insertion before testing, three or more rods during testing, and another 5 in the six months after testing.

The amount of 85Kr released during and after the TN-24P cask performance test with consolidated fuel is significantly higher than that released in previous cask testing with unconsolidated fuel. Before this test, four cask performance tests of similar duration and scope had been performed; only two indications of 85Kr release were observed. The magnitude of the releases in the previous tests and surveillance periods indicated that each was limited to a single rod cladding breach. The previous tests involved about 16,700 spent fuel rods, whereas this test involved about 9800 rods. It is hypothesized that the greater magnitude of 85Kr released in this test and post-test surveillance is because of additional cladding leaks caused by enlargement of incipient cladding flaws during pulling and flexing of the fuel rods during the consolidation process. The enlarged cladding flaws combined with cladding creep during cask testing and surveillance periods allowed leak paths to develop. The leakage has not affected operations.

4.0 COMPUTER CODE DESCRIPTIONS

Two thermal hydraulic computer codes have been used to support cask performance tests by simulating the thermal performance of spent fuel storage cask systems, COBRA-SFS and HYDRA. Both of these codes predict the steady-state three-dimensional thermal performance of the system based on finite difference solutions of the governing equation that define conservation of mass, momentum, and energy. A brief description of each code is included in this section. Additional details on the codes can be found in the individual performance reports (Creer 1986; McKinnon 1986, 1987a, 1987b, 1989, 1992) or in the code manuals (Rector 1986a, 1986b; Lombardo 1986; McCann 1987a, 1987b, 1987c). Both codes have undergone extensive review by the NRC for use in storage cask thermal performance analysis.

4.1 COBRA-SFS CODE DESCRIPTION

The COBRA-SFS (spent fuel storage) thermal hydraulics computer code has been used to simulate a wide range of dry spent fuel storage systems including single assembly and multiassembly systems, and ventilated concrete systems. The analysis has considered vertical and horizontal cask orientations, various backfill gases, and intact or consolidated spent fuel. The code contains thermal-hydraulic models for pressure drop, turbulent mixing, diversion cross-flow, buoyancy-induced flow recirculation, conduction, convection, and radiation heat transfer.

COBRA-SFS predicts steady-state three-dimensional velocity, pressure, and temperature distributions within spent fuel storage systems. The code uses an iterative procedure to solve finite-difference equations for mass, momentum, and energy conservation for an interconnected array of channels and structural members. Empirical relationships are used when needed to close the set of equations. The code uses subchannel representations with arbitrary flow and thermal connections; therefore, the user has a great deal of flexibility in modeling complex geometries. Although COBRA-SFS assumes that the fill medium is incompressible, it uses a thermally expandable model to produce buoyancy-driven circulating flows within the system. Heat is transported

throughout the system by conduction (fluid-to-fluid and solid-to-solid), natural convection, and planer radiation (rod-to-rod, rod-to-surface, and surface-to-surface).

The COBRA-SFS code is a steady-state lumped-parameter finite-difference computer code that predicts flow and temperature distributions in spent fuel storage systems and fuel assemblies under mixed and/or natural convection conditions. Derived from the COBRA family of codes, which have been extensively evaluated against in-pile and out-of-pile data, COBRA-SFS retains all the important features of the COBRA codes and extends the range of application to problems with two-dimensional radiation and conduction heat transfer. This capability permits analyses of single- and multi-assembly spent fuel storage systems with unconsolidated or consolidated fuel with a variety of fill media.

The energy equations for the coolant, rod cladding, fuel, and structural members are solved implicitly by iteration. Axial conduction in the structural members is considered. The radiation heat transfer model assembles a nonparticipating media and gray body radiation. It also allows two-dimensional radiant heat exchange among all solid members in an enclosure and is iteratively coupled to the rod and wall energy equations.

The flow field may be either user-prescribed or internally calculated as a function of the gravitational and dynamic pressure losses. Specifications of heat losses from the boundary may vary circumferentially and/or axially, and can include both radiation and convection heat transfer. Axial heat transfer from the subchannel model to plenum regions (regions above and below the fuel assemblies) can also be modeled.

4.2 HYDRA CODE DESCRIPTION

The HYDRA steady-state thermal hydraulics computer code is fully three-dimensional with user-oriented input. The governing equations in HYDRA that define the conservation of mass, momentum, and energy are solved using finite-difference formulations. The equations apply to single-phase, compressible flow. The momentum equation includes convection of momentum, Darcy drag, and orifice drag, and gravitational, pressure, and viscous force terms. Coupled heat transfer modes of conduction, convection, and radiation are accounted for

in conjunction with volumetric heat generation. Rod-to-rod and enclosure radiation models can be constructed by input. There is a significant degree of flexibility in specifying temperature boundary conditions. Output consists of steady-state temperatures, pressures, and velocities. The time-dependent conservation of energy equation with convection and heat sources is the basis for calculating the temperature field.

HYDRA uses a Cartesian coordinate system for the computational mesh in the inner cask cavity (fuel basket region). A cylindrical coordinate system is available for convenience in calculating temperatures in the surrounding cask body. When both coordinate systems are invoked to model a cask, the code will automatically align the two systems and enforce conservation of energy at their interface.

HYDRA has been designed to provide a user-oriented input interface, which eliminates the need for internal code changes. Any application for which the code is an appropriate choice can be completely described through the construction of an input file. The user may optionally request a formatted echo of the input file to confirm that the intended parameters are actually those used by the code. A selectable commentary monitoring the progress of the code toward a steady-state solution is available as well as a summary of energy balances. Finally, a tape may be written at the conclusion of a run, if the user wishes to restart the solution from its most recent point.

4.3 CODE PERFORMANCE

A summary of code performance is given in Table 4.1. The pretest predictions were completed before performance testing of the cask. The modeler had access to cask materials, design dimensions, and predicted decay heat output from the fuel. After a comparison to measured temperatures, the code input was modified to reflect better understanding of as-built dimensions of the cask, heat transfer coefficients, and fuel models. The post-test predictions reflect changes made to the models. Table 4.1 briefly lists the post-test model changes.

TABLE 4.1. Summary of Code Prediction Performance

CODE	CASK	Test Date Month/Year	Peak Temperature Range Measured, °C	Prediction Accuracy			
				Pretest		Post-Test	
				Profile	Peak	Profile	Peak
HYDRA	REA-2023	12/84-3/85	110-241	40	35	-	25
	CASTOR-V/21	9/85	347-395	60	48	25	-
COBRA-SFS	REA-2023	12/84-3/85	110-241	30	-	-	-
	TN-24P	1/86-2/86	206-266	38	19	30	16
	MC-10	6/86-7/86	130-212		30	35	26
	TN-24P[a]	1/88-2/88	205-280	34	34	26	13
	VSC-17[a]	10/88-12/90	312-392	15	15	-	-

(a) Consolidated fuel.

REA 2023 - HYDRA

Reviews of predictions and data support the conclusion that the surface-to-ambient heat transfer cannot be modeled accurately by conventional correlations. Conventional correlations result in conservatively high surface temperature predictions. Lacking meaningful improved correlation, measured surface temperatures were used in the post-test analysis.

The gaps between the copper conduction strips, the basket support structure, the copper shell of the basket, and the lead and cask body were not well defined. Modifications were made in the associated contact resistance based on observed temperature drops.

REA-2023 - COBRA-SFS

Changes were made in the fuel heat transfer model from a symmetric to an asymmetric rod heat flux model and the plenum regions were modified. The plenum film heat transfer coefficient was decreased by an order of magnitude in the post-test analysis.

CASTOR-V/21 - HYDRA

Three refinements to the input files were found to be uniformly warranted: 1) the exterior cask surface convection heat transfer coefficient was

increased; 2) the gap between the basket and the cask inner wall was reduced; and 3) the drag coefficients for flow channels between basket fuel tubes were added.

TN-24P - COBRA-SFS

A thorough comparison of the pretest predictions with data found the shape of the axial temperature profiles to be of concern. Consistent differences in all six simulations were noted, and the investigation led to the following model changes for the post-test simulations:

- Axial conduction was added to the aluminum basket. It had been neglected in the pretest analysis because of potentially large contact resistance at the basket plate interfaces.
- The plenum models at the bottom of the cask were modified to better model conduction of heat from the cask to the rail car.
- The modified surface-to-ambient heat transfer correlation was adjusted in the post-test simulations.

MC-10 - COBRA-SFS

In the post-test predictions, changes were made in basket-to-cask gap conductivities based on as-built measurements, input errors were corrected, and the surface emissivities values of several components were changed.

TN-24P loaded with consolidated fuel - COBRA-SFS

A more refined fuel model was used in the post-test predictions. The pretest fuel model incorporating two rings with 5 nodes was replaced with a model using 13 nodes and more concentric rings.

VSC-17 loaded with consolidated fuel - COBRA-SFS

No post-test analysis was performed.

5.0 DRY STORAGE PERFORMANCE TESTS

Cask performance tests consisted of 6 to 14 runs involving one or two loadings, usually three backfill environments, and one or two cask orientations. A test plan specified the order of the runs, spent fuel assembly load patterns, temperature and dose rate measurement locations, calibration requirements, and gas and crud sampling intervals. The test plan also addressed cask handling and fuel assembly characterization activities that were required before and after performance testing.

This section of the report contains a description of the dry spent nuclear fuel storage systems followed by a summary of the thermal and shielding performance of each system. The section concludes with some observation concerning cask/system handling.

5.1 CASK DESCRIPTIONS

Six spent nuclear fuel dry storage systems are briefly described. Table 5.1 gives a summary of the storage systems. Additional details on each of the systems are found in Appendix A.

REA 2023 Cask

The REA 2023 (McKinnon 1986; Wiles 1986) spent fuel storage cask consists of a double containment design with silicone rubber O-rings for sealing the primary lid of the inner cavity and a welded final closure on the secondary cover. The REA 2023 cask is shown in Figure 5.1. The cask has a smooth, painted, stainless steel outer skin; a lead/stainless steel gamma shield; and a water/glycol neutron shield. The fuel basket is constructed of stainless steel for criticality control, copper plates to conduct heat to the cask wall, and stainless steel for structural strength. The loaded cask is approximately 4.9 m (16 ft) tall, measures 2.22 m (7.3 ft) in diameter, and weighs approximately 100 tons. The basket is configured to hold 52 BWR spent fuel assemblies. The test fuel assemblies were of the GE 7 x 7 rod design. The REA 2023 BWR spent fuel storage cask design and manufacturing rights have been

TABLE 5.1. Summary of Casks, Baskets, and Fuel Used in the Performance Tests

	Mitsubishi MSF IV REA-2023	Gesellshaft fur Nuklear Services CASTOR V/21	Transnuclear TN-24P	Westinghouse MC-10	Sierra Nuclear Corporation VSC-17	Pacific Nuclear NUHOMS[2]
BODY						
Height, m	5	4.9	5	4.8	5.7	3.7 x 6.7 x 2.4
Diameter, m	2.5	2.4	2.3	2.7	2.7	--
Loaded Weight, tons	100	100	100	100	94	--
Material	SS, Lead	Nodular Cast Iron	Forged Steel	Forged Steel	Concrete with Steel Liner	Concrete
Seals, O-ring	Elastomer and Seal Weld	Elastomer and Metallic	Elastomer and Metallic	Elastomer and Metallic	O-ring/weld	Weld
Gamma Shielding	Lead	Cast Iron	Steel	Steel	Concrete and Steel	Concrete
Neutron Shielding	Liquid	Solid	Solid	Solid	Concrete	Concrete
External Surface	Painted	Painted, Horizontal Fins	Painted	Vertical Fins	Concrete	Concrete
FUEL						
Fuel Type[a]	BWR, GE 7 x 7	PWR, W 15 X 15	PWR, W 15 x 15	PWR, W 15 x 15	PWR, Consolidated	PWR, W 15 x 15
Source of Assemblies	Cooper	Surry	Surry	Surry	Surry & Turkey Point	H. B. Robinson
Burnup, GWD/MTU	24-28	24-35	29-32	24-35	26-35	<35
Cooling Time, yr	2.3-3.4	2.2-3.8	4.2	4.6-10.1	8.8-14.3	5+
Enrichment, wt%	2.5	2.9-3.1	2.9-3.2	1.9-3.2	2.5-3.2	<3.5
Decay Heat						
Assembly, W	235-370	1000-1800	832-919	400-700	700-1050	705-798
Average, W	290	1350	860	530	877	760
Cask Total kW	15.2	28.4	20.6	12.6	14.9	5320
BASKET						
Storage Locations	52	21	24	24	17	7
Basket Material	Stainless and Copper	Stainless	Aluminum	Aluminum and Stainless	Steel	Stainless and Aluminum
Criticality Control	Boral	Borated Stainless Steel	Borated Aluminum and Poison Rods	Boral		Boron Aluminum alloy

(a) GE refers to General Electric; W refers to Westinghouse
(b) Horizontal Storage System

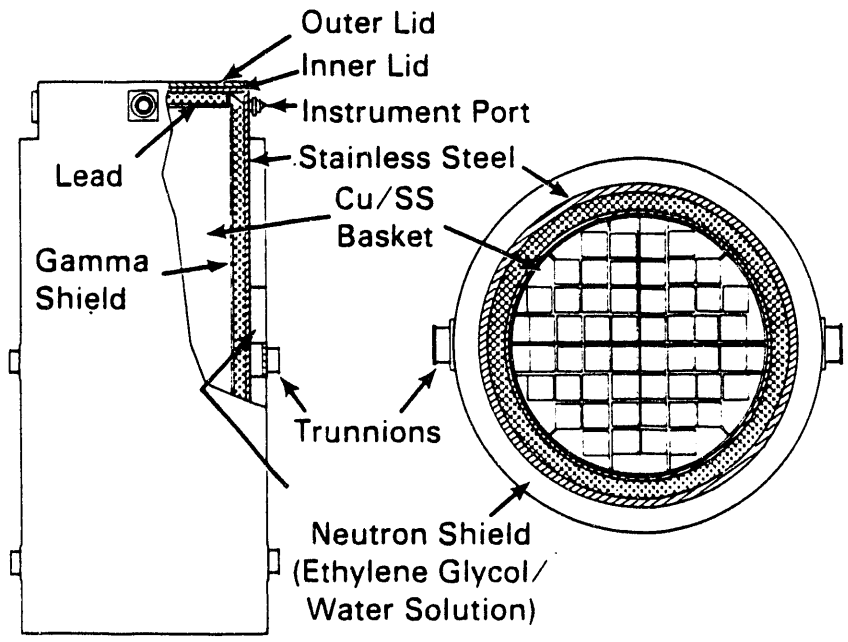

FIGURE 5.1. REA 2023 BWR Cask

acquired by Mitsubishi of Japan, and the cask model designation has been changed to MSF IV. The cask was performance tested at GE-Morris (Illinois) and is currently located at INEL.

CASTOR-V/21 Cask

The Castor-V/21 (Creer 1986) cask body is a one-piece cylindrical structure composed of ductile cast iron in nodular graphite form. The CASTOR V/21 is shown in Figure 5.2. This material exhibits good strength and ductility and provides effective gamma shielding. The overall external dimensions of the cask body include a height of 4.9 m (16 ft) and a diameter of 2.4 m (8 ft). The external surface has 73 heat transfer fins that run circumferentially around the cask, and is coated with epoxy paint for corrosion protection and ease of decontamination.

The spent fuel basket is a cylindrical structure of welded stainless steel plate, and borated stainless steel plate. The basket comprises an array of 21 square fuel tubes/channels that provide structural support and positive positioning of the fuel assemblies. A stainless steel primary lid and secondary lid are provided. The test fuel assemblies were of the Westinghouse

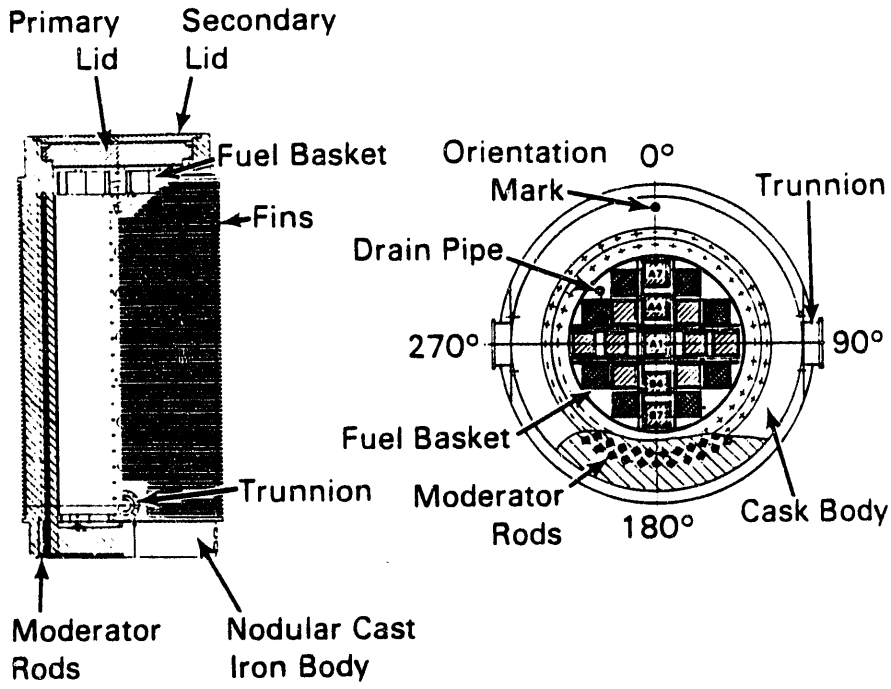

FIGURE 5.2. CASTOR V/21 PWR Cask

15 x 15 rod design. The secondary lid was not used during the CASTOR-V/21 cask performance test because of interference with fuel assembly instrumentation leads. Therefore, dose rates discussed in a later section of this document were obtained on the primary lid's exterior surface. Addition of the secondary lid will greatly reduce measured dose rate values. This cask was performance tested at INEL and demonstrated as part of the VP/DOE Cooperative agreement at VP's Surry Reactor.

TN-24P Cask

The TN-24P (McKinnon 1987a) cask has a forged steel body for structural integrity and gamma shielding, surrounded by a resin layer for neutron shielding, which is enclosed in a smooth steel outer shell. The TN-24P Cask is shown in Figure 5.3. The cask is 5.0 m (16 ft) long and measures 2.3 m (7.5 ft) in diameter; it weighs approximately 100 tons when loaded with unconsolidated PWR spent fuel. The cask has a cylindrical cavity that holds a fuel basket designed to accommodate 24 intact or consolidated PWR fuel assemblies.

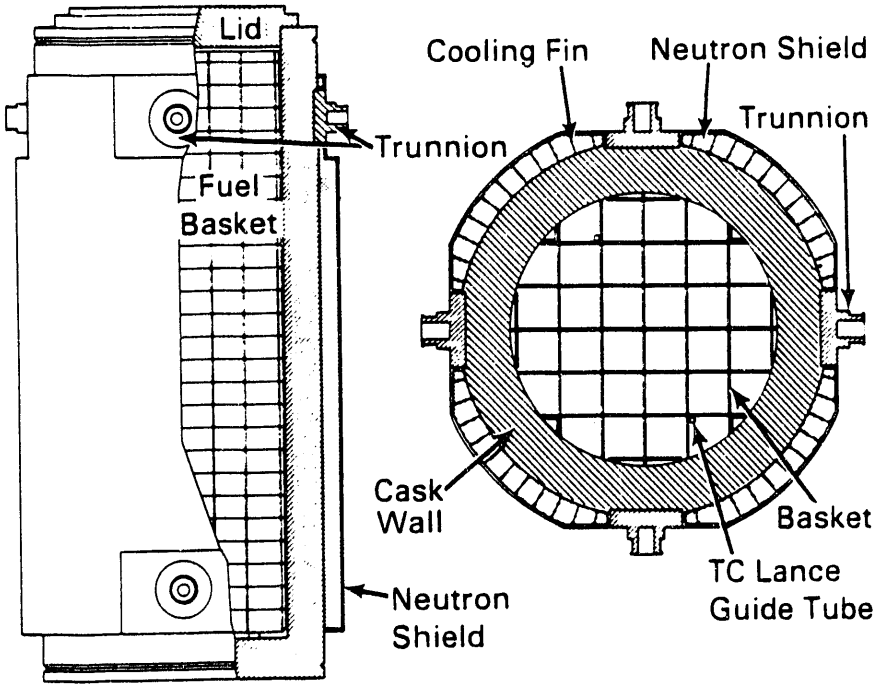

FIGURE 5.3. TN-24P PWR Cask

The basket is made of a neutron-absorbing material, borated aluminum, to control criticality. The cavity atmosphere is designed to be nitrogen or helium at a positive pressure.

The cask is sealed with a single lid. A protective cover, bolted to the body, provides weather protection for the lid penetrations. The test fuel assemblies were of the standard Westinghouse 15x15 rod design. This cask was performance tested at INEL with intact PWR fuel as part of the VP/DOE Cooperative Agreement. It was later performance tested with consolidated fuel by DOE and EPRI.

MC-10 Cask

The MC-10 PWR spent fuel storage cask (McKinnon 1987b) consists of a low-alloy forged steel body. The MC-10 cask is shown in Figure 5.4. The cask is 4.8 m (15.7 ft) long and measures 2.7 m (8.9 ft) in diameter; it weighs approximately 110 tons when loaded with unconsolidated PWR spent fuel. Neutron shielding is around the outside of the cask and vertical carbon-steel heat transfer fins pass through the neutron shield to augment cooling of the

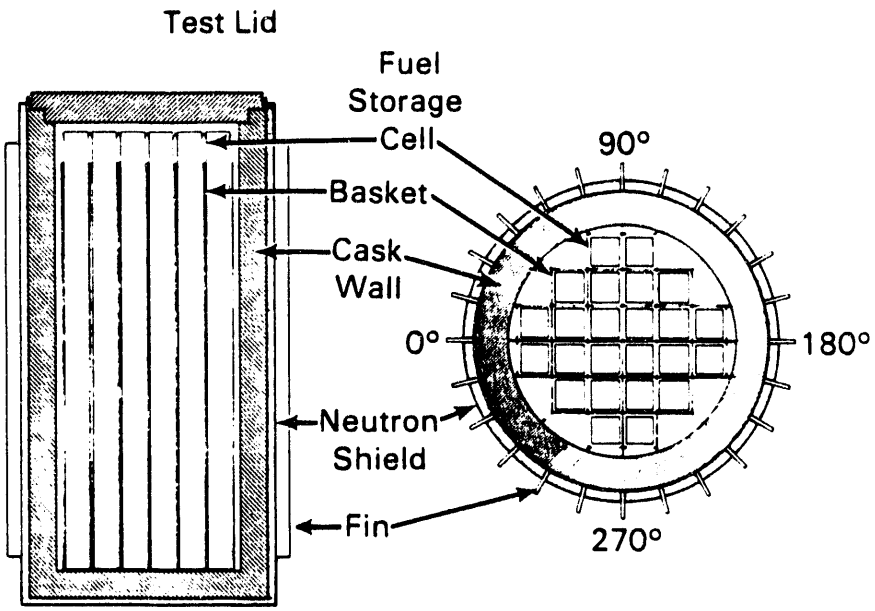

FIGURE 5.4. Westinghouse MC-10 PWR Cask

cask. The fuel basket within the cask is configured to hold 24 PWR spent fuel assemblies or 24 consolidated fuel canisters and is constructed of aluminum. Each of the 24 basket locations contains a removable stainless steel enclosure and neutron poison material for criticality control. The Surry spent fuel assemblies used during testing were of a standard Westinghouse 15 x 15 rod design. The cask is closed with two lids and a seal cover having both elastomer and metallic O-rings to seal the cask cavity from the environment.

The cask lid closure and seal system (LCSS) consists of four covers: shield, primary, seal, and protective covers. The LCSS was replaced with a single test lid for the performance test. The differences between the test lid and the LCSS caused the temperature measured on the surface of the test lid to be higher than it would be on the surface of the LCSS. The lack of a neutron shield and greater steel thickness for the test lid caused the gamma dose rate to be smaller and the neutron dose rate to be higher on the test lid than would be on the outer surface of the LCSS. This cask was tested at INEL and demonstrated at VP's Surry reactor as part of the VP/DOE Cooperative Agreement.

VSC-17 Cask

The VSC-17 spent fuel storage system (McKinnon 1992) is a passive device for vertical storage of 17 assemblies/canisters of irradiated nuclear fuel. The VSC-17 cask is shown in Figure 5.5. The commercial version of the cask is designed to hold 24 PWR fuel assemblies. The VSC-17 system consists of a Ventilated Concrete Cask (VCC) and a Multi-Assembly Sealed Basket (MSB). Decay heat, generated by the spent fuel, is transmitted through the containment wall of the MSB to a cooling air flow. Natural circulation drives the cooling air flow through an annular path between the MSB and the VCC and carries the heat to the environment without undue heating of the concrete cask. The annular air flow cools the outside of the MSB and the inside of the VCC.

The cask weighs approximately 80 tons empty and 110 tons loaded with 17 canisters of consolidated fuel. The VCC has a reinforced concrete body with an inner steel liner and a weather cover (lid). The MSB contains a guide sleeve assembly for fuel support and a composite shield lid that seals the

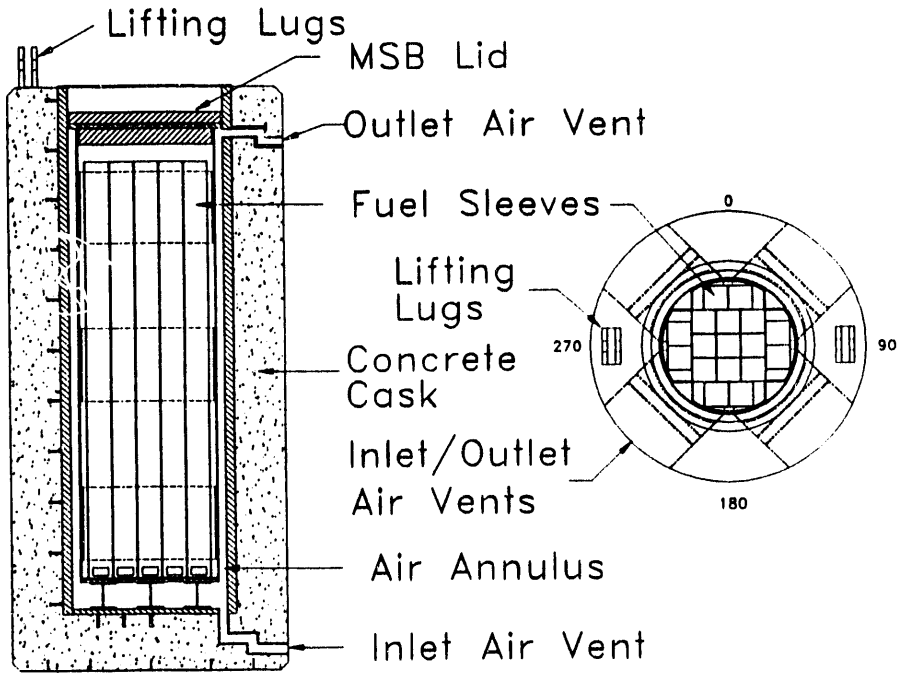

FIGURE 5.5. VSC-17 Cask

stored fuel inside the MSB. The cavity atmosphere is helium at slightly sub-atmospheric pressure. The helium atmosphere inside the MSB enhances the overall heat transfer capability and prevents oxidation of the fuel and corrosion of the basket components.

Consolidated Westinghouse 15x15 PWR spent fuel assemblies were used in the performance test. The performance test was part of a DOE/PSN Cooperative Agreement.

NUHOMS Cask System

The NUHOMS system (Strope 1990) is a passive device for horizontal dry storage of irradiated fuel assemblies. The NUHOMS System is shown in Figure 5.6. The fuel assemblies are confined in a helium atmosphere by a

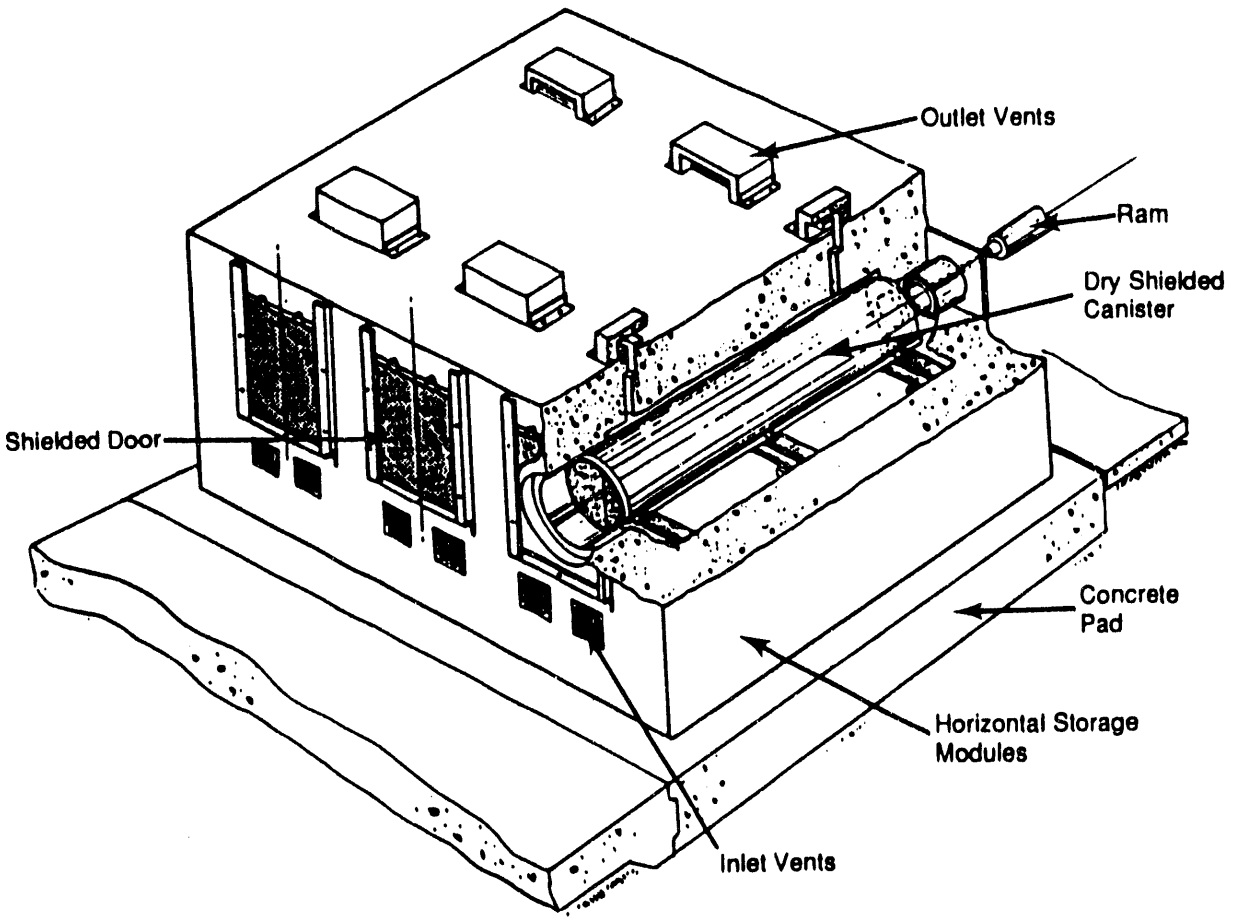

FIGURE 5.6. H.B. Robinson NUHOMS Dry Storage System

stainless steel canister. The dry shield canister (DSC) is protected and shielded by a massive reinforced concrete module. The reinforced concrete structure is roughly 22 ft long, 25 ft wide, and 12 ft high. The walls and roof of the module are approximately 3.5-ft thick, providing the primary biological shield and impact protection for the canister. The generic NUHOMS system consists of a basic unit of two modules arranged back-to-back. The system is expanded with additional two-module units placed beside the first until the required storage capacity is reached.

The demonstrated seven assembly DSC consists of a stainless steel cylindrical shell, which is made of rolled 0.6-in.-thick stainless steel. It has a diameter of 37 in. and is 180 in. long. The internal basket contains seven square fuel tubes made of a boron/aluminum alloy with stainless steel cladding. Commercial systems contain 24 fuel tubes per DSC. The test fuel assemblies were of the standard 15x15 rod PWR design. An IF 300 cask was used to move the dry shield canister from the reactor pool to the concrete storage module. The performance demonstration was conducted as part of a CP&L/DOE Cooperative Agreement.

5.2 THERMAL PERFORMANCE

Cask thermal performance tests consisted of 6 to 14 test conditions involving one or two loadings, usually three backfill environments, and one or two cask orientations. A test plan specified the order of the runs, spent fuel assembly load patterns, temperature measurement locations, and calibration requirements.

Cask thermal instrumentation consisted of 71 to 106 thermocouples, located in the fuel, the cask basket, or surface of the cask or concrete structure. The locations of the measurement can be inferred from data plots found in Appendix B of this report. The number and locations of thermocouples are listed in Table 5.2. Additional measurement location details are found within the original reports. All of the casks included one or two pressure monitors. The REA cask also included a weather station.

TABLE 5.2. Thermocouple Placements

Metal Cask	Internal			External			Total
	Ambient	Fuel	Basket	Top	Side	Bottom	
REA 2023	1	28	10	4	24	4	71
CASTOR V/21	3	42	12	6	23	6	92
TN-24P	3	42	26	6	23	6	106
TN-24P[a]	3	42	26	5	19	3	98
MC-10	3	42	12	3	22	3	91

Concrete Systems	Air		Fuel Canister			Concrete Structure				Total
	Inlet	Outlet	Canister	Fuel	Basket	Liner	Shield	Concrete	Surface	
VSC-17[a]	7	4	14	36	6	9	-	10	12	98
NUHOMS	2	12	18	10	9	-	10	14	10	85

(a) Performance test using consolidated fuel.

A summary of the core test conditions and peak fuel temperatures is found in Table 5.3. The peak fuel temperatures were estimated by extrapolating from measured temperatures using code predictions. In general, the temperature profiles follow the trends shown in Figure 5.7 (McKinnon 1986:5.36). Nondimensional temperatures in Figure 5.7 were established by subtracting average cask surface temperatures from fuel cladding temperatures and dividing by differences between maximum fuel temperatures and average surface temperatures. The horizontal and vertical vacuum profiles agree closely with one another and also with the measured gamma profile. Convection in the vertical helium and nitrogen runs shift the peak temperature upward in the cask. The larger shift in the nitrogen run is because of greater temperature differences with their associated density changes for nitrogen when compared to helium. The amount of the temperature shift is also related to the openness of the basket and fuel. The horizontal temperature profile was developed using temperature measurements with all three backfill gases. Axial and radial temperature profiles corresponding to the location of the peak temperature are contained in Appendix B. The tests are described in the following subsections.

TABLE 5.3. Peak Temperatures for Fully Loaded Storage System

Metal Casks	Orientation	Backfill	Cask Heat Load, kW		Ambient Temperature, °C	Wind Speed, m/sec	Estimated Peak Clad Temperature, °C
			Design	Actual			
REA 2023	Vertical	Helium	21	14.6	22		144
52 BWR	Vertical	Helium		14.9	-14	0.7	110
Assemblies	Vertical	Nitrogen		15.1	-4	3.1	151
(Hot fuel in	Vertical	Vacuum		15.2	24		227
center of	Vertical	Vacuum		15.2	-10	3.6	200
basket)	Horizontal	Helium		14.8	-8	4.2	113
	Horizontal	Nitrogen		15.0	-4	2.0	164
CASTOR V/21	Vertical	Helium	21	28.4	27		352
21 PWR	Vertical	Nitrogen		28.4	24		368
Assemblies	Vertical	Vacuum		28.4	25		424
(Hot fuel on	Horizontal	Helium		28.4	24		365
outside of	Horizontal	Nitrogen		28.4	24		405
basket)							
TN-24P	Vertical	Helium	24	20.6	18		221
24 PWR	Vertical	Nitrogen		20.6	20		241
Assemblies	Vertical	Vacuum		20.6	20		290
(Hot fuel in	Horizontal	Helium		20.5	18		215
center of	Horizontal	Nitrogen		20.4	21		256
basket)	Horizontal	Vacuum		20.3	19		280
24 PWR	Vertical	Helium	24	23.3	22		211
Canisters[a]	Vertical	Nitrogen		23.3	16		268
(Hot fuel on	Vertical	Vacuum		23.2	22		293
outside of	Horizontal	Helium		23.2	17		205
basket)	Horizontal	Nitrogen		23.2	22		252
	Horizontal	Vacuum		23.1	23		282
	Horizontal	Vacuum		23.1	24		282[b]
MC-10	Vertical	Helium	15	12.7	28		139
24 PWR	Vertical	Nitrogen		12.7	24		181
Assemblies	Vertical	Vacuum		12.6	23		217
(Hot fuel on	Horizontal	Helium		12.6	25		138
outside of	Horizontal	Nitrogen		12.6	26		204
basket)	Horizontal	Vacuum		12.6	27		213
Concrete Systems						Heat Source	
NUHOMS	Horizontal	Helium	7	5.3	21	7 PWR Fuel	181
(Random load	Horizontal	Helium	7	7	23	Electricity	201
of hot fuel)	Horizontal	Helium	7	13	19	Electricity	333
Block Inlets	Horizontal	Helium	7	7	28	Electricity	321
						Vent Blockage	
VSC-17	Vertical	Helium	17	14.9	21	None	321
17 PWR	Vertical	Nitrogen		14.9	24	None	376
Canisters[a]	Vertical	Vacuum		14.9	24	None	397
(Hot fuel in	Vertical	Helium		14.9	23	1/2 Inlets	334
center of	Vertical	Helium		14.9	23	All Inlets	378
basket)	Vertical	Helium		14.9	22	All Vents	381

(a) Consolidated fuel - 2:1 Consolidation ratio.
(b) The top and bottom of the cask were insulated during this run.

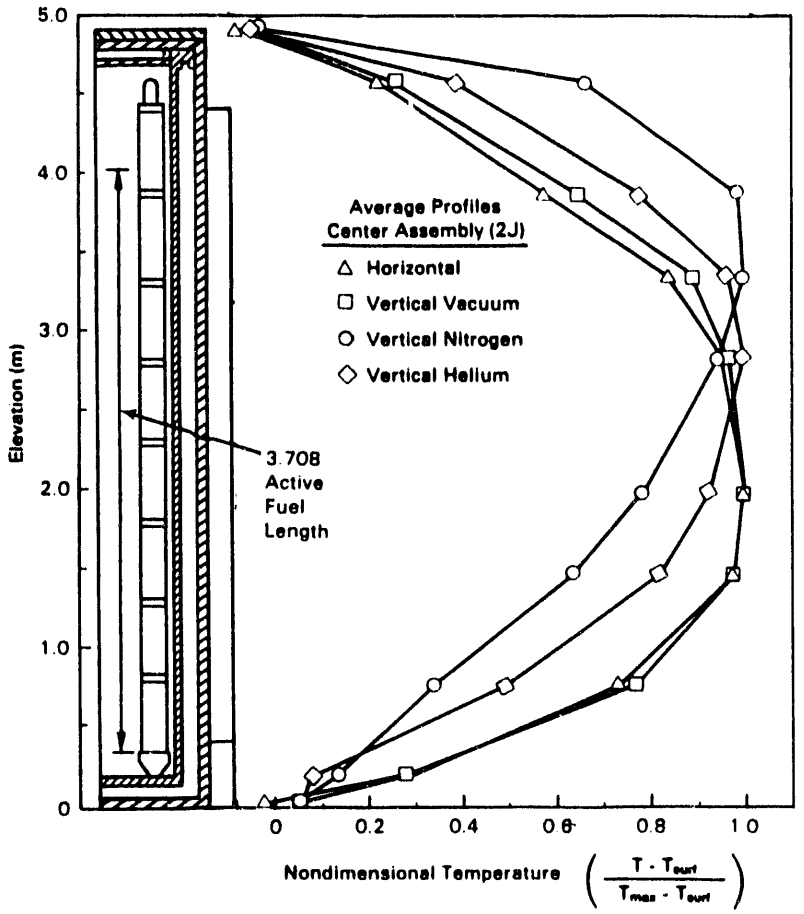

FIGURE 5.7. Effects of Cask Orientation and Fill Gas on Cask Axial Temperature Profiles

REA 2023

Based on pretest calorimetry, fuel assembly decay heat rates averaged 310 W/assembly to produce a total initial heat load in the cask of 15 kW (Table 5.3). Assembly decay heat rates ranged from 250 W to 390 W. The hotter fuel assemblies were located in the center of the basket, and the cooler assemblies were in the outer basket locations.

The cask test matrix included assessments of performance under conditions of partial and full loadings (28 and 52 assemblies), vertical and horizontal cask orientations, and three internal backfill environments (vacuum, nitrogen, and helium). Details concerning the partial load performance are found in McKinnon 1986. The final three test runs were conducted with the

neutron shield insulated to elevate cask surface temperatures beyond those expected during summer months. Results of the performance test runs and for the fully loaded uninsulated cask and for the various fill conditions and cask orientations are summarized in Table 5.3.

Measured peak cladding temperatures were 86°C, 118°C, and 170°C for a vertical, partially loaded cask (28 assemblies) at similar ambient temperatures with helium, nitrogen, and vacuum backfill environments, respectively. With the partially loaded cask oriented horizontally, corresponding peak cladding temperatures with helium and nitrogen backfills were 93°C and 116°C, respectively. Note that each peak temperature corresponds to a different ambient temperature.

Measured peak cladding temperatures with the cask fully loaded were higher than partial load temperatures. Vertical helium, nitrogen, and vacuum peak cladding temperatures at similar ambient temperatures were 110°C, 146°C, and 200°C, respectively. Corresponding horizontal helium and nitrogen temperatures were 113°C and 164°C, respectively. Insulation on the cask neutron shield resulted in vertical, full-load temperatures in helium, nitrogen, and vacuum of 185°C, 209°C, and 241°C, respectively.

GNS CASTOR V/21

Based on pretest ORIGEN2 predictions, fuel assembly decay heat generation rates totaled approximately 28 kW at the start of testing and 27 kW at the end of testing (Croff 1980). Thirteen of the twenty-one fuel assemblies had decay heat rates near 1 kW; the remaining eight assemblies had decay heat rates of approximately 1.8 kW at the start of the month-long test. The fuel assemblies were loaded in the cask with the hot assemblies in the outer regions of each quadrant. The selected fuel loading pattern was predicted to create a relatively flat radial temperature profile across the basket during testing.

The cask test matrix included assessments of performance with a full load of fuel (21 assemblies), vertical and horizontal cask orientations, and vacuum, nitrogen, and helium backfill environments.

Table 5.3 indicates that in a vertical cask orientation with nitrogen and helium backfills, peak cladding temperatures were less than the 380°C allowable. This was also the case for the horizontal helium test run. The vertical vacuum and horizontal nitrogen test runs resulted in peak cladding temperatures over 380°C, but not exceeding 425°C. None of the peak temperatures occurred in the high decay heat (1.8 kW) outer assemblies. In general, the cask heat transfer performance was concluded to be exceptionally good because it exceeded design expectations with the peak temperature in helium when the cask was dissipating approximately 28 kW. The peak temperature with 28 kW was less than that specified for the cask operating limit of 21 kW in the cask topical safety analysis report.

TN-24P

Loaded with unconsolidated fuel. Based on pretest ORIGEN2 predictions, fuel assembly decay heat generation rates totaled approximately 20.6 kW at the start of testing and 20.3 kW at the end of testing. The decay heat output of the assemblies ranged from 845 to 919 watts with an average output per assembly of 860 watts at the start of testing. The fuel assemblies had cooling times of 50 months at the start of testing. The load pattern placed the hot assemblies in the center of the basket and the cooler assemblies around the outside. This load pattern was selected to maximize fuel temperatures.

The cask test matrix included assessments of performance with a full load of fuel (24 assemblies), vertical and horizontal cask orientations, and vacuum, nitrogen, and helium backfill environments. The test matrix and corresponding measured peak guide tube temperatures and estimated peak cladding temperatures are presented in Table 5.3.

Table 5.3 indicates that peak cladding temperatures were less than the 380°C allowable for all fill gases and cask orientations tested. In general, the cask heat transfer performance was determined to be exceptionally good because the difference between the ambient and the peak cladding temperature in helium and nitrogen, when the cask was dissipating approximately 21 kW, was 100°C less than specified for the cask operating limit of 24 kW in the cask topical safety analysis report.

Loaded with consolidated fuel. A second series of tests was performed using the TN-24P cask loaded with 24 canisters of consolidated fuel. Based on pretest ORIGEN2 predictions, fuel rod decay heat generation rates totaled approximately 23 kW during testing. The decay heat output of the canisters of consolidated rods ranged from 700 to 1180 W with an average output per canister of 970 W at the start of testing. The fuel rods had cooling times of 6 to 12 years. The fuel loading pattern was expected to create a relatively flat radial temperature profile across the basket during testing with the cooler fuel canisters in the center of the basket and the hotter fuel canisters around the outside.

The cask test matrix included assessments of performance with a full load of consolidated fuel (24 canisters), vertical and horizontal cask orientations, and vacuum, nitrogen, and helium backfill environments. The test matrix and corresponding measured peak guide tube temperatures and estimated peak cladding temperatures are presented in Table 5.3. Peak cladding temperatures were estimated by using calculated guide tube-to-hot rod temperature differences from the COBRA-SFS computer code.

Table 5.3 indicates that peak cladding temperatures for all fill gases and cask orientations tested were less than 300°C. In general, the cask heat transfer performance was concluded to be exceptionally good, because the difference between the ambient and the peak cladding temperature in helium and nitrogen, when the cask was dissipating approximately 23 kW, was 100°C less than specified for the cask operating limit of 24 kW in the cask topical safety analysis report.

MC-10

Based on pretest ORIGEN2 predictions, fuel assembly decay heat generation rates totaled approximately 12.6 kW at the start of testing. The decay heat output of the 24 fuel assemblies at the beginning of testing ranged from 400 to 700 W with an average of 530 W. The cask was designed to accommodate fuel assemblies with an average decay heat output of 625 W or consolidated fuel canisters with 1250-W output. The fuel assemblies were loaded so the cooler assemblies were in the center of the cask and the hotter assemblies

were around the outside. The selected fuel loading pattern was predicted to create a relatively flat radial temperature profile across the basket during testing.

The cask test matrix included assessments of performance with a full load of fuel (24 assemblies), vertical and horizontal cask orientations, and vacuum, nitrogen, and helium backfill environments. The test matrix and corresponding measured peak guide tube temperatures and estimated peak cladding temperatures are presented in Table 5.3.

Table 5.3 indicates that peak cladding temperatures were more than 160°C less than the 380°C allowable for all test runs. The peak temperatures for the vacuum and nitrogen runs occurred in the hot assemblies (outer assemblies). In the helium runs, peak measured temperatures were located in a center assembly. In general, the cask heat transfer performance was determined to be exceptionally good because the peak measured temperatures in the cask, when the cask was dissipating approximately 12.6 kW, were 40 to 100°C less than anticipated based on an analysis presented in the cask topical safety analysis report.

VSC-17

Based on pretest ORIGEN2 predictions, fuel rod decay heat generation rates totaled approximately 14.9 kW during testing. The decay heat output of the canisters of consolidated rods ranged from 700 to 1050 W, with an average output per canister of 875 W at the start of testing. The fuel assemblies had cooling times of 9 to 15 years. The fuel loading pattern was expected to create a temperature profile that is peaked in the center; the hottest canisters of fuel were loaded in the center of the cask with cooler canisters of fuel loaded around the outside.

The cask test matrix included assessments of cask performance with a full load of consolidated fuel (17 canisters) for four ventilation blockage conditions and vacuum, nitrogen, and helium backfill environments. All tests were performed with the cask in a vertical orientation. The test matrix and corresponding measured peak temperatures and estimated peak cladding temperatures are presented in Table 5.3.

The data in Table 5.3 indicate that peak cladding temperatures for all fill gases and ventilation blockage conditions tested were less than 400°C. In general, the cask heat transfer performance was concluded to be good. The peak concrete temperatures were less than 72°C and were fairly insensitive to partial blockage of the inlet vents, and the peak fuel temperatures were less than 316°C for unblocked operation with a helium backfill and 15 kW in the cask.

NUHOMS

The NUHOMS system heat transfer test consisted of eight electrically heated test runs followed by two test runs with spent PWR fuel in the storage system. The first three electrically heated test runs were conducted with the DSC in the IF-300 transfer cask to evaluate the performance of the DSC/cask combination from the time it was loaded in the pool through vacuum drying of the DSC and during backfilling with helium in preparation for transfer to the horizontal storage module (HSM). Next, five electrically heated test runs were conducted with the DSC in the HSM to evaluate the performance of the dry storage system. These test runs simulated both the normal performance of the NUHOMS system and off-normal performance for air inlet/outlet blockages and higher decay heat levels.

The first heater test run in the HSM was designed to simulate the normal operation of the NUHOMS system. It was run with an electrical output simulating 1 KW per assembly, or a total of 7 KW per DSC. This was followed by a run with the air inlets to the HSM blocked. Then the outlets to the HSM were also blocked. The final heater test runs were performed at high and low power levels, 13 KW and 2 KW, respectively. Following the heater test runs, three DSCs were loaded with spent PWR fuel and placed in the HSM storage modules.

Table 5.3 summarizes the peak temperatures measured for several of the test runs. Appendix B gives additional temperature data. Ambient temperatures are also indicated. The electrically heated test runs conducted in the IF-300 cask simulated loading, vacuum drying, and backfilling the cask with helium. The temperature of the center fuel sleeve of the DSC basket increased from 50°C with the canister filled with water to 255°C during vacuum drying.

At the conclusion of the vacuum drying process, the canister was backfilled with helium and the peak temperature dropped to 138°C.

Following the electrically heated test runs conducted in the IF-300 cask, the DSC was placed in the HSM and another series of electrically heated test runs were conducted. The first run simulated normal operation of the cask. During normal operation, peak basket, heat shield, and concrete temperatures reached 201°C, 79°C, and 58°C, respectively. Blockage of the air inlet vents increased basket, heat shield, and concrete temperatures about 15°C. However, the temperature difference between the canister and the heat shield did not change appreciably indicating that the heat shield was still being cooled by convection. It appears that blocking the inlet vent did not significantly affect the heat dissipation capability of the module. With the inlet vents blocked, one of the outlet vents acts like an inlet.

The variable power level test runs show expected performance. This was accompanied by an increase in heat shield and concrete temperatures. However, the concrete temperatures were not much different from those for partial blockage. When the power was reduced to 2.2 KW, basket, heat shield, and concrete temperatures decreased as would be expected.

5.3 SHIELDING PERFORMANCE

Neutron and gamma dose equivalent rate measurements were taken on all the storage casks' exterior surfaces. Portable hand-held instruments were used at selected measurement locations on the cask surfaces. A summary of the numbers and locations of the measurements is given in Table 5.4. The thermoluminescent dosimeters (TLDs) and track etch dosimeters (TEDs) are small plastic chips that can be used to determine gamma and neutron dose rates. Their size allowed good definition of dose rate peaks. Experience showed that hand-held instruments did an adequate job of determining peaks, so the TLD/TED measurements were eliminated for the MC-10 cask. The spectral measurements were also eliminated because of the conditions obtained from the other casks showing that the radiation energy spectrum did not change significantly from cask to cask.

TABLE 5.4. Dose Rate Measurement Locations

Cast or System Measurement Locations	REA 2023	CASTOR V/21	TN-24P	TN-24P[(a)]	MC-10	VSC-17	NUHOMS
Cask/System Top							
Portable	19	23	24	16	21	29	33
TLD/TED	18	17	26				
Spectral	1	1	2				
Cask/System Side							
Portable	60	52	52	22	54	51	11
TLD/TED	29	40	49				
Spectral	2	1	2				
Cask/System Bottom or Ends							
Portable	16	12	22	16	14	--	24
TLD/TED	7	12	20				
Spectral	1	1	1				

(a) Performance test using consolidated fuel.

A typical surface dose rate profile is shown in Figure 5.8. System-specific dose rate profiles are found in Appendix C. The values for the various locations are given in Table 5.5. The dose peaks occurred at the end of the neutron shields, vent openings, or at parting planes associated with lids or closures.

Special attention should be given to a comparison of the gamma dose rate values for the TN-24P cask. Removal of the fuel assembly hardware resulted in a reduction of the gamma dose rate at the top of the cask by a factor of 3 to 4. The reduction in dose rate at the bottom of the cask was even more dramatic, on the order of 18 to 48. The hold down springs in the fuel rods provide a gamma source at the top of the cask after the upper end fittings are removed. This gamma source augments the gamma dose from the fuel. At the bottom of the cask the gamma source is primarily from the fuel.

In general, the overall shielding performance of each system was good and met the intended design goal except on the ends or at peaks on the side. With minor design refinements in the gamma and neutron shielding design, total dose rates can easily be reduced to less than the design goals.

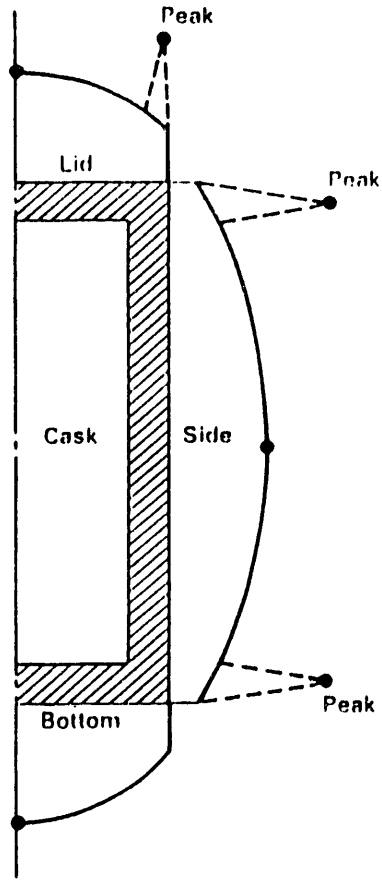

FIGURE 5.8. Representative Surface Radiation Dose Profile for Spent Fuel Storage Casks

TABLE 5.5. Measured Radiation Dose Equivalent (gamma/neutron), mrem/h

Cask or System Measurement Locations	REA 2023	CASTOR V/21	TN-24P	TN-24P[a]	MC-10[a]	VSC-17	NUHOMS
Center of Top	28/10	40/44	60/33[b]	15/32	13/58[b]	10/10	2/<0.5
Peak on Top	71/None	None	None	None	None	30/10	20/<0.5
Upper Peak on Side	37/8	134/15	33/22	11/17	None	70/1	None
Center of Side	14/5	39/16	13/3	7/3	18/18	26/1	2/<0.5
Lower Peak on Side	27/16	140/21	54/43	3/42	None	None	None
Center of Bottom	80/27	22/41	143/64	3/68	75/8	--	--
Front Face							15/2
Back Face							10/1
Design Goal (total)	<20	<200	<60	--	<68	<200	50-200
Design Heat Load, kW	20.8	21	24	24	15	17	7
Actual Heat Load, kW	15	28	21	23	13	15	5

(a) Performance test using consolidated fuel.
(b) Measurements taken without the neutron shield in place.

5.4 SYSTEM HANDLING - LESSONS LEARNED

General lessons learned during the cask handling associated with the performance test are as follows:

- Cask-handling procedures are site-specific, and procedures should be developed for each site. Cask design drawings and specifications, operating and maintenance manuals, and spare parts are helpful in cask-handling. Dry runs of the cask and associated equipment should be performed for all phases of cask handling and loading, including backfilling the cask with a cover gas and gas sampling. Dry (cold) runs with a nonirradiated dummy assembly were valuable in familiarizing personnel with cask-handling characteristics and in finalizing test procedures. Operational tests of project-specific equipment, especially that equipment used for remote operations, allowed problems to be resolved before the equipment was used with irradiated fuel.

- Approximately 1 hour was required to pump a cask down to 1 mbar and backfill with gas to 600 mbar. During a double pumpdown backfill operation, measured guide tube temperatures increased by <20°C during a 2-hour period. It is anticipated that evacuating and backfilling the cask after loading in a water basin will require a longer period and will result in larger temperature increases.

- The cover gas system used to evacuate, backfill, monitor, and obtain gas samples should be carefully designed. The difficulty associated with backfilling the cask with a pure (>99%) cover gas and obtaining gas samples without introducing air should not be underestimated. The cask should be pumped down and backfilled a minimum of two times to ensure purity (>99%) of the final cover gas.

- When loading dry, sealing surface protectors were used by INEL to ensure that crud or particles did not lodge on these surfaces and result in blemishes or scratches that could compromise the finish of the sealing surfaces.

- The method required to rotate the cask from a horizontal to a vertical orientation or vice versa using a center trunion is awkward; the standard method of using a shipping cradle as a pivot base is recommended. Contamination was not a major problem during fuel transfers in air between shipping and storage casks. About 4 total hours of decontamination were required to remove contamination on the personnel work platform between the storage and shipping casks.

- Total personnel exposures during cask testing effort were less than 1.8 man-rem. The exposure at a reactor or storage facility will be even lower because casks will not be incrementally loaded or continuously worked around.

- The cask's basket fuel storage cell openings size and wall smoothness should be designed for removal of fuel assemblies or canisters after extended storage. Allowances should be made for possible warpage and bowing of the fuel. Consideration should be given to formation of ledges or discontinuities that could grab a fuel assembly or canister. (Difficulty was encountered in removing consolidated fuel from the TN-24P cask. One of the canisters of fuel could not be removed.)

- If shielding material is used in cask lids, it should be completely isolated from the internal cask environment to prevent contamination of cask cover gas through off-gassing of the shielding material.

Specific lessons learned during the performance tests are listed below:

REA 2023

- During dry runs and after the primary head was installed under water and the head bolts torqued, it was discovered that the bolts, even though tightened to 27.7 kg m (200 ft lb), would loosen over time. The problem was traced to water trapped in the ends of the bolt holes, making the bolts behave as if they had bottomed out during torquing. When the cask sat for a period of time, the water leaked out through the threads and the bolts loosened. New bolts were procured with holes drilled in the centers to relieve the hydrostatic pressure. This solved the bolt-loosening problem, but left a vacuum-drying problem. The water remaining in the bolt threads during the vacuum-drying process was sufficient to corrode the bolts. The problem was finally solved by removing the cask completely from the water and drying the bolt holes, one at a time with each bolt removed, before finally installing the bolts. Personnel exposure (both neutron and gamma) associated with torquing the head in air on the decontamination pad did not differ significantly from that associated with torquing the head under water, because less time was needed to torque the head in air.

- After the cask was leak tight, it was vacuum dried to remove residual moisture. The vacuum-drying procedure was designed to remove moisture from the cask in such a way that ice was not formed. No effort was required to minimize the vacuum-drying time because of the relatively low heat load in the cask.

- The cask's external surface was decontaminated each time it was removed from the basin. Cask decontamination was performed to remove smearable surface contamination that accumulated on the cask surface during underwater loading and unloading in the basin. The method used to decontaminate the cask was simply manual scrubbing with a detergent and water solution, followed by rinsing and drying. To evaluate the possibility of radioactive contamination leaching from the cask surface, the cask was surveyed when it was

delivered to the storage area (outgoing survey) and when it was returned to the basin area (incoming survey). Any increase in smearable activity over this duration was indicative of leaching of radioactive material out the surface.

- The outer surface of the cask is made entirely of stainless steel; that portion of the cask comprising the neutron shield tank is painted. This was done to ease the decontamination effort and to improve the emissivity of the surface. The painted area of the cask could usually be decontaminated with a reasonable effort, except when the paint softened as a result of higher surface temperatures. During insulated cask test runs, the paint became very soft and the insulation stuck to the paint. From conversations with Carboline, the paint is supposed to be hard and stable to over 235°C when properly cured. Apparently, the paint was not properly cured and, because the cask was wrapped with insulation, the insulation adhered to the surface. When the insulation was removed, it separated, and part of it remained embedded in the paint. This made the surface fuzzy, and it had to be hand-scraped with razor blades several times to remove the fuzz. However, the cask was successfully decontaminated after it was finally unloaded, without having to remove the paint. After the conclusion of the performance test, the cask was shipped to INEL. Over a period of time, the surface of the cask developed smearable radiation and the surface of the cask was painted to fix it.

- The REA 2023 cask interior was decontaminated to below Class A licensing limits by flushing it with water, even when a small leak was present in a fuel rod. Significant amounts of crud were not found in the cask after the fuel was unloaded. The cask exterior can be decontaminated using soap and water in a manner similar to that used for transportation casks.

- Decontamination times for the REA cask after the partial and full loadings were not excessive, and generally required three to four shifts to complete.

CASTOR V-21

- When the cask cavity was pumped down, hot gases removed from the cask tended to soften the vacuum hose near the cask valve tree. Occasionally, the hose would collapse.

- When the cask was backfilled through the valve tree after the pump-down, the gas supply hose collapsed. The vacuum in the cask removed gas from the hose faster than the gas supply system could provide it at the system set pressure.

- When the cask was backfilled, the pressure transducer indicated the gas supply pressure rather than the cask cavity pressure. The transducer was mounted on the valve tree just above the cask lid

disconnect. Operating technicians shut the gas flow off and allowed the system pressure to equalize. If the cavity pressure was not at the desired level, the flow was started and stopped as required to get the desired final pressure.

- The dual elastomer/metallic O-ring sealing technique used in the CASTOR-V/21 cask performed exceptionally well during many repetitive on/off lid operations. Similar high-quality lid gaskets that can withstand repetitive use are desirable if incremental loading is to be performed.

TN-24P

- Minor contamination occurred on the personnel work platform between the casks. About 4 hours of decontamination were required before personnel could continue hands-on work for cask shipping and interim storage activities.

- The fuel assembly grapple lower assembly and tool fingers became highly contaminated after each fuel unloading. The lower assembly was decontaminated and bagged between each use.

MC-10

- Contamination was of the same level as TN-24P.

VSC-17

- During VSC-17 testing, unusual pressure behavior of the internal cask was encountered. The internal pressure was found to increase at a rate that could not be explained by the thermal expansion associated with heating of the gas in the cask, and the change in the gas constituents could not be explained (e.g., increases in hydrogen and organics). As a result, the cask had to be pumped down and back-filled with inert gases several times to maintain backfill gas purity.

  Evaluation of this phenomena determined that the RX-277 neutron shielding in the lid was primarily responsible for the unusual pressure behavior. The initial pressure rise (beyond that expected) was caused by water vapor being driven out of the RX-277 homogeneous mixture during heatup of the cask after fuel loading. The second contributor was hydrogen off-gassing of the RX-277, which was a function of cask temperature increase. The first event was confirmed when water was found in the sediment bowl of the vacuum pump each time the cask was re-evacuated for backfilling. The second event was confirmed through routine gas sample analysis that detected increasing hydrogen levels in the cask as the temperature increased.

Test data from Reactor Experiments, Inc., the manufacturers of the RX-277, confirmed the hydrogen release phenomena as a function of temperature increase. The problem is considered unique to the VSC-17 test cask design because holes had to be drilled through the test lid to install the TC lances. The holes penetrated the RX-277; consequently, there is a path from the RX-277 material to the MSB internal environment. If the hole through the RX-277 had been lined and sealed from communication with the cask cavity, off-gassed water vapor and hydrogen would not have entered the cask cavity. The VSC-24 does not have this problem because the RX-277 will be contained within the lid and will not have the TC penetrations into the cask cavity.

Other contributions to the unusual cask pressure behavior in the form of organics are believed to be residual fabrication cutting fluids or similar materials that off-gassed from surfaces during cask heatup.

The behavior led to a number of unplanned evacuation and backfill operations and to considerably more gas sampling/analyses than originally planned.

In the period 12/31/90 to 1/28/91, a small increase in hydrogen was detected and the pressure in the cask changed from 795 to 802 mbar. At the end of the test program, the cask was then evacuated and backfilled to a stabilized pressure of 802 mbar. The pressure remained constant for the next two months.

NUHOMS

- NUHOMS had several problems in the areas of Load Tests, Air Evacuation Test, Annulus Seal Test, Weld Mockups, Dry Shield Canister Coatings, Vacuum Drying, and Construction of Roadbeds. The explanation of each problem and its solution can be found in the original report (see Strope 1990).

6.0 CASK DEMONSTRATIONS AT SURRY POWER STATION

When the spent fuel pool at Surry Power Station Units 1 and 2 was designed and constructed in the early 1970s, VP assumed that reprocessing would be available. Fuel reprocessing has not become available since that time. The Surry Power Station fuel storage pool has been reracked to the extent possible and now has a capacity of 1044 spent PWR fuel assemblies. In 1986 the capacity of the pool was reached, requiring that an average of 75 fuel assemblies be removed each year to maintain a full core reserve margin of 157 fuel assemblies.

In August 1983, in response to DOE's SCAP, VP proposed a program involving cask performance testing at a federal site in support of a licensed demonstration at the Surry Power Station. A Cooperative Agreement was signed by VP and the DOE in March 1984. Cask testing in support of the Surry Power Station ISFSI was conducted at INEL TAN by the DOE, EG&G Idaho, and PNL. Results of those cask tests have been discussed previously in this report.

VP's portion of the Cooperative Agreement involved the selection and purchase of casks to be tested at TAN, selection and transport of spent fuel assemblies to TAN, and the design, licensing and operation of a dry cask storage ISFSI at the Surry Power Station. Table 6.1 gives a summary of the VP licensing effort.

In October and November 1986, the first two Castor V/21 storage casks, supplied by General Nuclear System, Inc. (GNSI), were loaded with spent fuel assemblies and placed at the Surry Power Station ISFSI (McKay 1989). The first NAC-I28 cask was loaded and placed at the ISFSI in March 1991 (Batalo and Wakeman 1992). The MC-10 cask was loaded and placed at the ISFSI in November 1991. The CASTOR X/33 cask is expected to be loaded in mid 1993.

A similar demonstration of a NUHOM's system was conducted through a Cooperative Agreement with CP&L at their H. B. Robinson reactor site. The results of that demonstration were discussed earlier in this report.

TABLE 6.1. Cask and ISFSI Licensing Submittals from the VP/DOE/EPRI Cooperative Agreement Program

Description	Date to NRC	Date Approved
Surry ISFSI License Application, Safety Analysis Report and Environmental Report	10/02/82	07/02/86
Use of Burnup/Boron Credit Casks	12/13/88	
Use of MC-10 Casks	01/13/89	02/15/90
Use of NAC-I28 Casks	06/21/89	05/16/90
Use of CASTOR X Casks	05/03/91	
Use of NAC-I28 Cask without Impact Limiters	12/24/91	
GNSI CASTOR V/21	12/16/83	09/30/85
Westinghouse MC-10	12/20/84	09/30/87
NAC-26 S/T	06/05/87	03/29/88
NAC-C28 S/T	02/17/88	09/29/88
GNSI CASTOR X/28 and X/33	07/01/88	
NAC-I28 S/T	11/17/88	02/01/90

7.0 REFERENCES

Barner, J. O. 1985. Characterization of LWR Spent Fuel MCC - Approved Testing Material - ATM-101. PNL-5109 Rev. 1, Pacific Northwest Laboratory, Richland, Washington.

Batalo, D. P., and G. H. Wakeman. 1992. Surry Power Station Independent Spent Fuel Storage Installation: Design and Operation of the Nuclear Assurance NAC-I28 Spent Fuel Dry Storage Cask. PNL-8012/EPRI, Electric Power Research Institute, Palo Alto, California.

Creer, J. M., R. A. McCann, M. A. McKinnon, J. E. Tanner, E. R. Gilbert, R. L. Goodman, D. H. Schoonen, M. Jensen, C. Mullen, D. Dziadosz, and E. V. Moore. 1986. CASTOR-V/21 PWR Spent Fuel Storage Cask Performance Testing and Analysis. PNL-5917/EPRI NP-4887, Electric Power Research Institute, Palo Alto, California.

Croff, A. G. 1980. ORIGEN-2--A Revised and Updated Version of the Oak Ridge Isotope Generation and Depletion Code. ORNL-5621, Oak Ridge National Laboratory, Oak Ridge, Tennessee.

Guenther, R. J., D. E. Blahnik, T. K. Campbell, U. P. Jenquin, J. E. Mendel, L. E. Thomas, and C. K. Thornhill. 1988. Characterization of Spent Fuel Approved Testing Material--ATM-103. PNL-5109-103, Pacific Northwest Laboratory, Richland, Washington.

Johnson, A. B., Jr., J. C. Dobbins, F. R. Zaloudek, E. R. Gilbert, and I. S. Levy. 1987. Assessment of the Integrity of Spent Fuel Assemblies Used in Dry Storage Demonstrations at Nevada Test Site. PNL-6207, Pacific Northwest Laboratory, Richland, Washington.

Johnson, A. B., Jr., and E. R. Gilbert. 1983. Technical Basis for Storage of Zircaloy-Clad Spent Fuel in Inert Gases. PNL-4835, Pacific Northwest Laboratory, Richland, Washington.

Lombardo, N. J., J. M. Cuta, T. E. Michener, D. R. Rector, and C. L. Wheeler. 1986. COBRA-SFS: A Thermal-Hydraulic Analysis Code: Volume III - Validation Assessments. PNL-6049 Vol. III, Pacific Northwest Laboratory, Richland, Washington.

McCann, R. A. 1987a. HYDRA-II: A Hydrothermal Analysis Computer Code: Volume I - Equations and Numerics. PNL-6206, Volume 1, Pacific Northwest Laboratory, Richland, Washington.

McCann, R. A., R. S. Lowery, and D. L. Lessor. 1987b. HYDRA-II: A Hydrothermal Analysis Computer Code: Volume II - User's Manual. PNL-6206, Volume 2, Pacific Northwest Laboratory, Richland, Washington.

McCann, R. A. 1987c. HYDRA-II: A Hydrothermal Analysis Computer Code: Volume III - Verification/Validation Assessments. PNL-6206, Volume 3, Pacific Northwest Laboratory, Richland, Washington.

McKay, H. S., B. H. Wakeman, J. M. Pickworth, S. D. Routh, and W. C. Hopkins. 1989. An Independent Spent-Fuel Storage Installation at Surry Station: Design and Operation. PNL-6843/EPRI NP-6032, Electric Power Research Institute, Palo Alto, California.

McKinnon, M. A., J. W. Doman, J. E. Tanner, R. J. Guenther, J. M. Creer and C. E. King. 1986. BWR Spent Fuel Storage Cask Performance Test, Volume 1: Cask Handling Experience and Decay Heat, Heat Transfer, and Shielding Data. PNL-5777, Vol. 1, Pacific Northwest Laboratory, Richland, Washington.

McKinnon, M. A., J. M. Creer, T. E. Michener, J. E. Tanner, E. R. Gilbert, R. L. Goodman, D. H. Schoonen, M. Jensen, C. Mullen, D. Dziadosz, and E. V. Moore. 1987a. The TN-24P PWR Spent Fuel Storage Cask: Testing and Analysis. PNL-6054/EPRI NP-5128, Electric Power Research Institute, Palo Alto, California.

McKinnon, M. A., J. M. Creer, T. E. Michener, J. E. Tanner, E. R. Gilbert, R. L. Goodman, D. H. Schoonen, M. Jensen, C. Mullen, D. Dziadosz, and E. V. Moore. 1987b. The MC-10 PWR Spent Fuel Storage Cask: Performance Testing and Analysis. PNL-6139/EPRI NP-5268, Electric Power Research Institute, Palo Alto, California.

McKinnon, M. A., T. E. Michener, M. F. Jensen, and G. R. Rodman. 1989. Testing and Analyses of the TN-24P PWR Spent-Fuel Dry Storage Cask Loaded with Consolidated Fuel. PNL-6631/EPRI NP-6191, Electric Power Research Institute, Palo Alto, California.

McKinnon, M. A., R. E. Dodge, R. C. Schmitt, L. E. Eslinger, and G. Dineen. 1992. Performance Testing and Analyses of the VSC-17 Ventilated Concrete Cask. PNL-7839/EPRI TR-100305, Electric Power Research Institute, Palo Alto, California.

Rector, D. R., C. L. Wheeler, and N. J. Lombardo. 1986a. COBRA-SFS: A Thermal-Hydraulic Analysis Computer Code: Volume I - Mathematical Models and Solution Methods. PNL-6049 Vol. I, Pacific Northwest Laboratory, Richland, Washington.

Rector, D. R., J. M. Cuta, N. J. Lombardo, T. E. Michener, and C. L. Wheeler. 1986b. COBRA-SFS: A Thermal-Hydraulic Analysis Code: Volume II - User's Manual. PNL-6049 Vol. II, Pacific Northwest Laboratory, Richland, Washington.

Strope, L. A., M. A. McKinnon, D. J. Dyksterhouse, and J. C. McLean. 1990. NUHOMS Modular Spent-Fuel Storage System: Performance Testing. PNL-7327/EPRI NP 6941, Palo Alto, California: Electric Power Research Institute.

Vinjamuri, K., E. M. Feldman, C. K. Mullen, A. E. Arave, B. L. Griebenow, J. H. Browder, P. E. Randolph, and W. J. Mings. 1988a. Dry Rod Consolidation Technology Project Quick-Look Report. EGG-WM-7852, EG&G Idaho, Idaho Falls, Idaho.

Vinjamuri, K., E. M. Feldman, C. K. Mullen, B. L. Griebenow, A. E. Arave, and R. C. Hill. 1988b. Dry Rod Consolidation Technology Project at the Idaho National Engineering Laboratory. EGG-WM-8059, Idaho National Engineering Laboratory, Idaho Falls, Idaho.

Wiles, L. E., N. J. Lombardo, C. M. Heeb, U. P. Jenquin, T. E. Michener, C. L. Wheeler, J. M. Creer, and R. A. McCann. 1986. BWR Spent Fuel Storage Cask Performance Test: Volume II - Pre- and Post-Test Decay Heat, Heat Transfer, and Shielding Analyses. PNL-5777, Vol. II, Pacific Northwest Laboratory, Richland, Washington.

APPENDIX A

CASK DESCRIPTIONS

APPENDIX A

CASK DESCRIPTIONS

A.1 REA 2023 CASK AND ASSOCIATED INSTRUMENTATION

The REA 2023 cask was specifically designed for BWR fuel and specially instrumented for performance testing. Since the cask was built and tested, Mitsubishi Heavy Industries, Ltd., of Japan has obtained design and fabrication rights and markets the cask as an MSF IV. The cask consists of a double containment design with silicone rubber O-rings for sealing the primary or inner cavity and a welded final closure on the secondary cover. The cask has a smooth, painted stainless steel outer skin; a lead/stainless steel gamma shield; and a water/glycol neutron shield. The fuel basket is constructed of stainless steel-clad Boral for criticality control, copper plates to conduct heat to the cask wall, and stainless steel for structural strength. The loaded cask holds 52 assemblies, is approximately 5 m (16 ft) tall, is 2.5 m (8 ft) in diameter, and weighs approximately 100 tons.

The containment vessel, or cavity shell, is 1.91 cm (0.75 in.) hot-rolled and annealed 304 stainless steel. The cavity bottom plate is 5.08 cm (2 in.) stainless steel. The outer cylindrical shell and bottom plate are also 5.08 cm (2 in.) stainless steel. Thicknesses of lead shielding are 10.80 cm (4.25 in.) in the sidewall and 8.26 cm (3.25 in.) in the bottom.

The neutron shield is a 15.2 cm (6 in.) annular tank, divided into two sections and extending from the bottom of the cask to 50.8 cm (20 in.) below the top of the cask. The annular tank contains 3800 liters (1000 gal) of a 50/50 ethylene glycol/water solution. Within the neutron shield are the trunnion supports, to which the lifting trunnions may be externally bolted.

The bottom section of the neutron shield is an expansion tank. It begins 0.64 cm (0.25 in.) from the cask bottom and extends up 40 cm (15.75 in.). The neutron shield cavity has top and bottom fill and drain plugs, and the expansion tank has a bottom drain plug.

The inner or primary cover is constructed of a 2.5 cm (1.0 in.) stainless steel bottom plate and a 5.08 cm (2.0 in.) top plate, and contains 7.62 cm (3.0 in.) of lead between the two plates. It is secured to the cask body by 36 high-strength bolts. Sealing is obtained by two silicone rubber O-rings. A hole through the top plate, located between the O-rings, permits checking for leak tightness.

The outer or secondary cover is constructed of 5.08 cm (2.0 in.) stainless steel plate. It has a stainless steel angle welded around its periphery to mate with a similar angle at the top of the outer wall of the cask body. These angles are seal-welded after loading to provide high integrity and long-term leak tightness.

Two 1.27-cm- (0.5-in.-) diameter drain lines penetrate the cavity bottom plate and lead. Vent/sampling lines penetrate the cavity wall and lead near the top of the cask, slightly below the primary cover.

Four instrument ports were located on the cask and were used for testing. These instrument ports provided pass-throughs for internal thermocouples and pressure sensors. Seventy type K thermocouples (TCs) were used to monitor temperatures of the cask and fuel. Thirty-eight of these TCs were located inside the cask; the remaining 32 were mounted on the surface of the cask. Twelve internal type K thermocouples were located on the basket of the REA cask. Four of these thermocouples were attached to the bottom of the basket by REA during the installation of the basket. The remaining eight were placed between the slots of the basket in the small gaps formed between the copper plates and the Boral tubes.

A unique feature of the REA cask characterization test program was the Thermocouple Attachment Device (TAD) used to measure the surface temperature of the center rod of a 7x7 fuel assembly. Seven fuel bundles were instrumented with TADs. The TAD installation was done in conjunction with the first incremental loading.

All fuel instrumentation was done underwater in the GE-MO unloading basin. A special TAD installation tool (referred to as a TAD-pole) was designed, fabricated, and used to install the TAD-mounted thermocouples. The

TAD-pole was basically a 40-ft-long manipulator with a "master" end located above water and a "slave" end located underwater. The TAD-pole was used to pick up the TAD from a vertical position ("T" bar handle pointed up), rotate it to a horizontal position, insert it into a BWR fuel bundle, and rotate it 90 degrees to lock it in place.

The REA cask is designed to operate with nitrogen or helium backfill environments. The internal gas pressure should be positive with respect to the atmosphere--50 to 70 kPa (7 to 10 psig). The pressure transducer mounted on the cask provides a means of detecting leaks during long-term storage.

The cask body has eight attachment points or trunnion supports for bolt-on trunnions. Four of these are located near the top, spaced 90° apart, and are used for lifting the cask in the vertical position. Two trunnion supports, 180° apart, are at an elevation slightly above the center of gravity of the cask. These trunnions are used when lifting the cask in the horizontal position and for rotating the cask from a vertical to a horizontal position or vice versa. The other two trunnion supports are near the bottom of the cask and are located 180° apart. These supports were used for securing the impact limiter to the cask during testing at GE-MO.

The basket was fabricated in four quadrants, which are placed in the cask cavity. Contact is made between the outer cylindrical copper shells of the basket quadrants and the inner wall of the cask, thus minimizing thermal resistance. Each quadrant has thirteen 15.2 cm (6 in.) square spent fuel tubes, each of which contains one fuel assembly. Each fuel tube consists of concentric inner and outer square shrouds that integrally encapsulate Boral neutron absorber plates. The Boral plates extend above and below the active lengths of the fuel assemblies. These tubes are essentially identical to tubes currently licensed for use in spent fuel storage basins. Copper strips are used as the outer boundary of each quadrant and as internal ribs to effectively transfer heat from inner spent fuel assemblies/fuel tubes to the outer copper shells and cask inner wall. Other structural members of the basket are made of stainless steel. The basket rests on the bottom of the cask and has cutouts on the bottom edge to permit water drainage and backfill gas circulation.

A.2 CASTOR-V/21 CASK AND ASSOCIATED INSTRUMENTATION

The cask body is a one-piece cylindrical structure composed of ductile cast iron in nodular graphite form. This material exhibits good strength and ductility and provides effective gamma shielding. The overall external dimensions of the cask body include a height of 4886 mm (16 ft) and a diameter of 2385 mm (8 ft). The external surface has 73 heat transfer fins that run circumferentially around the cask and is coated with epoxy paint for corrosion protection and ease of decontamination.

The cask body wall, excluding fins, is 380 mm (15 in.) thick. Incorporated within the wall of the body are polyethylene moderator rods to provide neutron shielding. Two concentric rows of these 60 mm (2.3 in.) nominal diameter rods are distributed around the cask perimeter. Two lifting trunnions are bolted on each end of the cask body.

The diameter of the inner cavity is 1527 mm (5 ft), and the overall inner cavity length is 4152 mm (163 in.). Precision-machined surfaces are provided at the open end of the cask cavity for positive gasket sealing, and bolt holes are included at these locations to secure the two cask lids. The interior cavity surfaces, including sealing surfaces, have a galvanic applied nickel plating.

The spent fuel basket is a cylindrical structure of welded stainless steel plate, and borated stainless steel plate, having a boron content of approximately 1% for criticality control. The basket's comprises an array of 21 square fuel tubes/channels that provide structural support and positive positioning of the fuel assemblies. The basket's overall height is 4110 mm (13.5 ft) including the four 130-mm-diameter (5-in.) pedestals that support the basket and fuel weight on the bottom of the cask cavity. The basket outside diameter of 1524 mm (5 ft) fits tightly in the cask cavity inner diameter of 1527 mm (5 ft). The depth of each fuel tube is 4050 mm (13.3 ft). A spacing of 74 mm (3 in.) is present between the top of the basket cavity and the underside of the primary lid, thus accommodating a fuel assembly length of 4124 mm (162 in.) and supporting convection heat transfer. The final assembly

results in a clearance of approximately 60 mm (2.3 in.) between the top of the fuel assemblies and the bottom of the primary lid for a reference fuel assembly of 4064 mm (160 in.).

The basket layout results in inter-fuel tube spaces that act as flux traps for criticality control and channels to support free convection heat transfer. The basket design ensures a subcritical configuration under worst-case conditions, and the basket structure physically protects the fuel under normal and accident conditions.

A pipe with an inner diameter of 42 mm (1.6 in.) and a lead-in funnel at the top is welded to the side of a fuel tube near the outer circumference of the basket. The pipe location corresponds to a penetration in the primary lid and the low side of the slope in the cask cavity bottom. This pipe provides a path for a flanged pipe used to fill and drain the cask.

A stainless steel primary lid, 1785 mm (6 ft) in diameter and 290 mm (12 in.) thick, is provided. Forty-four bolt holes are machined near the lid perimeter to secure the lid to the cask body. Two grooves machined around the lid underside, inside the bolt circle, are provided for O-ring gaskets. The inner groove accepts a metal O-ring, which serves as the first barrier between stored fuel and the environment. The outer groove accepts an elastomer O-ring. A 10-mm-diameter (0.5-in.) penetration through the lid provides access to the annulus between the two seals to perform post-assembly leak testing. This penetration is plugged when not in use.

Three penetrations through the lid are provided for various cask operations. A 35-mm-diameter (1.4-in.) straight-through penetration is used for water fill/drain operations. This penetration is located near the perimeter of the lid and is normally sealed with two flanges equipped with elastomer O-rings. This location corresponds to the pipe attached to the fuel basket. The other two penetrations, spaced next to each other and covered by a single flange, are also located near the lid perimeter, but 180 degrees from the fill/drain penetration. The through-lid penetration at this location is equipped with a quick-disconnect fitting used for vacuum drying and backfilling with gas. The second penetration at this location leads to the lower edge of the lid. Although not needed for the CASTOR-V/21, this penetration could

be used for leak-testing an optional third lid gasket. This penetration is sealed by a gasketed seal plug in addition to the top cover flange.

The primary lid used during testing was not a standard lid and has 10 additional penetrations for fuel assembly guide tube instrumentation (TC lances). Nine of the penetrations are machined with 18 mm (0.7 in.) holes through the lid and countersunk (20 mm, 0.8 in.) to accept the TC lances and 105-mm-diameter (4 in.) flanges. The tenth penetration has a hole through the lid for a TC lance and accepts a 140-mm-diameter (5.5 in.) flange. The pattern of the 10 fuel assembly instrumentation penetrations was selected to measure radial temperature profiles across the basket in the spent fuel assemblies. The pattern was developed using pretest temperature predictions of the undocumented HYDRA thermal hydraulics computer program.

The stainless steel secondary lid is 2007-mm (79 in.) in diameter and is 90 mm (3.5 in.) thick. Forty-eight bolt holes are machined near the lid perimeter to secure the lid to the cask body. Two concentric grooves located inside the bolt circle on the underside are provided for a metal O-ring/elastomer O-ring sealing system of the same design as that used on the primary lid. Three normally sealed penetrations are provided for various cask operations. A 10-mm-diameter (0.4 in.) penetration through the lid provides access to the annulus between the two seals for post-assembly seal testing. A gasketed seal plug is used to close this penetration.

A second penetration is equipped with a quick-disconnect fitting, which is used for vacuum drying and gas backfilling of the primary/secondary inter-lid space. A 130-mm-diameter (5 in.) cover plate and gasket secured by six 12 mm (0.5 in.) bolts is in place when this penetration is not used. The third penetration provides a pressure sensing port between the inter-lid space and a pressure switch mounted in the secondary lid. The pressure switch is the primary component of the cask seal monitoring system.

The secondary lid was not used during the CASTOR-V/21 cask performance test because of interference with fuel assembly instrumentation leads. Therefore, dose rates discussed were obtained on the primary lid exterior surface. Addition of the secondary lid will greatly reduce measured dose rate values.

Seven of the 21 Surry PWR spent fuel assemblies were instrumented with TC lances (tubes). Each TC lance had six TCs installed in the 8-mm-diameter (0.315 in.) tube. Lances were inserted through instrumentation penetrations in the primary test lid and into selected guide tubes of the seven assemblies. Standard elastomer O-rings in the TC lance flanges were used to establish seals between the cask inner cavity containing spent fuel and the outside environment.

Note that two additional TC lances were inserted through the lid, but not into assembly guide tubes. These two TC lances were used to measure gas temperatures near the center and edge of the fuel basket.

A.3 TN-24P CASK AND ASSOCIATED INSTRUMENTATION

The TN-24P cask has a forged steel body for structural integrity and gamma shielding, surrounded by a resin layer for neutron shielding, which is enclosed in a smooth steel outer shell. The loaded cask weighs approximately 100 tons. The cask has a cylindrical cavity that holds a fuel basket designed to accommodate 24 intact PWR fuel assemblies. The basket is made of a neutron-absorbing material, borated aluminum, to control criticality. The cavity atmosphere is designed to be nitrogen or helium at a positive pressure.

The cask is sealed with a single lid. A protective cover, bolted to the body, provides weather protection for the lid penetrations. Two concentric metallic O-rings are provided for sealing the lid to the cask body, and an elastomer O-ring is used with the protective cover. The body is fitted with three pairs of removable trunnions for handling and transport. A polyethylene neutron shielding disk is attached to the lid when the cask is in storage. If the cask is stored in a horizontal orientation, a neutron shielding disk must also be attached to the cask bottom.

The major differences between the TN-24P test cask and standard TN-24 casks occur in cask body thickness, basket material, and neutron shield structure. These differences are listed in Table A.1.

The TN-24P basket is composed of borated aluminum plates, while the standard TN-24 basket is assembled from copper-clad borated stainless steel

TABLE A.1. Differences Between TN-24 Prototype (TN-24P) and Standard TN-24 Casks[a]

Parameter	TN-24	TN-24P
Cask Body		
Cask OD, cm (in.)	225 (88.5)	228 (89.8)
Steel shell thickness, cm (in.)	24 (9.5)	27 (10.6)
Bottom thickness, cm (in.)	26.7 (10.5)	28 (11.0)
Outer shell thickness, cm (in.)	1.9 (0.75)	1 (0.39)
Bottom chamber	yes	no
Neutron shielding annulus	Resin in aluminum	Resin butts against cans that butt cask body and is against cask body between copper fins and outer shell
Shell penetrations	None	One
Lid		
Lid thickness, cm (in.)	26.7 (10.5)	28.5 (11.2)
Lid bolts (No. x dia, in.)	48 x 1.50	40 x 1.65
Neutron shielding thickness, cm (in.)	7 (2.75)	10.7 (4.2)
Penetrations	2	1
Basket		
Material	Borated stainless	Borated steel with copper aluminum cladding
Plate size (height x thickness, in.)	41 x 0.6 (16.2 x 0.22)	16 x 1 (6.3 x 0.39) 0.3 (0.118 in. copper)
Construction	Full interlocking plates	Semi-interlocking plates with connecting angles
Instrumentation	No internal	Internal thermocouples
Protective Cover	1.9 (0.75-in. thick) bolted to body	0.8 (0.315-in. thick) attached by clamps
Loaded weight on storage pad (lb)	83.5 MT(184,000)	87.1 MT(192,000)

(a) Data presented were provided by M. Mason of Transnuclear, Inc., June 20, 1985.

plates. The TN-24P has an instrument penetration in the cask body containing thermocouples that are attached to the basket. The standard TN-24 contains no instrumentation penetration.

These differences impact the cask performance in two ways: 1) the dose rate for standard TN-24 casks will be higher than for the TN-24P test cask due

to differences in wall thickness and 2) temperatures in standard TN-24 casks will be higher due to basket materials and neutron shield structure.

The remainder of this section describes the TN-24P cask.

The cask body is a one-piece cylindrical structure composed of forged steel. The overall external dimensions of the cask body include a length of 5063 mm (16.6 ft) and a diameter of 2281 mm (7.5 ft). All surfaces except sealing surfaces are coated with a deposit of zinc-aluminum alloy. Sealing surfaces are clad with stainless steel. Internal surfaces have an aluminum titanium oxide overcoat; exterior surfaces are covered with white silicone paint.

The cask body consists of a 270-mm-thick (10.6-in.) cylindrical shell welded to a 280 mm (11 in.) bottom plate. A neutron shield containing L-shaped copper plates is welded to the cylindrical shell. The copper plates are welded to the inner surface of the neutron shield and provide enhanced heat conduction through the resin compound of the neutron shield. The cask can accommodate six bolted trunnions for handling and tie-down, four near the top and two near the bottom. Finally, the cask body has an instrumentation orifice sealed by a metallic gasket.

The diameter of the inner cavity is 1455 mm (57.3 in.), and the overall inner cavity length is 4150 mm (163.4 in.). Precision-machined surfaces are provided at the open end of the cask cavity for positive gasket sealing, and bolt holes are included at these locations to secure the cask lid and protective cover.

The basket comprises an array of 24 fuel tubes/channels that provide structural support and positive positioning of the fuel assemblies. The basket is composed of stacked interlocking plates constructed of aluminum and boron. The plates are 10 mm (0.4 in.) thick and 160 mm (6.3 in.) wide and vary in length depending on their position in the basket. Each layer of the basket is bolted to four uprights that are used to tie the basket together in the axial direction and support the basket. The uprights provide a 45 mm (1.8 in.) gap between the bottom of the basket and the bottom of the cask. This gap plus the 29-mm (1.1-in.) gap between the top of the basket and the

cask lid provide convection paths for the gas in the cask. The basket overall height is 4121 mm (162.2 in.). The position of the basket within the cask is maintained by bars welded to the interior surface of the cask. The bars act as guides for the interlocking plates.

Two aluminum tubes are welded to the aluminum basket in two locations that do not interfere with the fuel. The tube locations match penetrations in the lid used to insert TC lances and provide temperature readings typical of the basket.

A carbon steel lid, 1720 mm (5.6 ft) in diameter and 285 mm (11.2 in.) thick, is provided. The lid is fastened to the cask body with 40 bolts matching index marks on the lid and cask for proper alignment. Sealing is ensured by a double O-ring metallic gasket installed in a stainless steel-coated lid groove. A 5-mm-diameter (0.2-in.) penetration through the lid provides access to the annulus between the two seals to perform post-assembly leak testing. Additional sealing is obtained by a Viton O-ring fitted between the protective cover and a groove in the top surface of the cask wall.

An operations orifice is located in the lid for access to the internal cavity. It consists of a plug extended by a base acting as a radiation trap, a tightening ring, and an orifice plate. Sealing of this penetration is ensured by an O-ring metallic gasket fitted on the orifice plate. Sealing is monitored through a test orifice closed by a test plug.

A neutron shielding drum is bolted to the lid. It consists of granular polypropylene wrapped in a carbon-steel drum. The drum is composed of a flat circular head closed with a circular welded plate. Its finished size is 105.5 mm (4.2 in.) thick by about 1700 mm (70 in.) in diameter. To facilitate operations, test plugs in the lid and operations orifice plate are easily accessible while the drum is in place.

A protective cover fits over the lid and neutron shielding drum. This cover consists of a carbon-steel ellipsoidal head and a flange equipped with one rubber O-ring gasket. The cover measures 1815 mm (71.5 in.) in diameter and is 498 mm (19.6 in.) deep. It is fastened to the body of the cask using eight bolts and clamps. Two penetrations are provided in the protective cover

for instrumentation leads and for leak-checking the attached cover. The interspace between the lid and the protective cover contains the pressure monitoring loop. This loop pressurizes and monitors the space between the double O-ring metallic gaskets during long-term storage. It also pressurizes and monitors the operations orifice seal. The loop consists of connections to the lid and operations spaces to be monitored, a pressure monitoring tank, a reference pressure tank, a pressure sensor, and two thermocouples. The thermocouples provide data concerning whether pressures changes are due to temperature changes or leakage.

A non-standard lid with nine penetrations for thermocouple lances was used during the performance testing. Eight of the penetrations are machined with 18-mm (0.7-in.) holes through the lid and countersunk (20 mm, 0.8 in.) to accept the TC lances and 105-mm-diameter (4-in.) flanges. The ninth penetration has a hole through the lid for a TC lance and accepts a 140-mm-diameter (5.5-in.) flange. The pattern of the nine fuel assembly instrumentation penetrations was selected to measure radial temperature profiles across the basket in the spent fuel assemblies. Cask evacuation, gas backfill, pressure monitoring, and gas sampling were done using the instrumentation port through the side of the cask. The test lid used a single Viton O-ring and 20 bolts instead of the double O-ring metallic seal and 40 bolts used with the primary lid. Like the primary lid, the test lid was 1725 mm in diameter and 285 mm thick. However, the neutron shielding drum, protective cover, and pressure monitoring loop were not used during the performance test. Gas backfilling, gas sampling, and pressure monitoring were performed through the instrumentation port by means of a cross manifold when the test lid was on the cask.

A Leybold Heraeus model MAC 2000 pressure transducer was used to measure cask cavity pressures. The transducer had a range of 0 to 2000 mbar and a stated accuracy of 0.02% of full scale. The transducer was connected to the quick-disconnect penetration provided in the primary lid of the cask. Fourteen type K TCs were permanently attached to the inner wall and basket of the cask. An additional 54 TCs were placed in the fuel assemblies and basket using TC lances. Each TC lance had six TCs installed in an 8-mm-diameter (0.315-in.) tube. Lances were inserted through instrumentation penetrations

in the primary test lid and into selected guide tubes of seven fuel assemblies and into two simulated guide tubes attached to the basket. Standard elastomer O-rings in the TC lance flanges were used to establish seals between the cask's inner cavity containing spent fuel and the outside environment.

The selected axial and cross-sectional locations of the TC lance thermocouples facilitated redundancy, evaluations of temperature symmetry, and determinations of axial and radial temperature profiles in both vertical and horizontal orientations.

A.4 MC-10 CASK AND ASSOCIATED INSTRUMENTATION

The MC-10 cask is approximately 4.8-m (15.7 ft) long, measures 2.7 m (8.9 ft) in diameter, and weighs approximately 95 tons (empty). The cask has a low alloy forged steel body for structural integrity and gamma shielding, surrounded by a solid hydrogenous material for neutron shielding. Additional neutron absorption and criticality control are provided by Boral plates in the basket portion of the cask. The cask has a cylindrical cavity that holds a fuel basket designed to accommodate 24 PWR fuel assemblies. Four trunnions bolted to the cask wall are used for all cask-handling operations.

The cask closure system consists of four covers: shield, primary, seal, and protective covers. A metallic O-ring seal is used to seal the shield cover, and both metallic and elastomer O-rings are used with the primary cover. The seal cover can be welded to the cask body.

The containment vessel consists of a 254-mm-thick (10-in.) cylindrical forged alloy steel wall welded to a 254-mm-thick (10-in.) bottom plate. The vessel cavity measures 172.7 mm (68 in.) in diameter and is 413 mm (162.6 in.) long.

Twenty-four 25.4-mm-thick (1 in.) carbon-steel fins are welded to the outside wall of the containment vessel. The fins run axially along the outside wall, are attached by full-length fillet welds, form a heat path through the neutron shield, and act as an impact limiter. An annular cavity is formed

around the outside of the cask by welding 3.2-mm-thick (0.125-in.) plates to adjacent fins. The plates and protruding stainless steel fins form an outer protective skin for the alloy steel vessel.

The alloy steel vessel base plate is protected in a similar manner except that the fins welded to the base plate do not protrude beyond the protective skin. The bottom skin is twice as thick (6.4 mm [0.25 in.]) as the cylindrical skin.

Radiation shielding for the cask is provided by the steel in the cask wall and a layer of neutron absorber. The steel in the cask wall and skin provide the gamma shielding for the cask. Neutron shielding is provided using the cavities formed between the vessel wall and the skin. These cavities are filled with BISCO NS-3, a neutron-absorbing hydrogenous material produced by Brand Industries. The cavities filled with this material provide more than 63.5 mm (2.5 in.) of neutron shielding around the outside of the cask.

The overall external dimension of the cask body, excluding the fins, is 4.798 m (15.74 ft) long by 2.39 m (7.8 ft) in diameter. The fins extend about 170 mm (6.64 in.) beyond the skin surface on the side of the cask, giving the cask a total envelope of 4.798 m (15.74 ft) in length by 2.7 m (8.9 ft) in diameter.

The basket assembly consists of a one-piece fabricated aluminum grid system and 24 stainless steel fuel storage cells. The basket is fabricated using 10.2-mm-thick (0.400-in.) by 3.8-m-long (149-in.) aluminum plate. Half-length slots allow assembly of the plates in an egg-crate fashion. Plate intersections are joined using a full-length fillet weld to form an uninterrupted heat transfer path and to provide structural rigidity. Perimeter edges of basket plates are fit into guide blocks welded to the inside diameter of the cask vessel.

A removable storage cell is contained in each of the 24 grid locations. Each cell consists of an enclosure, neutron poison material, and limiter blocks. The enclosure is a 1.9 mm thick (.075 in.) by 4.1 m long (160 in.) stainless steel plate formed to provide a 222-mm-square (8.75-in.) envelope for fuel assembly storage. The upper ends of the enclosure walls are flared

to serve as funnels to facilitate fuel loading. Attached to the outside of each wall of the cell is a Boral plate for the absorption of neutrons and control of criticality. The Boral plates (boron carbide particles in an aluminum matrix sandwiched between two pieces of Type 1100 aluminum) are attached to the cell walls by stainless steel wrappers welded to the cells.

The storage cells are centered in the aluminum basket using spacer blocks on the four corners of the cells at various elevations along the length of the cell. The bottom set of spacer blocks protrudes 6.4 mm (0.25 in.) below the bottom of the cell and rests on the vessel floor. The gap between the bottom of the cell and the vessel floor helps to facilitate draining and provides a convection path for gas circulation.

The MC-10 cask uses a redundant closure and seal system consisting of three cover plates: the shield, the primary cover, and the seal cover.

The shield cover is an alloy steel plate 127 mm (5 in.) thick by 1918 mm (75.5 in.) in diameter. The underside of the shield cover is machined for a spring-energized metallic O-ring held in place by six retainer clips. The O-ring groove and matching seal surface of the vessel are clad with stainless steel to provide a good seal. The shield cover is attached to the vessel using thirty-six 1.5-in.-diameter studs and nuts. Four alignment pins are provided to help in remote handling of the shield cover. The cover includes four tapped holes to interface with lifting equipment.

The primary cover is a carbon-steel plate 88.9 mm (3.5 in.) thick by 2181 mm (85.88 in.) in diameter. Like the shield cover, the primary cover includes four tapped holes to interface with lifting equipment. It is bolted to the cask vessel using thirty-six 1.375-in. bolts. The underside of the primary cover is machined for an elastomer and spring-energized metallic O-ring assembly. The O-ring assembly is held in place with six screws. Two penetrations with dual spring-energized metallic O-ring seals are provided to permit leak-testing of the main O-ring assembly. The primary cover is positioned on a stainless steel-clad seat that is recessed into the low alloy steel containment vessel just above the shield cover.

The seal cover is a carbon-steel plate 25.4 mm (1 in.) thick by 2213 m (87.12 in.) in diameter. It is bolted to the primary cover using twelve 1.125-in. studs at the twelve spacer bosses welded to the top surface of the seal cover. Four of the bosses are tapped to interface with lifting equipment.

The final protective cover is the closure cover. This cover is a steel weldment, approximately 127 mm (5 in.) thick by 2.4 m (94.5 in.) in diameter, containing neutron shielding material. Twelve clearance holes in the cover align with seal cover bosses and studs. The cover is fastened using 114 mm (4.5 in.) knurled nuts. Elastomer O-rings between the nuts and cover provide a water-tight seal. Four nuts are welded to the protective cover top to interface with lifting equipment.

The LCSS was replaced with a single test lid for the performance test. The test lid was 279 mm (11 in.) thick and was fastened to the primary cover sealing surface. The differences between the test lid and the LCSS will cause the temperature measured on the surface of the test lid to be higher than that on the surface of the LCSS. The LCSS has several contact resistances between steel plates and the neutron shield. The lack of a neutron shield and greater thickness of steel for the test lid will cause the gamma dose rate to be smaller and the neutron dose rate to be higher for the test lid than for the LCSS.

The vessel wall has three penetrations: a drain port at the cask base, a vent port, and an instrument port. The drain and vent ports are identical in design. The vessel was bored and tapped to accept a straight-thread union fitting with metallic V-ring seals. A quick-disconnect plug is installed on the union fitting. Two covers with spring-energized metallic O-rings are fastened over the quick-disconnect plugs. A neutron shield cover is fastened over the port covers.

The instrument port is of a similar design except that an adaptor fitting with metallic V-ring seals is threaded into the tapped hole for mounting a pressure transducer. Clearance is provided between the two cover plates to

allow for passage of the transducer lead wires. Both covers include a feed-through fitting with elastomer O-ring seals for the transducer lead wire. The neutron shield is notched for routing the lead wire to the data acquisition system.

A Leybold-Heraeus model MAC 2000 pressure transducer was used to measure cask cavity pressures. The transducer had a range of 0 to 2000 mbar and a stated accuracy of >0.02% of full scale. The transducer was connected to the quick-disconnect penetration provided in the primary lid of the cask via the valve tree. The signal from the transducer was conditioned and read out on the data acquisition system (DAS) described in a later section.

Fifty-four TCs were placed in the fuel assemblies and basket using TC lances. Each TC lance had six TCs installed in an 8-mm-diameter (0.315-in.) tube. Lances were inserted through instrumentation penetrations in the primary test lid and into selected guide tubes of seven fuel assemblies and into two simulated guide tubes attached to the basket. Standard elastomer O-rings in the TC lance flanges were used to establish seals between the cask inner cavity containing spent fuel and the environment outside the cask.

The exterior surface of the cask was instrumented with 34 iron/constantan type J TCs. Only during horizontal testing were TCs placed on the bottom of the cask. The TC patterns on each surface were selected to provide appropriate axial, radial, and circumferential temperature profiles.

A.5 VSC-17 CASK AND ASSOCIATED INSTRUMENTATION

The VSC-17 spent fuel storage system is a passive device for storing 17 assemblies/canisters of irradiated nuclear fuel. The VSC-17 system consists of a VCC and an MSB. Decay heat, generated by the spent fuel, is transmitted through the containment wall of the MSB to a cooling air flow. Natural circulation drives the cooling air flow through an annular path between the MSB and the VCC and carries the heat to the environment without undue heating of the concrete cask. The annular air flow cools the outside of the MSB and the inside of the VCC.

The cask weighs approximately 80 tons empty and 110 tons loaded with 17 canisters of consolidated fuel. The VCC has a reinforced concrete body with an inner steel liner and a weather cover (lid). The MSB contains a guide sleeve assembly for fuel support and a composite shield lid that seals the stored fuel inside the MSB. The cavity atmosphere is helium at slightly sub-atmospheric pressure. The helium atmosphere inside the MSB enhances the overall heat transfer capability and prevents oxidation of the fuel and corrosion of the basket components.

The ventilated concrete cask is a one-piece cylindrical structure. It provides structural support, shielding, and natural convection cooling for the MSB. The concrete wall thickness (20 inches) is sufficient to limit exterior surface radiation dose rates to less than 200 mrem/h for intact fuel. The air inlet and outlet vents are steel-lined penetrations that have non-planar paths to minimize radiation streaming.

The internal cavity of the concrete cask is formed by a steel cylindrical liner and a flat bottom plate. Reinforcing studs are welded to the cylinder to connect the steel and the concrete. An outer rebar cage is formed by vertical hook bars, horizontal ring bars, and reinforcing at the bottom of the cask. The vertical horizontal hook bars engage the reinforcement at the cask bottom to completely encase the cask. The heavily reinforced cask bottom is 56 cm (22 inches) thick.

The cask is made of Type II Portland Cement, 145 lb/ft^3, 4000 psi concrete. Plasticizers and vibration were used during placement of the concrete to ensure complete filling of all volumes between embedments and to prevent void formation under horizontal surfaces. Two lifting lug assemblies are embedded at the top face of the cask and are designed to vertically lift the cask. The cask has rounded edges to mitigate potential damage to the cask if it were dropped accidently. The rounded edges eliminate the sharp corners at the cask top and bottom where chipping, spilling, and loss of material are more likely to occur in a drop accident. Reinforcement in these potential impact areas and a 0.25-inch steel plate on the bottom of the cask will also help reduce concrete material loss from a drop accident.

The depth of the cask cavity was selected to accommodate an MSB for BWR assemblies. A MSB support assembly was provided with the shorter PWR MSB to prevent blockage of flow to the outlet air vents.

The annular air flow path is formed by the air inlet ducts, the gap between the MSB exterior and the liner interior, and air outlet ducts. To minimize radiation streaming, the air inlet and outlet ducts contain two or more sharp bends. The ducts also have relatively thick steel walls to reduce surface radiation doses.

The cask weather cover plate provides additional shielding and provides a cover to protect the MSB from the environment. The cover is bolted in place and has a sheet rubber seal.

The 17-PWR-element MSB consists of an outer shell assembly, a shield lid, and the fuel guide sleeve assembly. The MSB is fabricated from pressure vessel steel. The fuel guide sleeve assembly is fabricated from welded square steel tubes. The shell and internals are coated with Everlube 812.

Structural support in the lateral direction is provided by a curved basket support structure located at each end and in the center of the basket. Sufficient radial clearance is maintained between the shell and the storage sleeve assembly so that differential thermal expansion during operation will not cause load transfer between the two structures.

The MSB seal system is designed to ensure the leak tightness of the MSB. If defects should develop in individual fuel rods during long-term storage, any activity released would be contained within the MSB.

The MSB shield lid has two steel sections that sandwich some neutron shielding material. The test lid has one penetration (with quick disconnect fitting) for the vacuum drying/helium backfilling system and seven penetrations for TC lances. Two O-rings, one metallic and one elastomer, are provided for sealing the lid to the MSB. The metal seal provides long-term stability while the elastomer seal ring serves to functionally test the cask seal system. However, the credit for the elastomer seal was not used in the

cask safety analysis. The annulus formed between metal and elastomer O-rings, along with the test penetrations through the lid, were means to verify that a proper seal had been obtained.

The shield lid is bolted to the MSB after fuel insertion. Two permanent alignment pins, installed in the MSB flange, help to correctly position the lid on the cask.

The MSB is also lifted from above. Lifting of the MSB when it is empty (and without the shield lid) is performed by using the four lifting eyes welded symmetrically to the inside of the MSB shell. Four turnbuckles with jaw end fittings are used in this lift. The lifting eyes are sized to lift the empty MSB into the VCC. Lifting of the shield lid is performed by using a solid lid lift fixture that allows leveling of the lid.

Differences between the VSC-17 and VSC-24, a commercial cask of the same basic design, are listed in Table A.2. Major differences include cask capacity with its associated diameter and weight. Lid attachment methods are also significantly different. The diameter of the VSC-17 was constrained by the existing cask transporter at the test site. To minimize dose rates, the VSC-17 used a thicker steel inner liner because of a relatively thin concrete cask wall. The net effect of the wall thickness differences was expected to increase the unconsolidated spent fuel dose rate from the test cask compared to the dose rate from the VSC-24 (200 mrem/h versus 50 mrem/h, respectively). The commercial cask relies on a welded closure, whereas the test cask used O-ring seals and bolted lids so fuel could be easily removed during testing and subsequent activities.

The large capacity of the commercial cask would be expected to result in sightly higher fuel and concrete temperatures; however, the approximate temperatures of the commercial cask may be extrapolated from those obtained from the VSC-17.

A.6 NUHOMS CASK AND ASSOCIATED INSTRUMENTATION

The major components of the system are an HSM made of reinforced concrete, a stainless steel DSC, an onsite transfer cask, and a special

TABLE A.2. Differences Between the VSC-17 Test Cask and the Commercial VSC-24 Cask i c Only

Parameter, in.	VSC-24	VSC-17
Cask Body		
Cask Outside Diameter	132	105
Cask Height	209	226
Multi-Assembly Sealed Basket		
Capacity	24 PWR	17
Internal Atmosphere	Helium	Helium
Material	Steel	Steel
Height	176-189	181
Lid Gamma Shield	Steel	Steel
Lid Neutron Shield	RX-277	RX-277
Lid Penetrations	2	8
Lid Attachment Method	Welded	Bolted
Lid Seal Arrangement	Seal Weld	Metal O-ring
Instrumentation	None	Pressure TCs in Concrete TC Lances (test)
Loaded weight on storage pad (lb)		
MSB (Loaded, w/Lids)	63,900	44,640
VCC (Empty, w/O Cover Plate)	192,300	155,570
VCC & MSB (Loaded w/B&W Fuel)	257,310	189,270
VCC & MSB (Loaded w/Con. Fuel	--	211,960

trailer. Each storage module houses a single canister containing seven intact PWR assemblies. The DSC provides containment for the fuel assemblies and the cover gas and includes an internal basket to maintain the assemblies in a critically safe configuration. The transfer cask provides shielding and protection for the DSC when it is moved from the reactor spent fuel pool to the HSM. The special-purpose trailer is used to move the transfer cask containing the loaded DSC to the HSM and provides the alignment required to mate the cask with the module. The HSM provides shielding and missile protection for the canister during long-term storage. In operation, the DSC is inserted into the

transfer cask and lowered into the reactor spent fuel. The spent fuel assemblies are placed in the canister basket and a lead shield plug is placed on the open end of the canister. The cask is then removed from the pool and transferred to the cask decontamination area where the water is removed from the cask and canister, the top shield plug is seal welded to the canister, and the canister is vacuum dried and backfilled with helium. The cask lid is then bolted on and the cask is decontaminated, placed on the trailer, and transported to the HSM. At the HSM, the cask lid is removed, the transfer cask is aligned with a docking port on the module, and the DSC is pulled from the cask into the module by a hydraulic ram extended through a port on the back of the module. To complete the installation, a 2-in. thick shielded door is lowered and welded in place to cover the docking port.

The reinforced concrete for a three-module design is roughly 22 ft long, 25 ft wide, and 12 ft high. The walls and roof of the module are approximately 3.5 ft thick, providing the primary biological shield and impact protection for the DSC. Each module is isolated from the others by concrete inner walls and contains a large docking port in one end and a small access port in the other. When the transfer cask is aligned with the docking port, a hydraulic ram is extended through the small access port to grapple the DSC and pull it onto a set of rails extending through the small access port from the docking port toward the back of the module. When the DSC is in place, its outer skin is cooled primarily by convective air currents generated in the module by the elevated temperature of the DSC.

The NUHOMS system is designed to be a totally passive storage system and requires no safety-related instrumentation. However, two of the HSMs and two DSCs were instrumented with thermocouples to provide thermal data to characterize the performance of the NUHOMS system as part of the CP&L/DOE project.

The generic NUHOMS system designed by PNFS consists of a basic unit of two modules arranged back-to-back. The system is expanded with additional two-module units placed beside the first until the required storage capacity is reached (2x2 array).

The generic configuration requires an onsite transfer cask with an access port in the bottom to allow a hydraulic ram to push the canister from

the cask into the module. Because the IF-300 does not have an access port, the hydraulic ram had to be inserted through the back of the module to pull the canister into the module. To allow access to the back of the modules, the system used in the ISFSI was configured so that the three modules are side-by-side (1x3 array).

For reference, the modules have been arbitrarily numbered HSM-1 through HSM-3 from left to right as viewed from the docking port end (front) of the modules. The three-module monolith is symmetrical about the axial centerline of the center module (HSM-2). Taking advantage of this symmetry, half of the structure (all of HSM-3 and half of HSM-2) was instrumented with thermocouples to provide an estimate of the thermal performance of the overall structure. The two storage modules were instrumented with 54 type J thermocouples (iron-constantan), most of which are imbedded in concrete in three vertical planes along the length of the storage modules, one at the axial center of the modules, and one at either end near the outlet vent. The center array contains 18 thermocouples while the arrays near the vents contain 10 each. In addition, 16 thermocouples have been placed on the sheet metal heat shields located between the top of the canisters and the module ceilings. Each thermocouple is a continuous run of thermocouple wire from its location in the module to a terminal board near the DAS. A short run of thermocouple extension wire connects the terminal board to the DAS.

Two airflow transducers were installed in the module air inlets during electrically heated test runs. The early data from the transducers were erratic and judged to be unreliable. An investigation found that the transducers were full of water and completely inoperative. The transducers were replaced late in the spent fuel test but again proved to be unreliable. Data from these transducers were not used in the evaluation.

The DSC provides the primary containment and structural support for the spent fuel assemblies in storage. The DSC consists of a stainless steel cylindrical shell with shield plugs at each end and an internal basket to support seven PWR spent fuel assemblies.

The cylindrical shell is made of rolled 0.6-in.-thick stainless steel, 37 in. in diameter, and 180 in. long. The shielded end plugs contain approximately 5 in. of lead in a stainless steel casing and are welded to the outer shell. The shield plugs reduce the radiation dose to operating personnel during canister loading, drying and sealing operations and during transfer procedures at the HSM.

The internal basket of the DSC contains seven square fuel tubes made of a boron/aluminum alloy with stainless steel cladding. The tubes are designed to support the fuel assemblies and maintain criticality control during the fuel-loading process in the spent fuel pool.

During the fuel-loading process, the DSC is vacuum dried and backfilled with a helium cover gas at 1 atmosphere, then sealed with welds at all penetrations. The helium cover-gas provides an inert atmosphere to limit oxidation of the spent fuel and provides a relatively high thermal conductivity to optimize the transfer of decay heat to the outer shell of the canister.

Two DSCs, arbitrarily numbered DSC-1 and DSC-2, were instrumented to provide thermal data to support the demonstration. Each DSC contains 25 type J thermocouples to monitor the temperature of the outer shell of the canister, the end caps, the center spacer disc, and the center guide tube in five of the stored fuel assemblies. The thermocouple leads are routed to the end of the canister and exit through a specially designed fitting that provides a redundant seal to maintain canister integrity. The leads are then terminated in a multi-pin connector. A continuous run of thermocouple extension wire connects the mating plug to a terminal board near the data acquisition system. A short run of thermocouple extension wire connects each thermocouple pair on the terminal board to the DAS.

The cask used by CP&L to transfer the loaded DSCs from the reactor building to the ISFSI is a GE IF-300 transportation cask licensed by the NRC. The cask can be configured to transport either PWR or boiling water reactor (BWR) fuel by changing the internal basket and the closure head. The BWR configuration holds 18 assemblies, and the PWR version has a capacity of 7 assemblies. Both configurations weigh approximately 135,000 lb fully loaded.

The cask body is nominally 64 in. OD, 37.5 in. ID, and 169 in. long. The cask contains an inner basket that provides structural support and criticality control for the contained fuel assemblies. The cask body, bottom and closure head are made of stainless steel, clad-depleted uranium to provide radiation shielding. The outer body of the cask is encircled by a thin-walled corrugated stainless steel water jacket extending axially over the active length of the contained fuel assemblies to provide neutron shielding. The bottom of the cask and the closure heads are fitted with an array of radial fins designed to absorb impact energy in the event of an accident.

The fuel rods in a fuel assembly are arranged in a square array with 15 rod locations per side and a nominal rod-to-rod centerline pitch of 0.563 in. Of the possible 225 rod locations per assembly, 20 are occupied by guide tubes for control rods and burnable poison rods, and one central thimble is reserved for in-core instrumentation. The remaining 204 locations contain fuel rods.

APPENDIX B

THERMAL DATA

APPENDIX B

THERMAL DATA

This appendix contains the fuel load patterns and a collection of temperature plots taken from the performance reports. In the data plots, the temperature points have been connected with lines to help the reader. On the plots that show COBRA-SFS or HYDRA code predictions, the lines represent the predictions and the data points are not connected. The data will be presented for each cask or storage system.

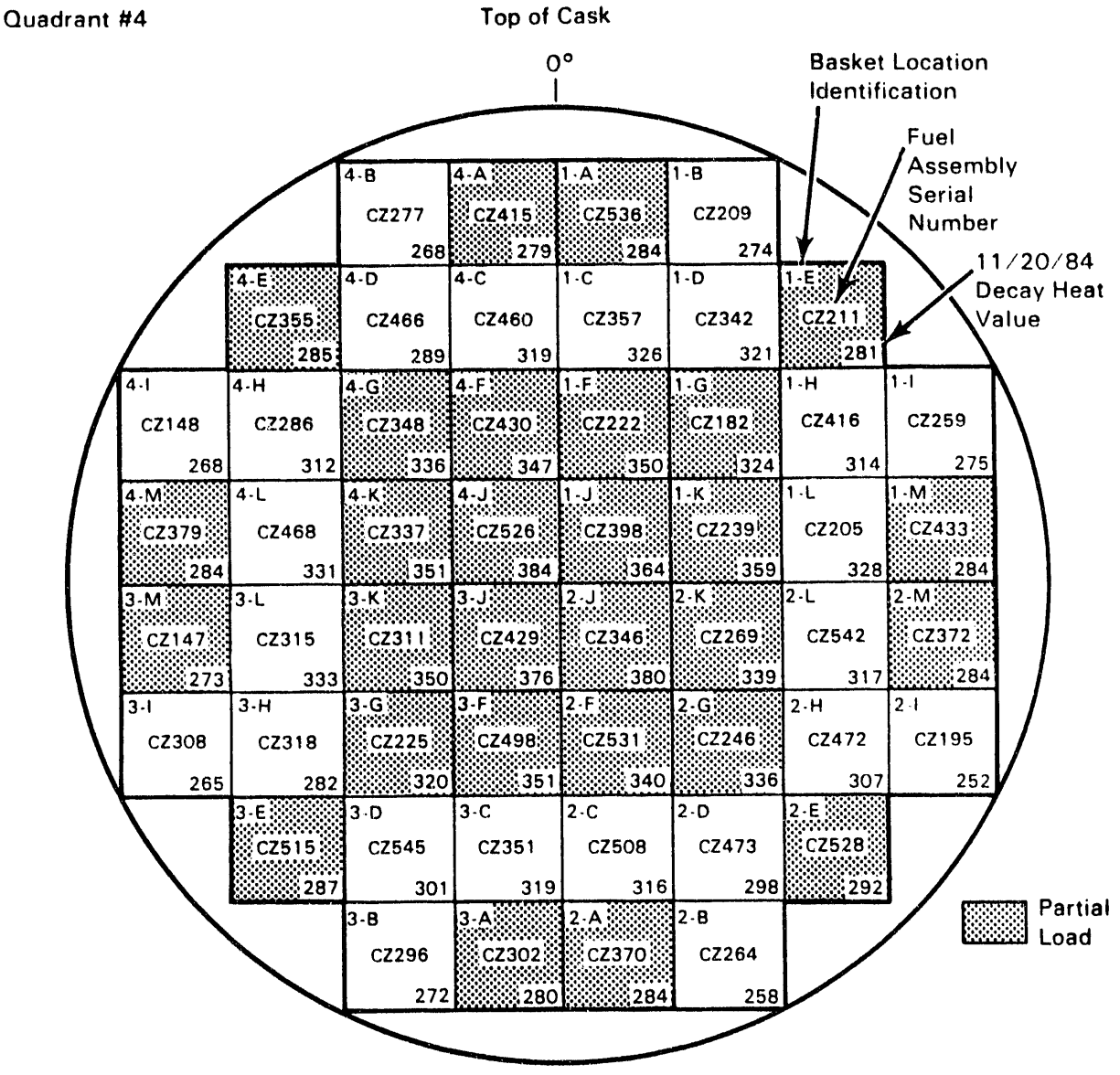

FIGURE B.1. BWR Spent Fuel Load Pattern for the REA-2023 Cask (McKinnon 1986: p. 3.18)

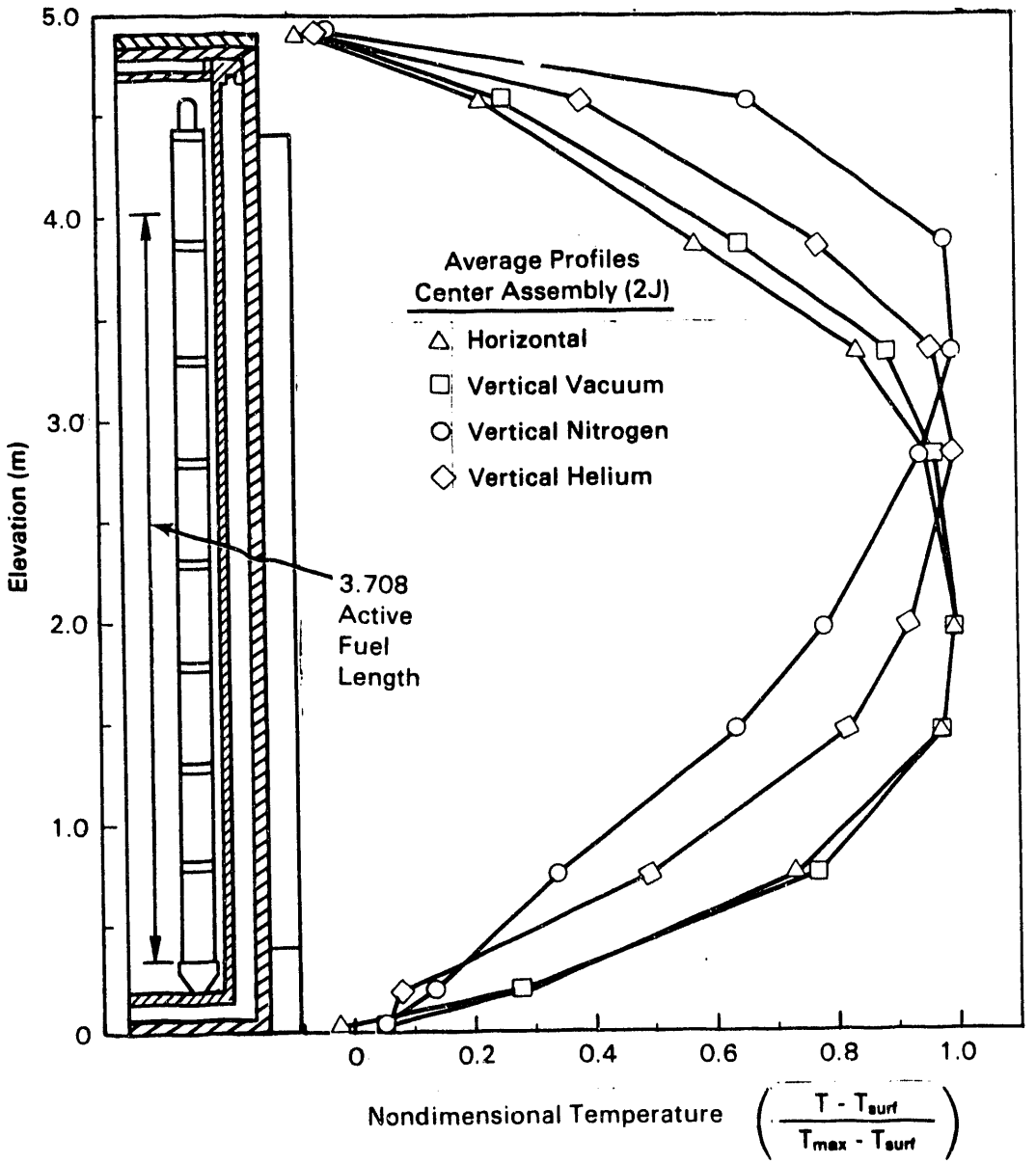

FIGURE B.2. Normalized Axial Fuel Temperature Profiles for the REA-2023 Cask Showing the Effect of Fill Gas and Cask Orientation (McKinnon 1986: p. 5.36)

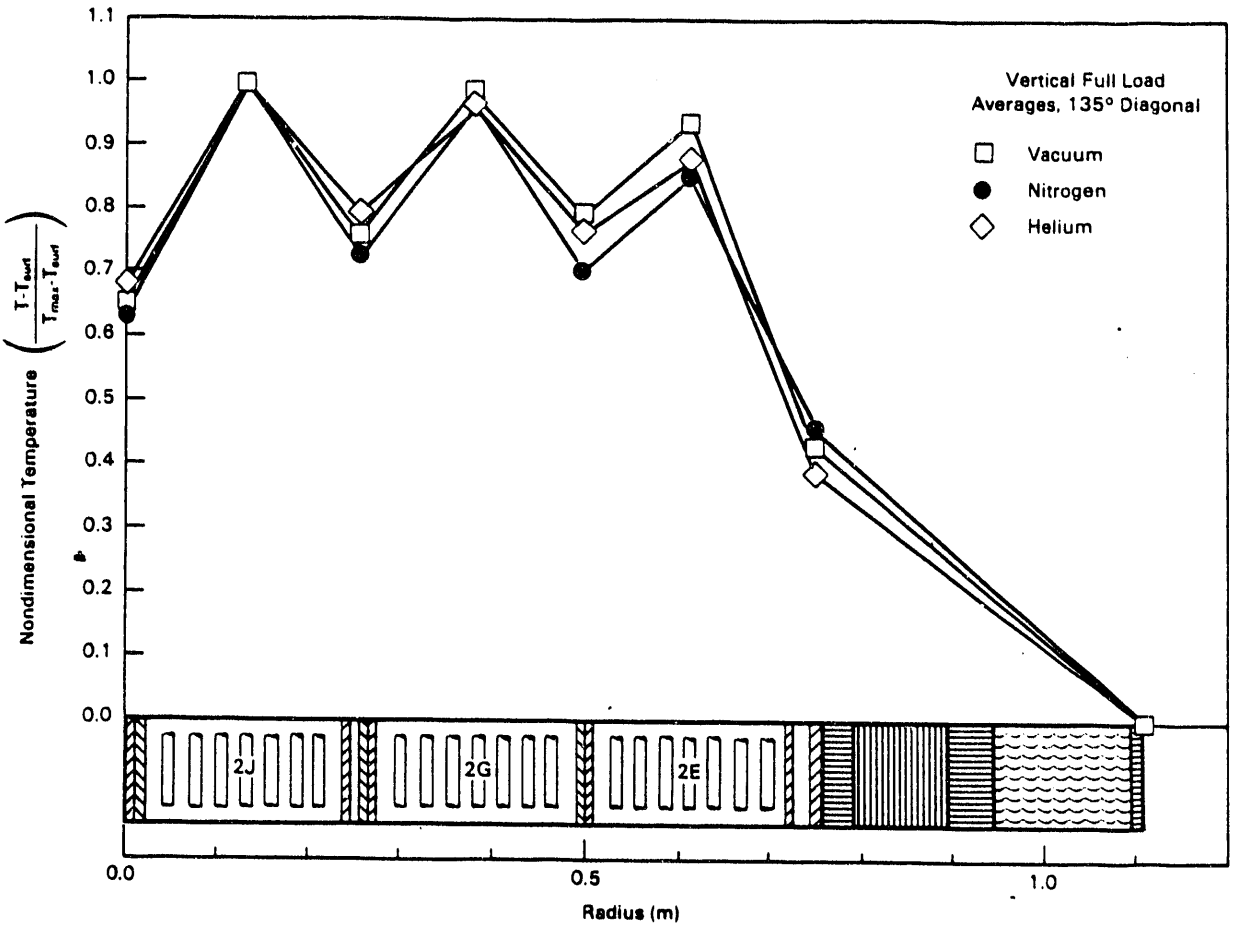

FIGURE B.3. Normalized Radial Fuel Temperature Profiles for the REA-2023 Cask Showing the Effects of Fill Gas and Cask Orientation (McKinnon 1986: p. 5.38)

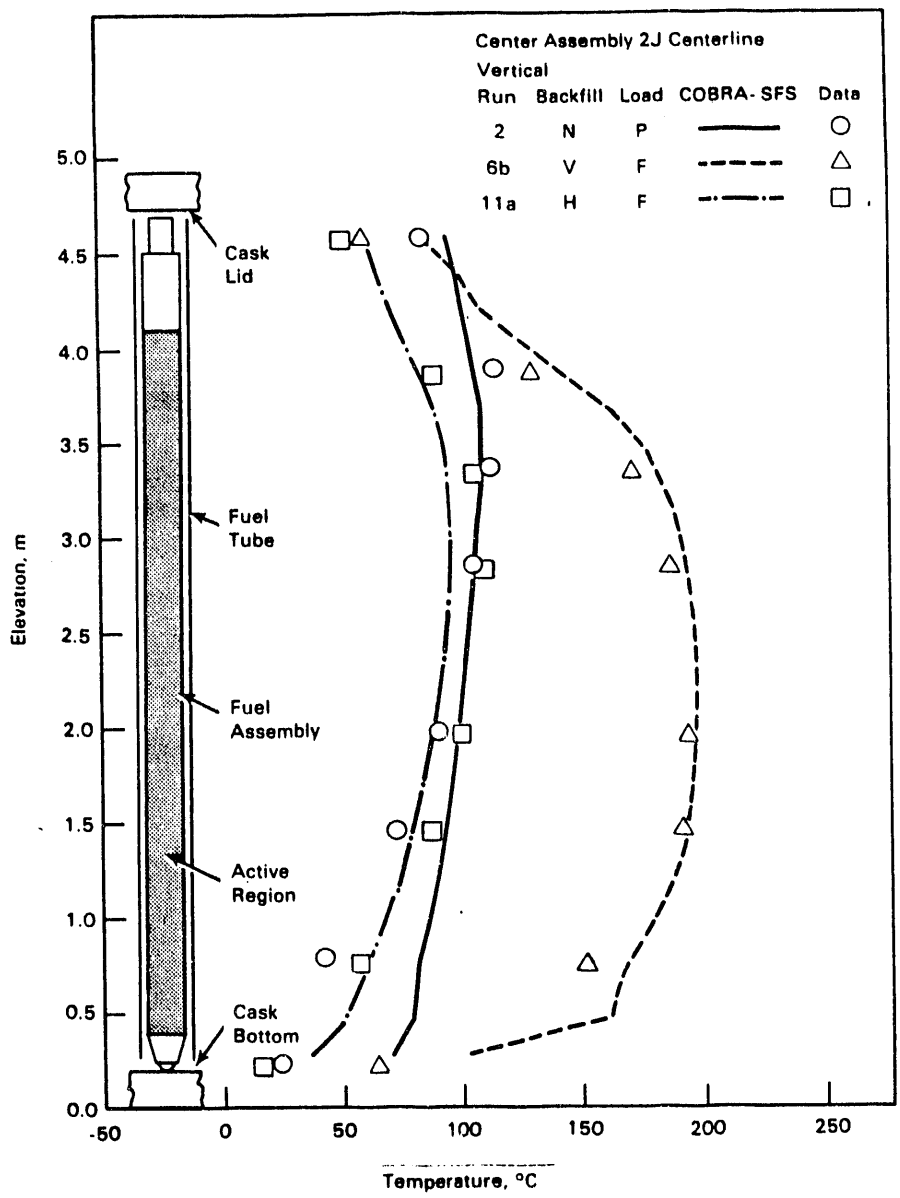

FIGURE B.4. HYDRA Pretest Predictions of REA-2023 Cask, Center Assembly Axial Temperature Profiles Compared to Full Load, Vertical Vacuum, Nitrogen, and Helium Data (Wiles 1986: p. xi)

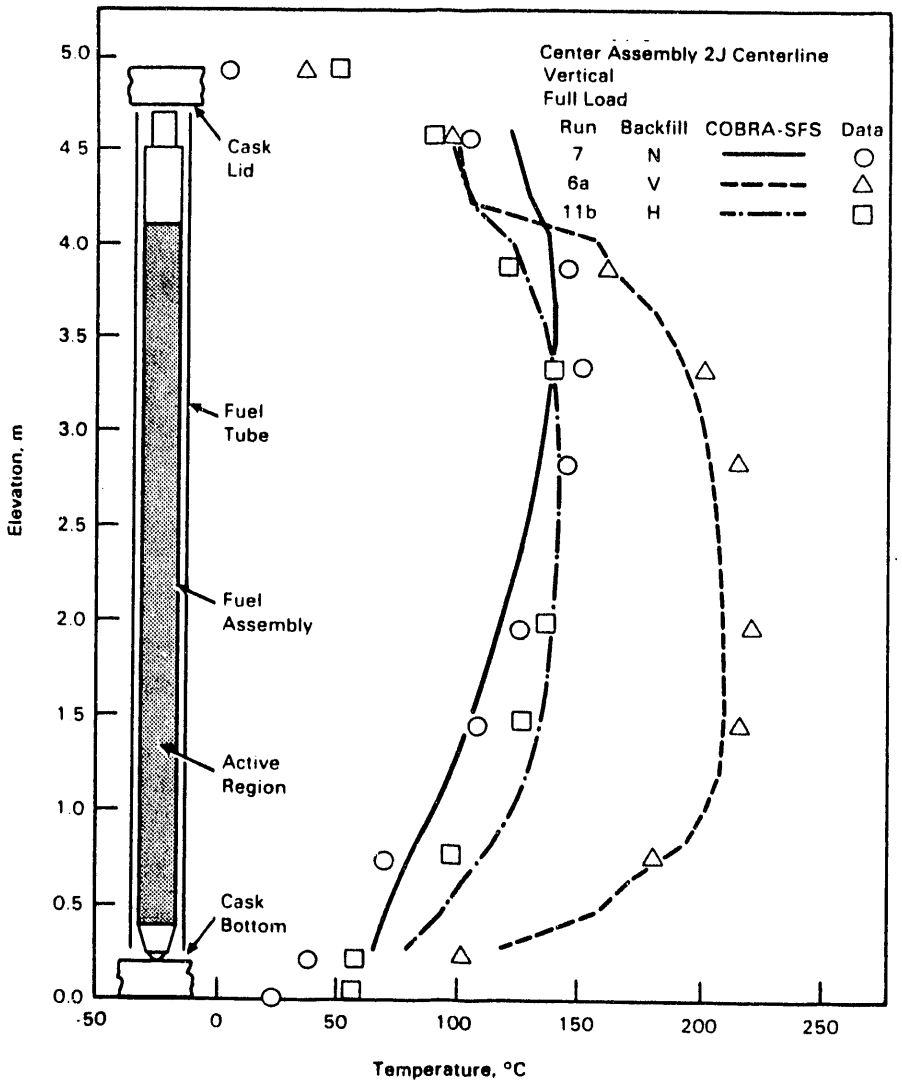

FIGURE B.5. COBRA-SFS Pretest Prediction of REA-2023 Cask, Center Assembly Axial Temperature Profiles Compared to Vertical, Full Load, Vacuum, Nitrogen, and Helium Data (Wiles 1986: p. xiv)

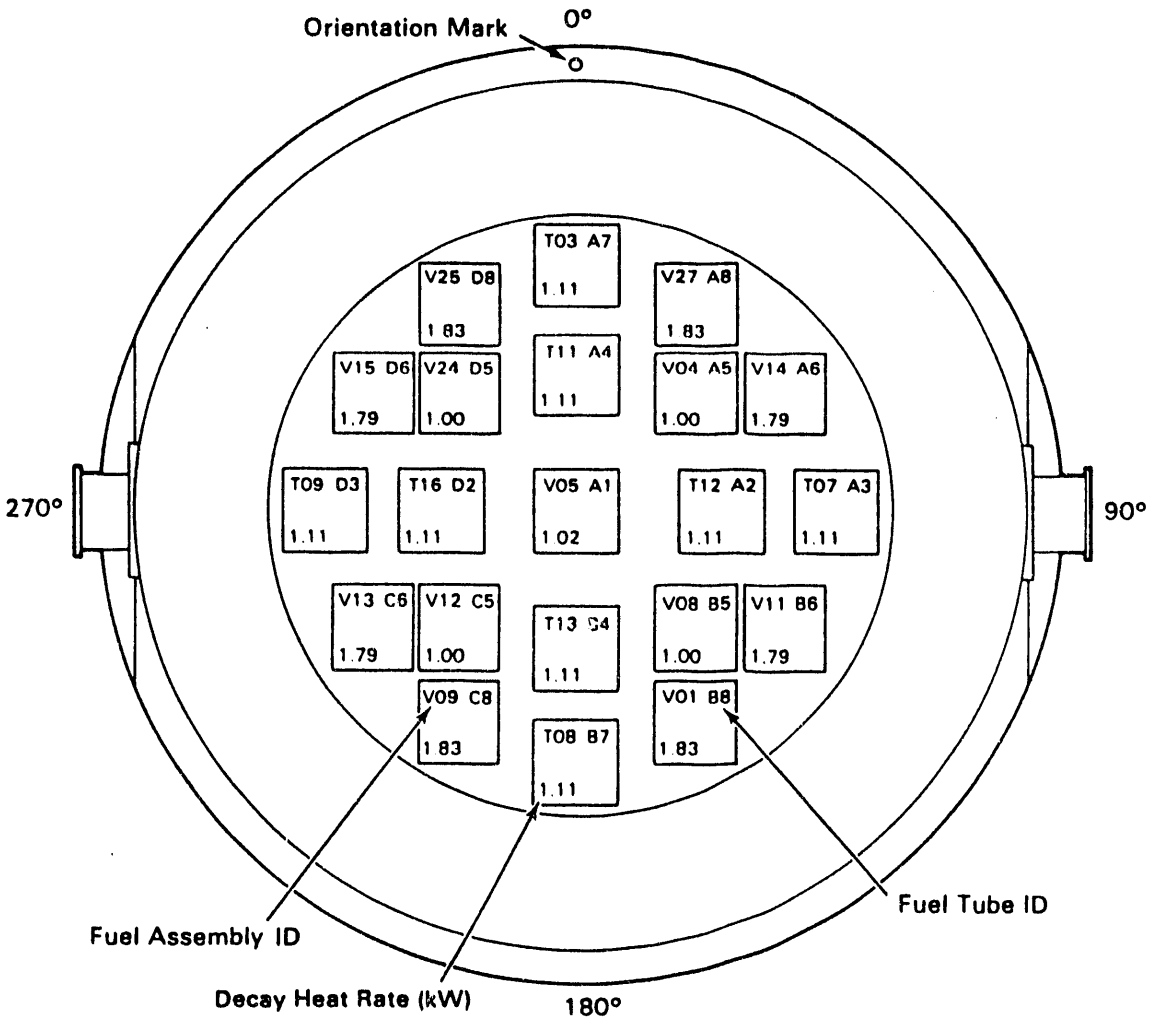

FIGURE B.6. PWR Spent Fuel Load Pattern for the CASTOR-V/21 Cask (Creer 1986: p. 3-22)

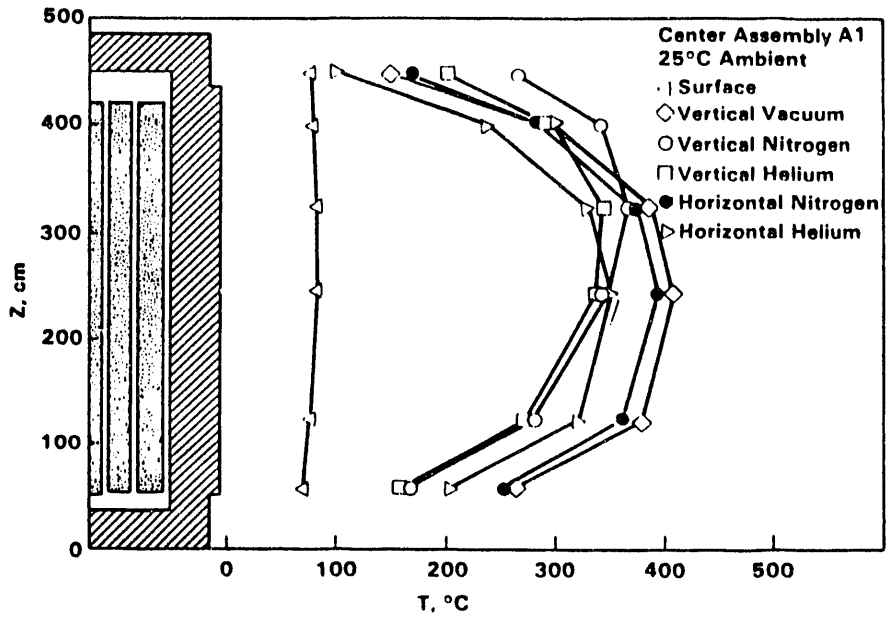

FIGURE B.7. Center Assembly Axial Temperature Profiles for the CASTOR-V/21 Cask Loaded with PWR Spent Fuel (Creer 1986: p. S-6)

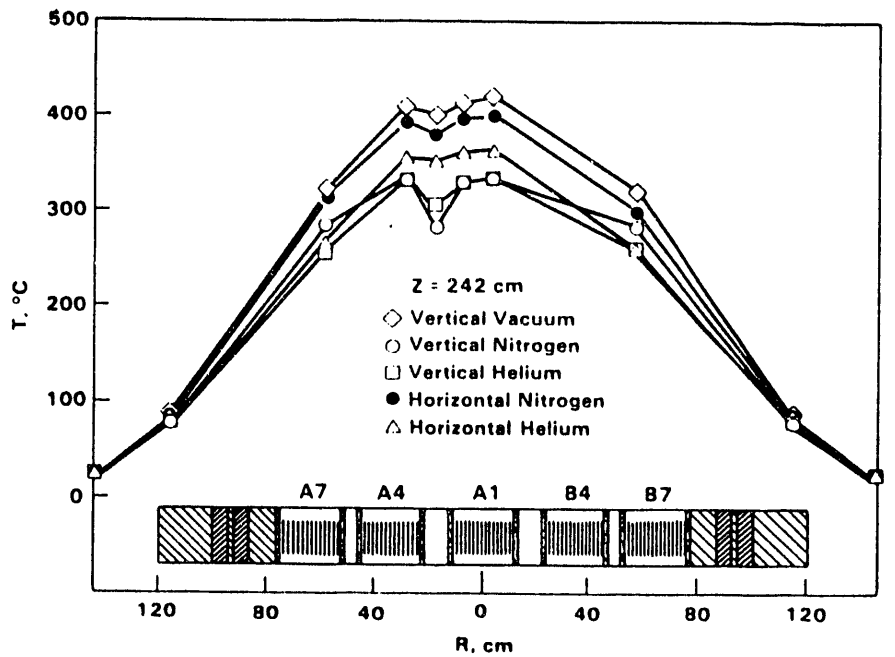

FIGURE B.8. Radial Temperature Profiles Near the Peak Axial Temperature Location for the CASTOR-V/21 Cask Loaded with PWR Spent Fuel (Creer 1986: p. S-7)

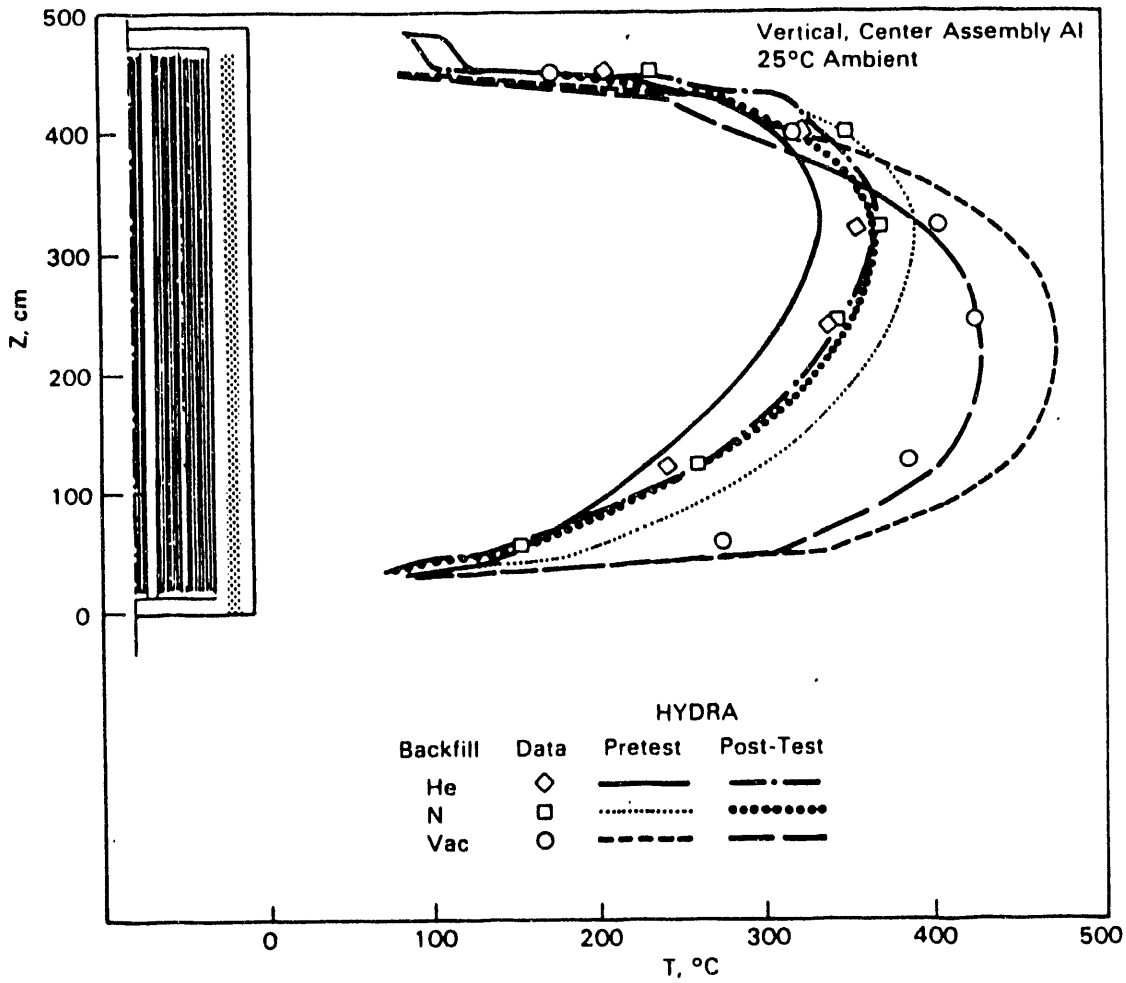

FIGURE B.9. Axial Temperature Profile Predictions for the CASTOR-V/21 Cask Compared to Vertical, Vacuum, Nitrogen, and Helium Data (Creer 1986: p. S-9)

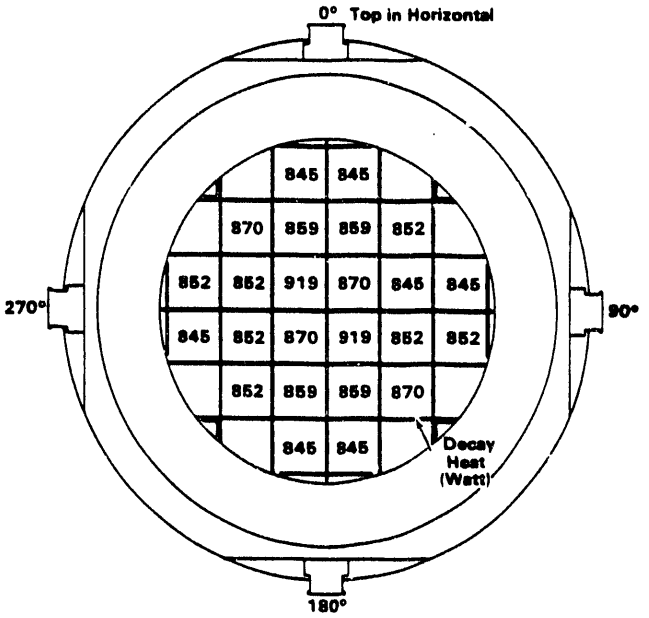

FIGURE B.10. PWR Spent Fuel Load Pattern for the TN-24P Cask (McKinnon 1987a: p. 3-28)

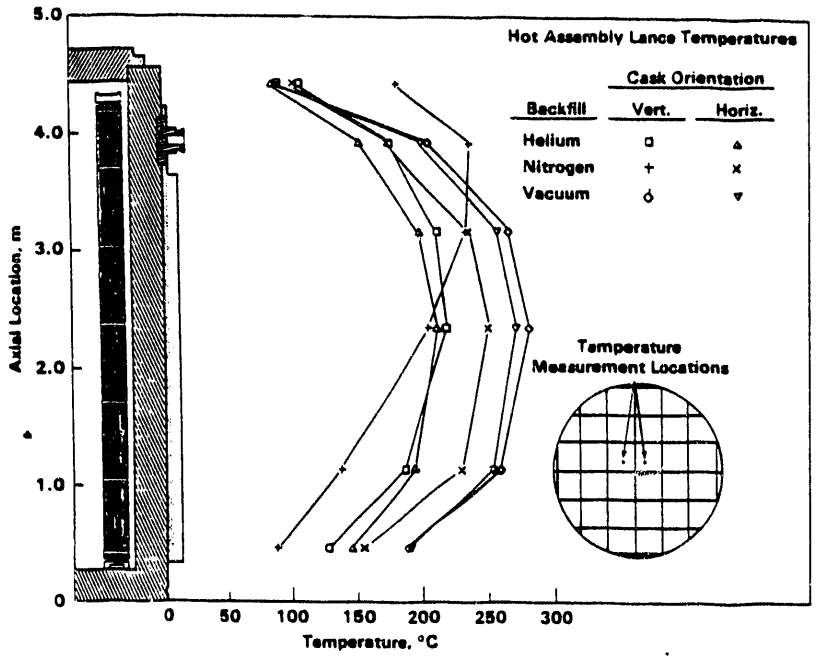

FIGURE B.11. Center Fuel Assembly Axial Temperature Profiles for the TN-24P Cask Loaded with PWR Spent Fuel (McKinnon 1987a: p. S-7)

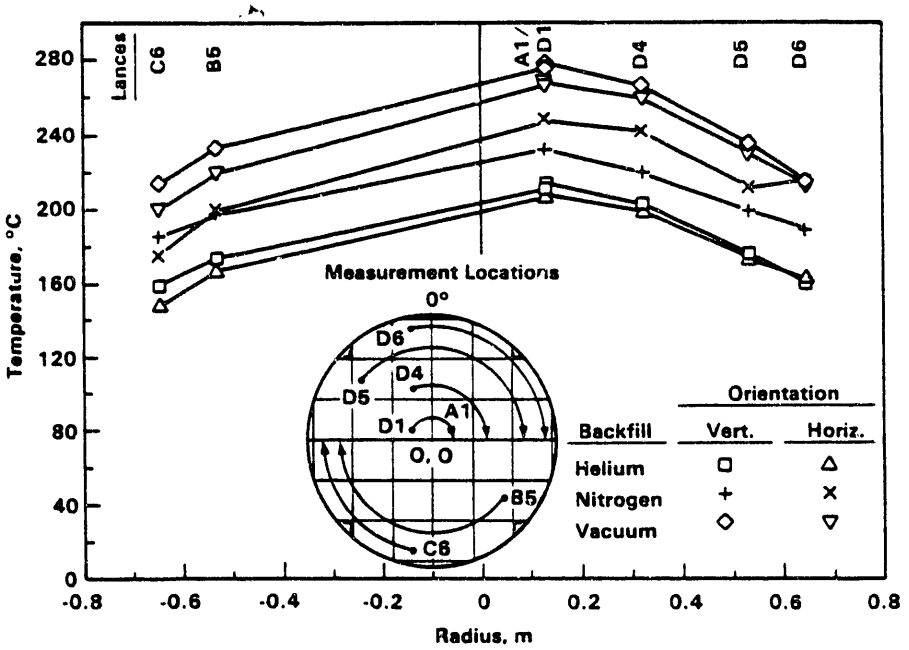

FIGURE B.12. Radial Temperature Profiles Near the Peak Axial Temperature Location for the TN-24P Cask Loaded with PWR Spent Fuel (McKinnon 1987a: p. S-8)

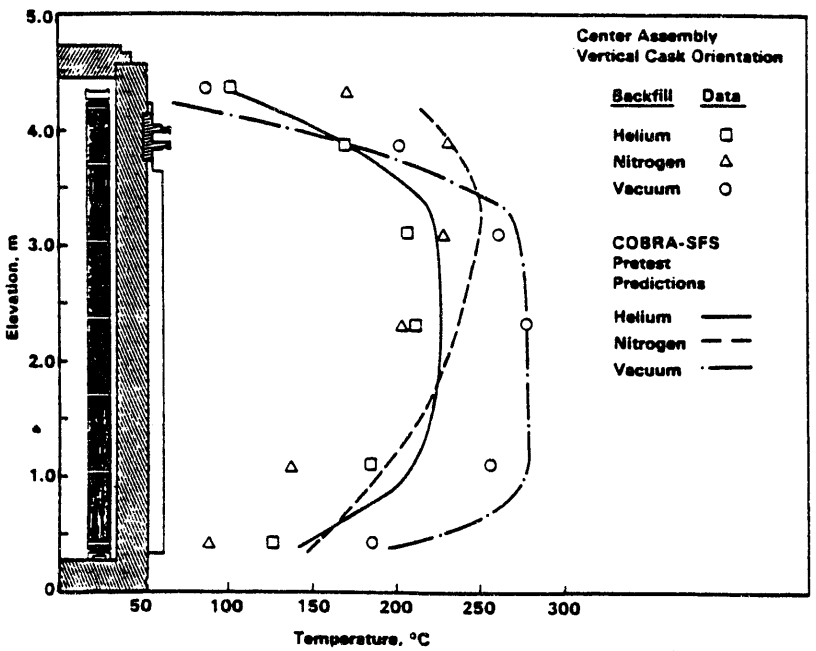

FIGURE B.13. Pretest Axial Temperature Profile Prediction for the TN-24P Cask Loaded with PWR Fuel Compared to Vertical, Vacuum, Nitrogen, and Helium Data (McKinnon 1987a: p. S-10)

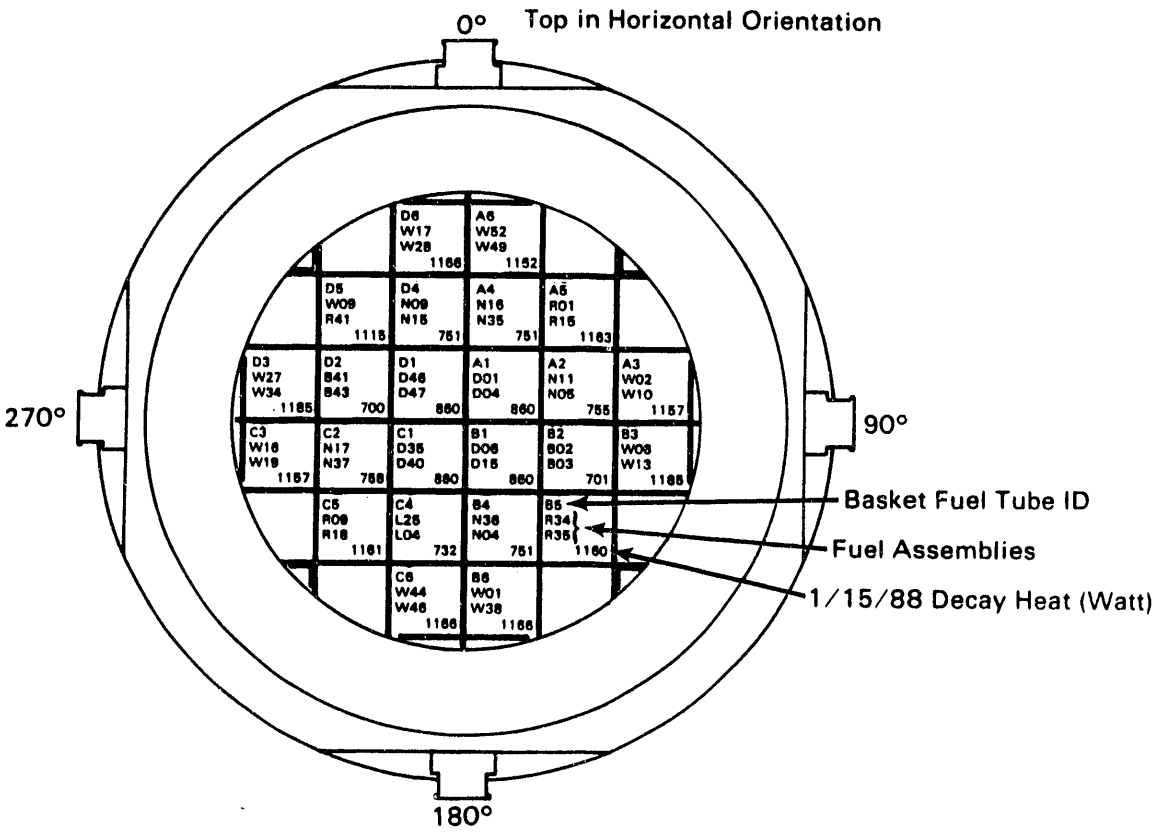

FIGURE B.14. Spent Fuel Load Pattern for the TN-24P Cask Loaded with Consolidated PWR Spent Fuel (McKinnon 1989: p. 3-26)

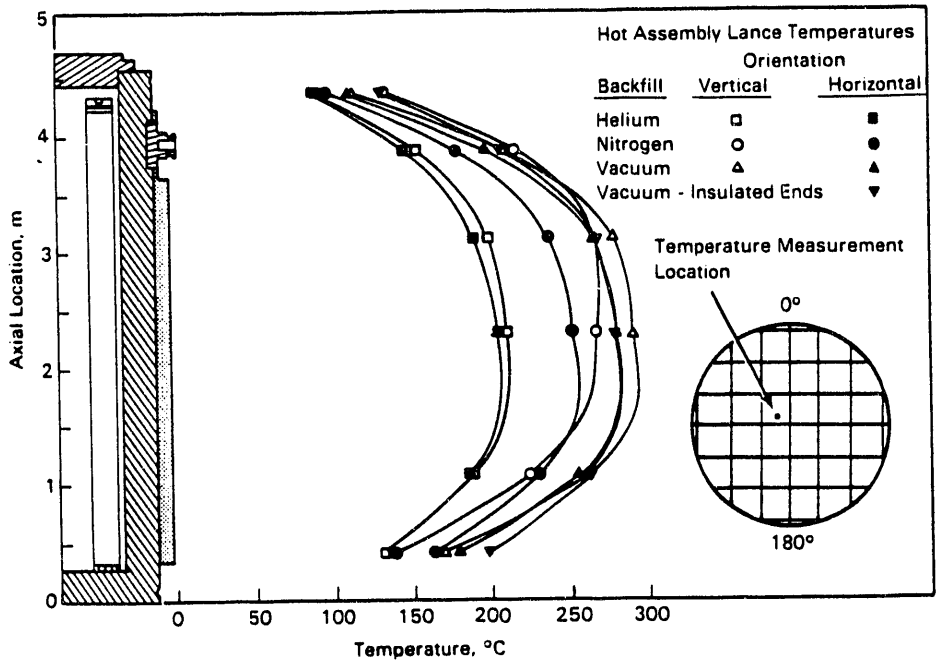

FIGURE B.15. Center Fuel Canister Axial Temperature Profiles for the TN-24P Cask Loaded with Consolidated PWR Spent Fuel (McKinnon 1989: p. S-7)

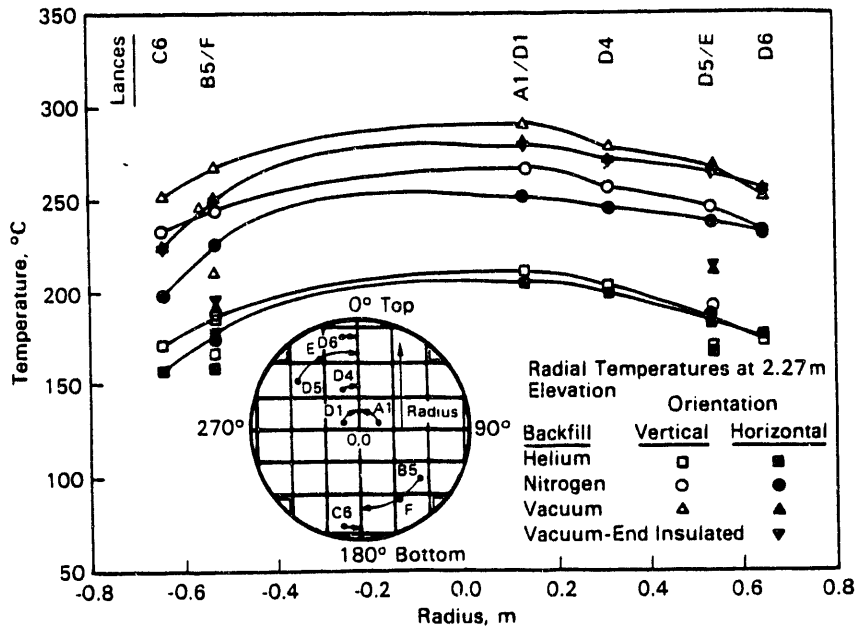

FIGURE B.16. Radial Temperature Profiles Near the Peak Axial Temperature Location for the TN-24P Cask Loaded with Consolidated PWR Spent Fuel (McKinnon 1989: p. S-8)

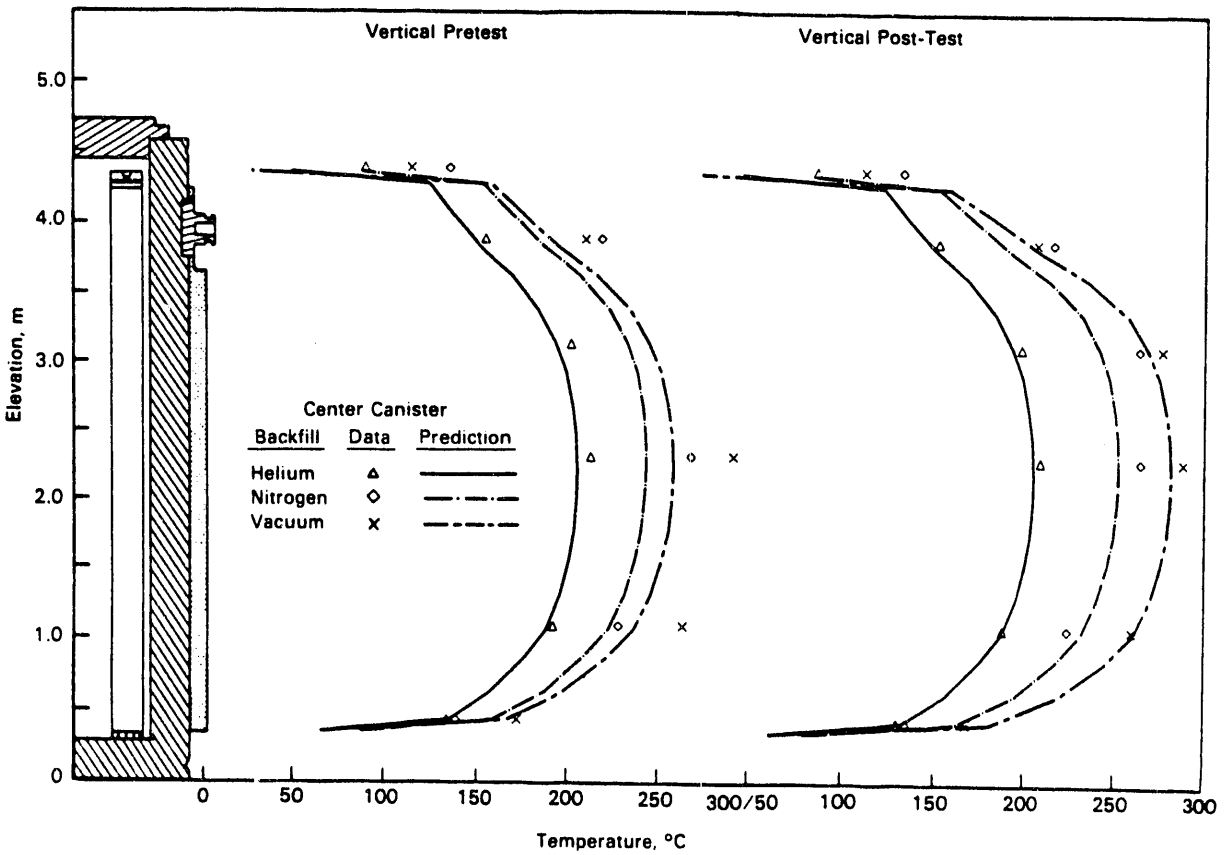

FIGURE B.17. Axial Temperature Profile Prediction for the TN-24P Cask Loaded with Consolidated PWR Spent Fuel Compared to Vertical, Vacuum, Nitrogen, and Helium Data (McKinnon 1989: p. S-11)

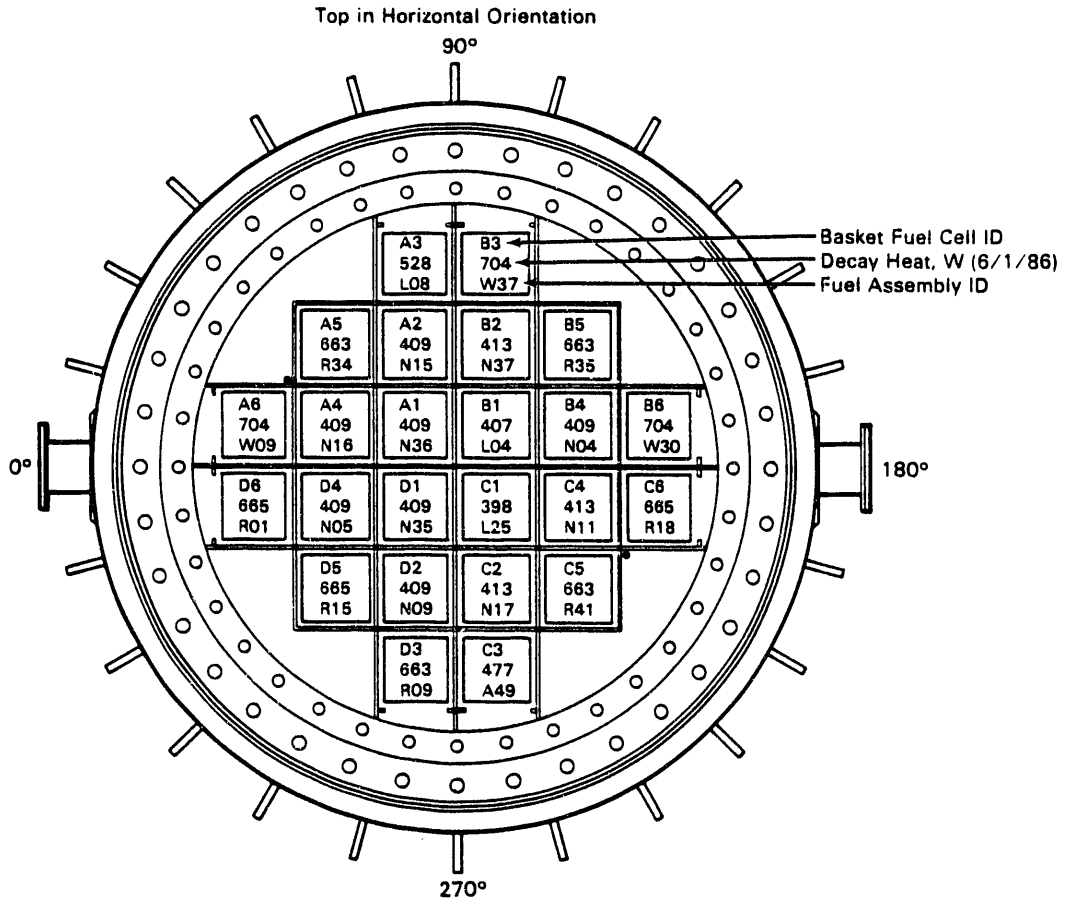

FIGURE B.18. PWR Spent Fuel Load Pattern for the MC-10 Cask (McKinnon 1987b: p. S-4)

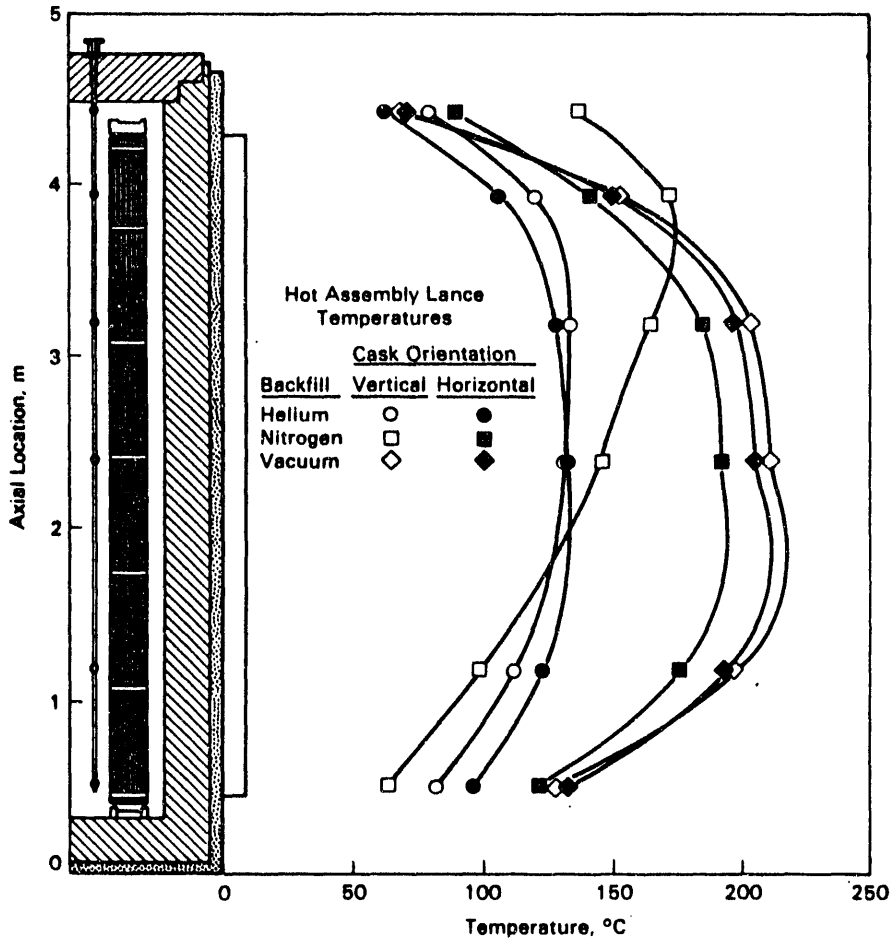

FIGURE B.19. Center Fuel Assembly Axial Temperature Profiles for the MC-10 Cask Loaded with PWR Spent Fuel (McKinnon 1987b: p. S-8)

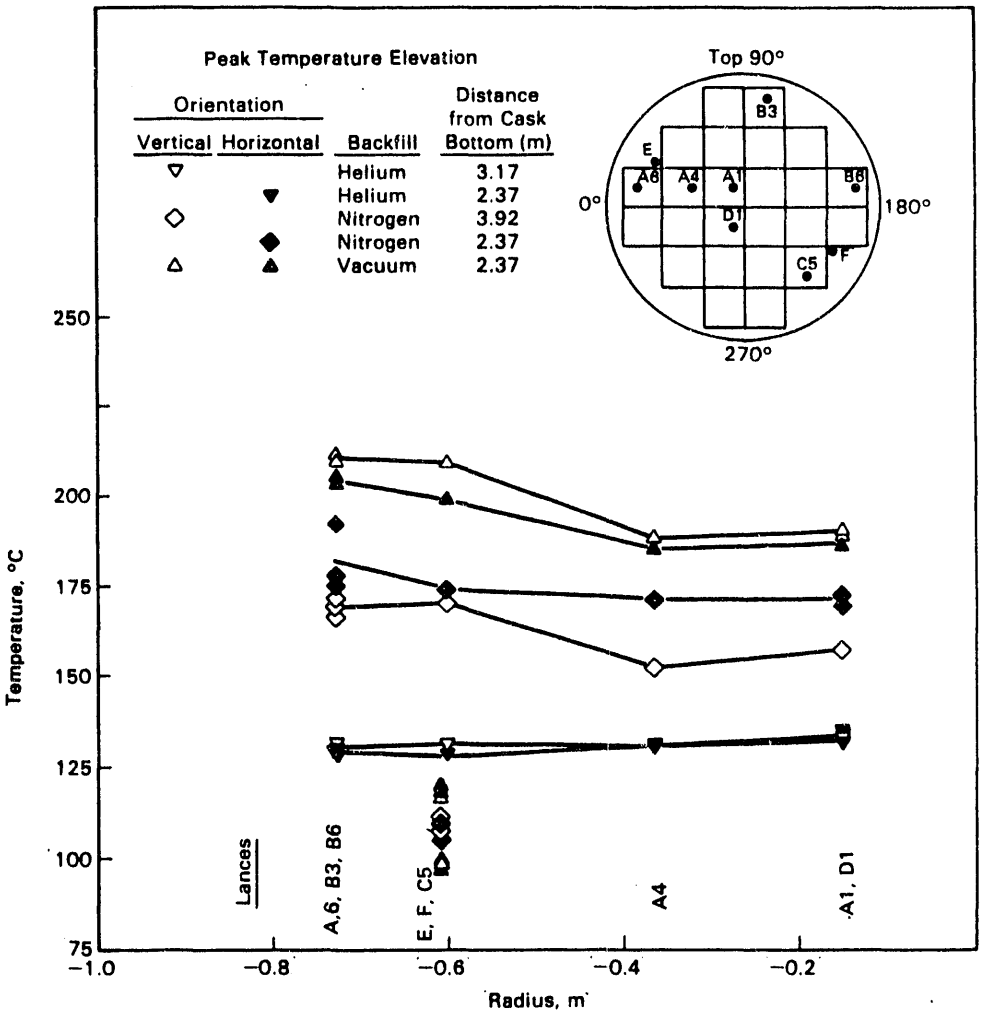

FIGURE B.20. Radial Temperature Profiles Near the Peak Axial Temperature Location for the MC-10 Cask Loaded with PWR Spent Fuel (McKinnon 1987a: p. S-9)

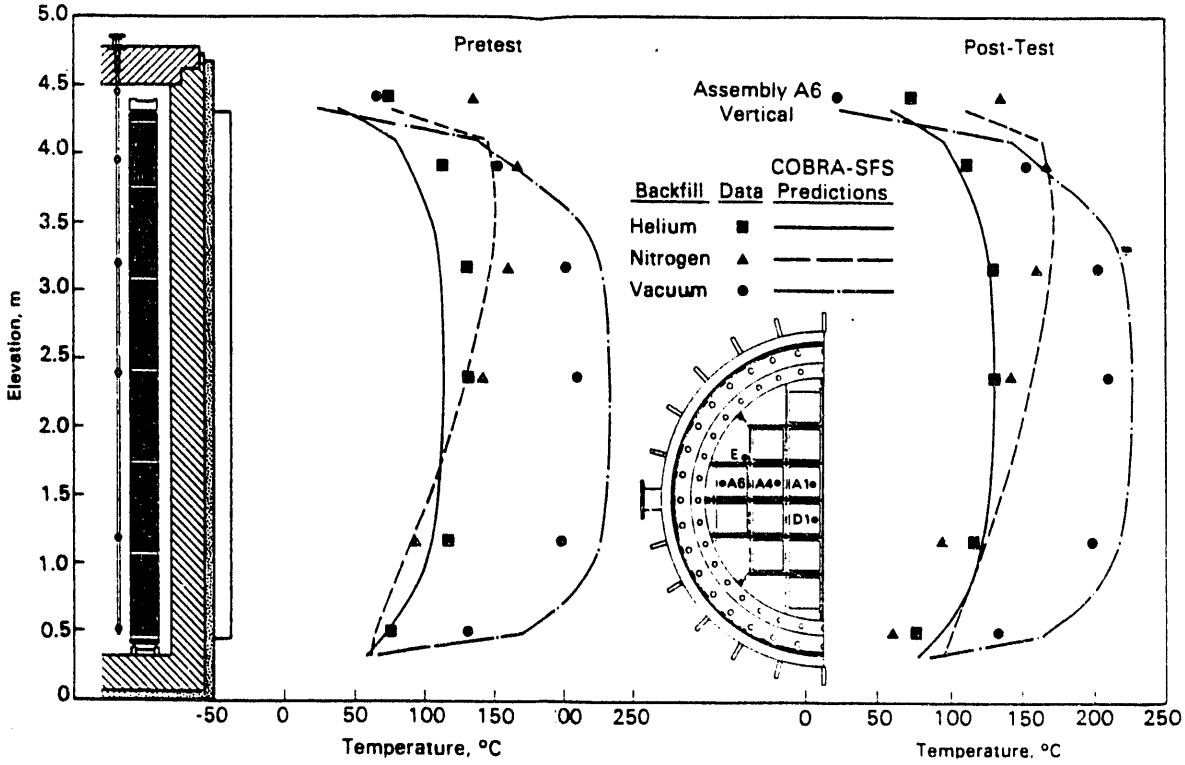

FIGURE B.21. Axial Temperature Profile Prediction for the MC-10 Cask Loaded with PWR Spent Fuel Compared to Vertical, Vacuum, Nitrogen, and Helium Data (McKinnon 1987b: p. S-10)

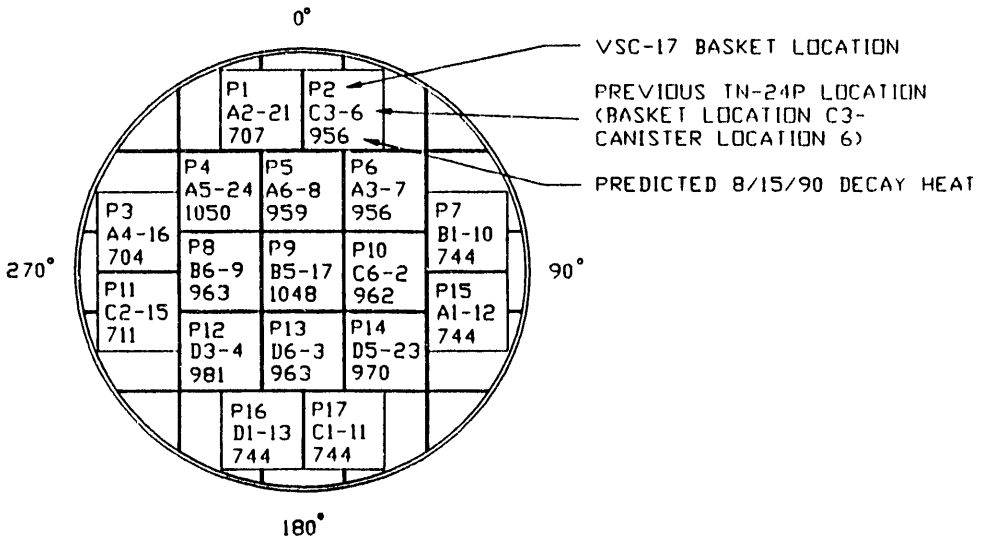

FIGURE B.22. Spent Fuel Canister Load Pattern for the VSC-17 Ventilated Concrete Cask Loaded with PWR Consolidated Spent Fuel (McKinnon 1992: p. 3-18)

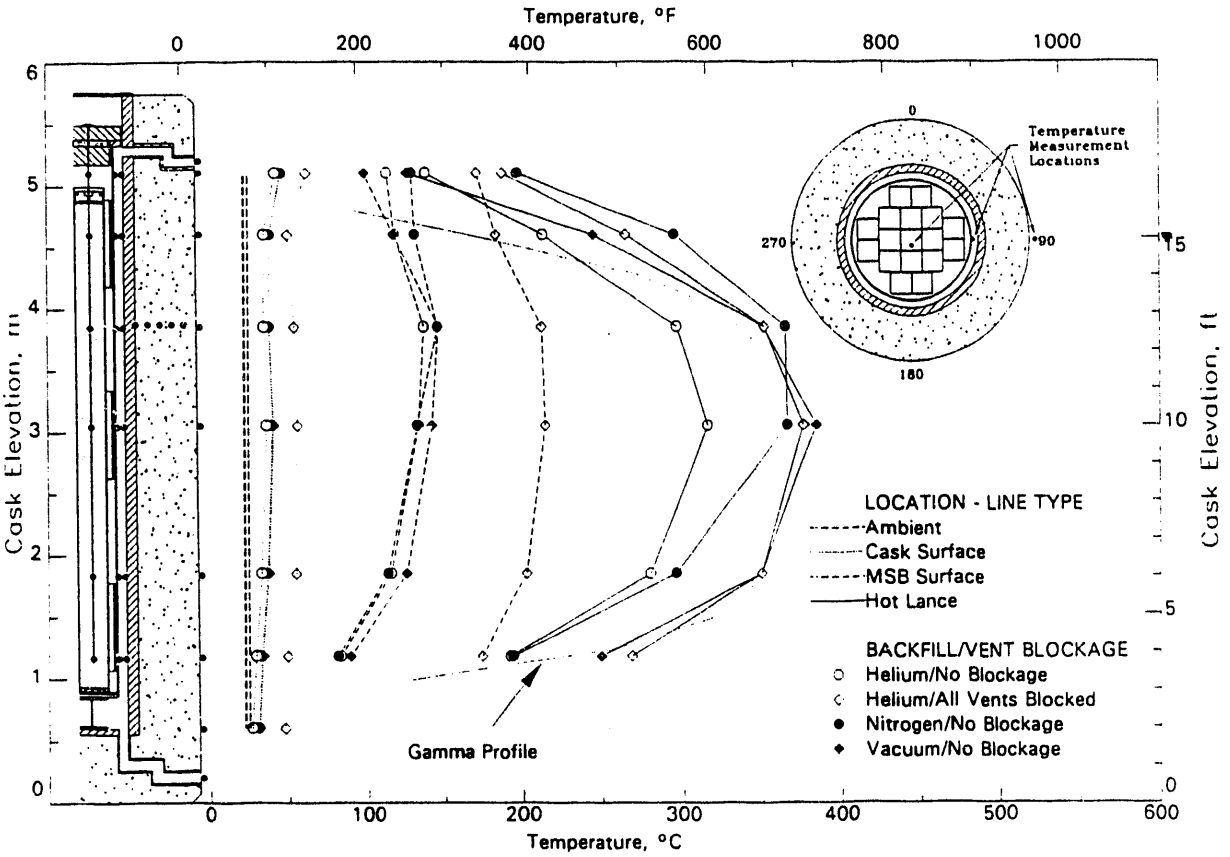

FIGURE B.23. Effect of Gas Environment and Vent Blockage on the Center Fuel Canister Axial Temperature Profiles for the VSC-17 Cask Loaded with Consolidated PWR Spent Fuel (McKinnon 1992: p. S-7)

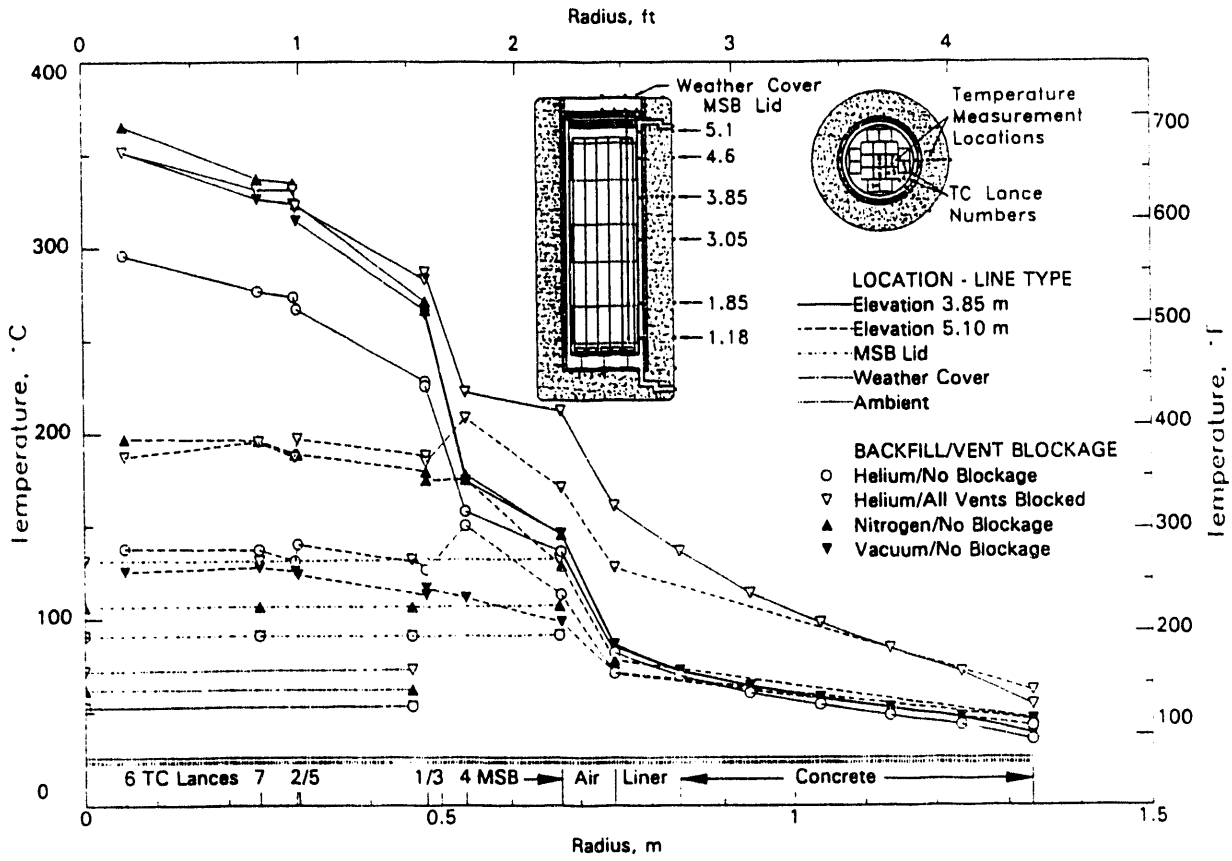

FIGURE B.24. Effect of Gas Environment and Vent Blockage on the Radial Temperature Profiles Measured Near the Peak Axial Temperatures in the VSC-17 Cask Loaded with Consolidated PWR Spent Fuel (McKinnon 1992: p. S-8)

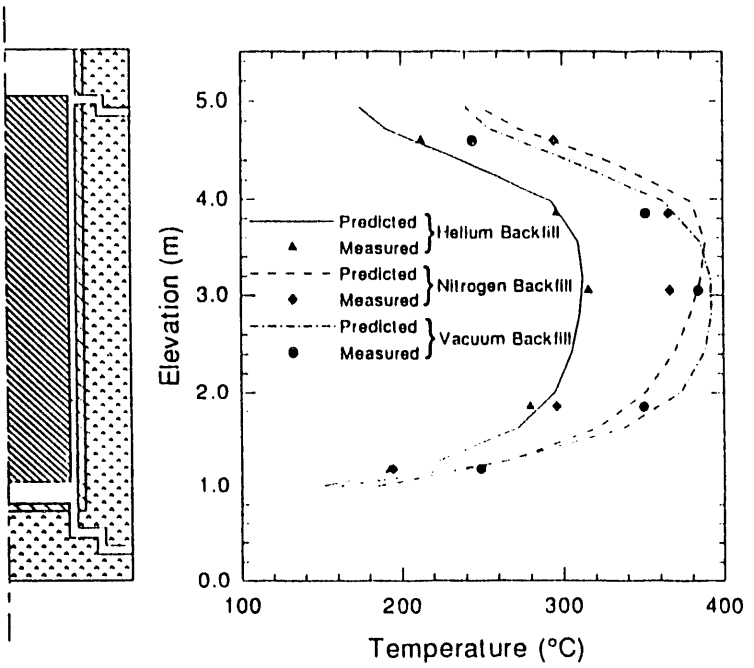

FIGURE B.25. Pretest Axial Temperature Profile Predictions for the VSC-17 Cask Compared to Vacuum, Nitrogen, and Helium Data (McKinnon 1992: p. S-9)

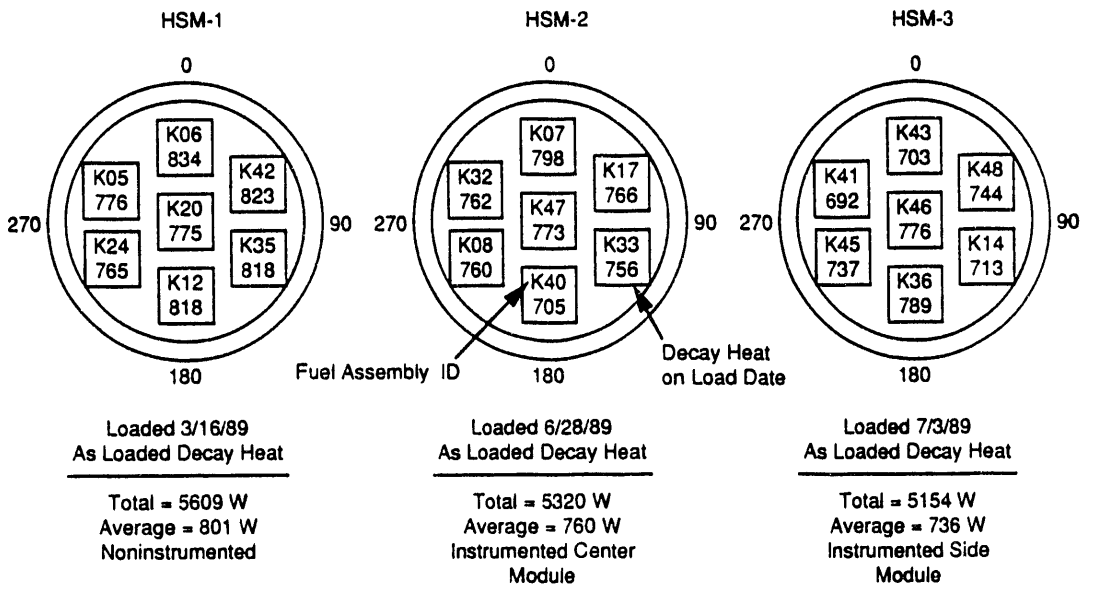

FIGURE B.26. PWR Spent Fuel Load Pattern for the NUHOMS Demonstration at CP&L (Strope 1990: p. 3-16)

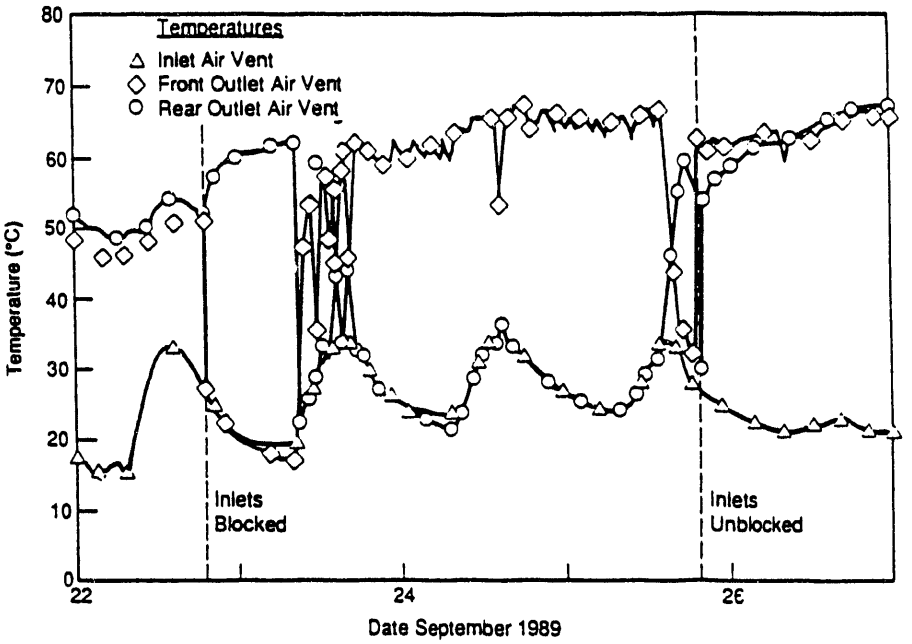

FIGURE B.27. Inlet and Outlet Air Temperature Measurements for the NUHOMs System. Air Temperatures Demonstrate that an Outlet Acts Like an Inlet when the Inlet is Blocked (Strope 1990: p. 4-11).

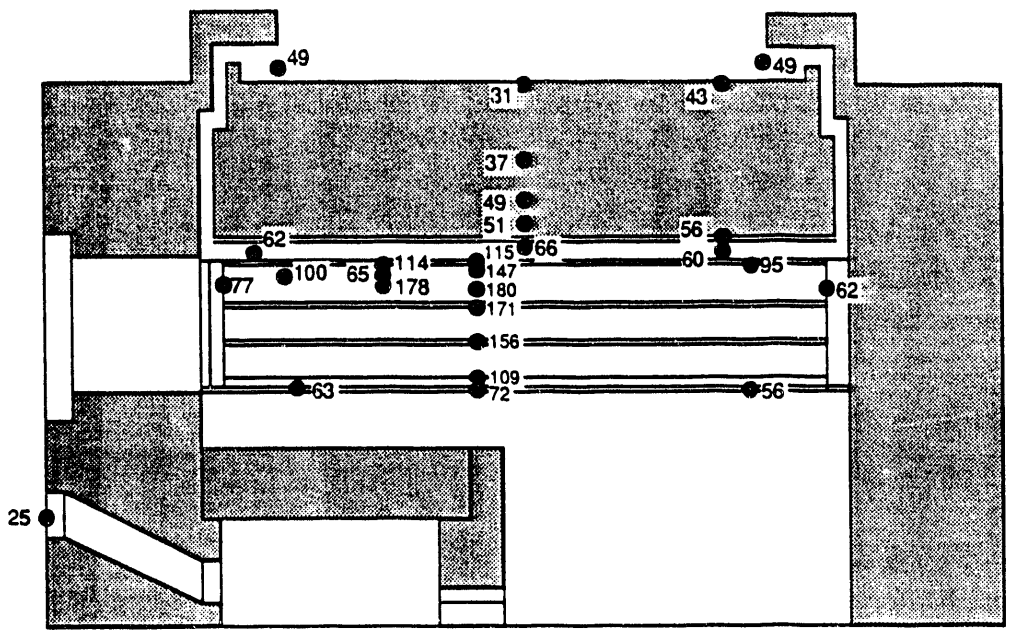

FIGURE B.28. Temperature in the Center Module of the CP&L Demonstrated NUHOMS System on September 21, 1989, with all Modules Loaded with PWR Spent Fuel (Strope 1990: p. 4-22)

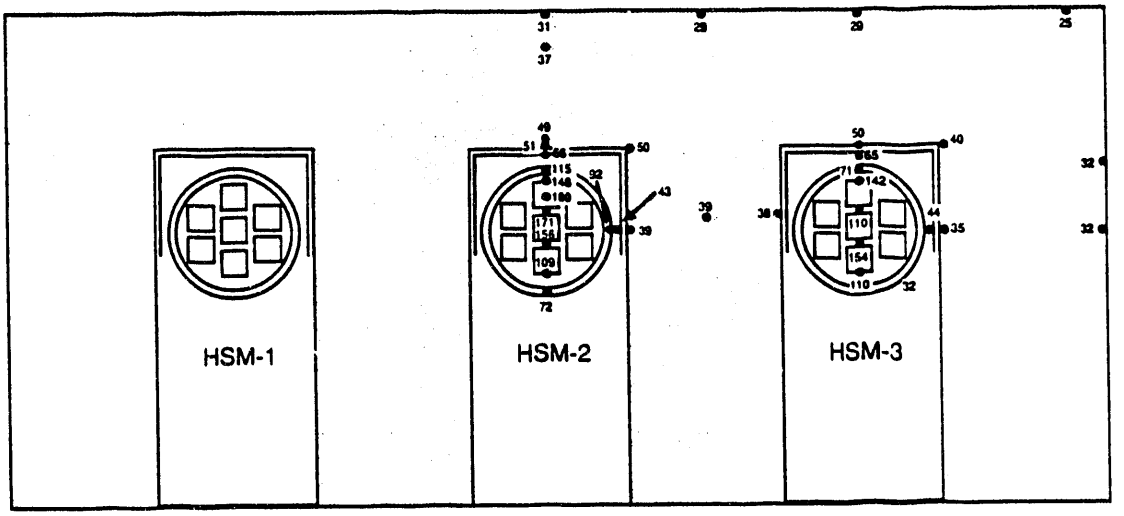

FIGURE B.29. Temperatures in the Center of the CP&L Demonstrated NUHOMS System on September 21, 1989, with all Modules Loaded with PWR Spent Fuel (Strope 1990: p. 4-24)

APPENDIX C

SHIELDING DATA

APPENDIX C

SHIELDING DATA

This appendix contains a collection of plots taken from the performance reports listed in the reference section. Only data points should be considered because the lines are provided for clarity and may not represent actual profiles. The performance report also contain dose information at 1 and 2 meters from the casks at selected locations. The references for the plot in this appendix are included in the figure titles. Table C.1 includes summary information on dose rates. In general, radial spreading smoothes out the peaks and valleys in dose rate observed at the surface of the cask. Table C.1 also includes information on design heat loads and actual heat loads for each storage system. The heat loads can be used to extrapolate dose rates to design conditions. Notice should be taken of fuel type in cask. Consolidation of fuel significantly reduces gamma dose rates.

TABLE C.1. Measured Radiation Dose Equivalent (gamma/neutron), mrem/h

Cask or System Measurement Locations	REA 2023	Castor V/21	TN-24P	TN-24P[a]	MC-10	VSC-17[a]	NUHOMS
Center of Top	28/10	40/44	60/33[b]	15/32	13/58[b]	10/10	[illegible]
Peak on Top	71/None	None	None	None	None	30/10	[illegible]
Upper Peak on Side	37/8	134/15	33/22	11/17	None	70/1	None
Center of Side	14/5	39/16	13/8	7/8	18/18	26/1	[illegible]
Lower Peak on Side	27/16	140/21	54/43	8/40	None	None	None
Center of Bottom	80/27	22/41	143/64	3/66	75/8	--	--
Front Face							15/2
Back Face							10/1
Design Goal (total)	<20	<200	<60	--	<68	<200	50-100
Design Heat Load, kW	20.3	21	24	24	15	17	7
Actual Heat Load, kW	15	21	21	13	13	15	[illegible]

(a) Performance test using consolidated fuel
(b) Measurements taken without the neutron shield in place

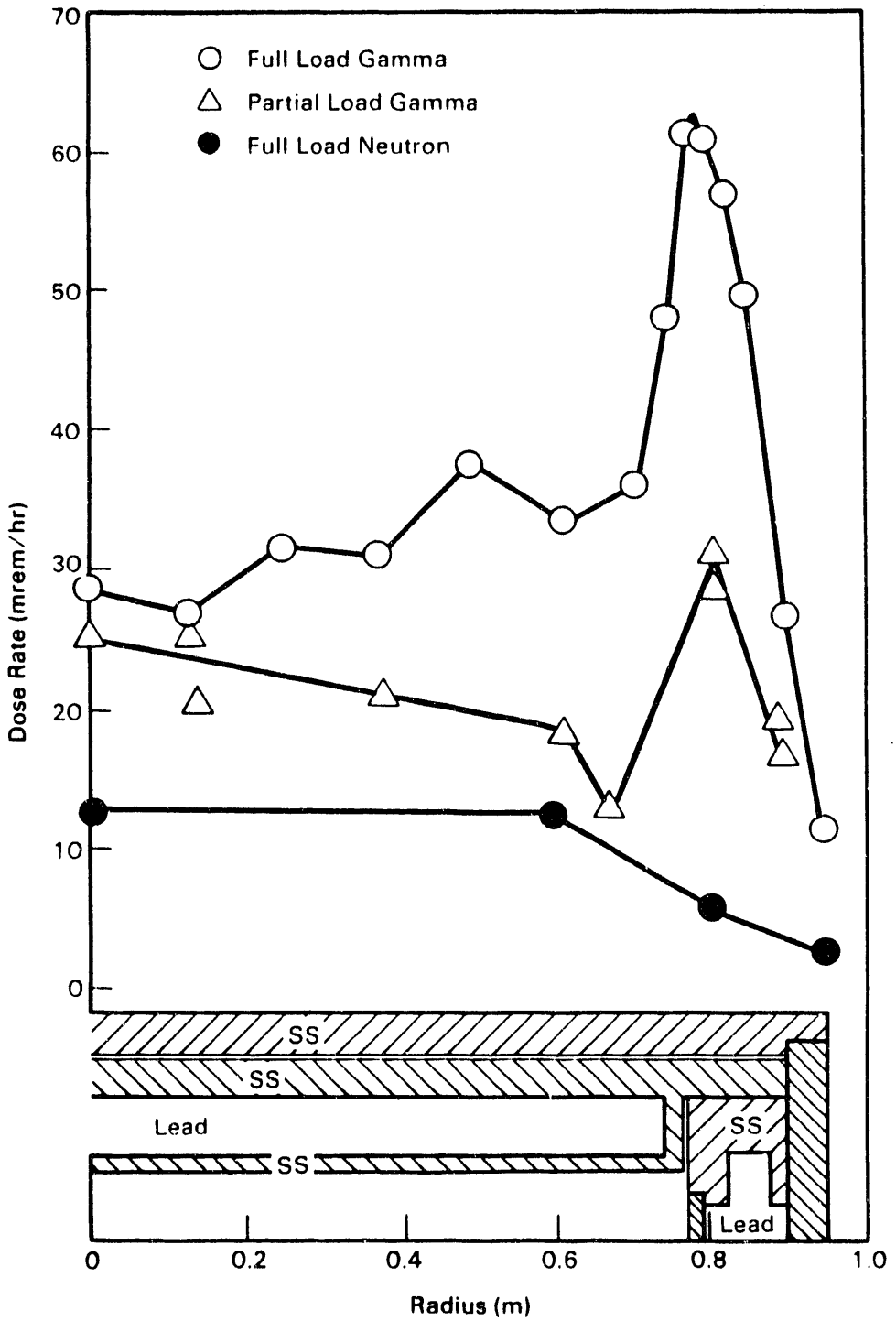

FIGURE C.1. Surface Dose Rate Profiles on the Lid of the REA-2023 Cask Loaded with BWR Spent Fuel (McKinnon 1986: p. 5.52)

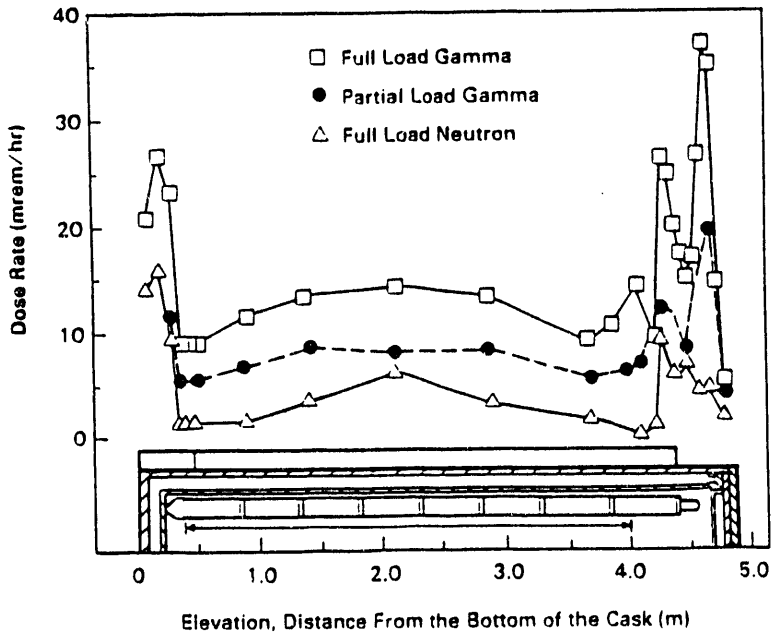

FIGURE C.2. Surface Dose Rate Profiles on the Side of the REA-2023 Cask Loaded with BWR Spent Fuel (McKinnon 1986: p. 5.51)

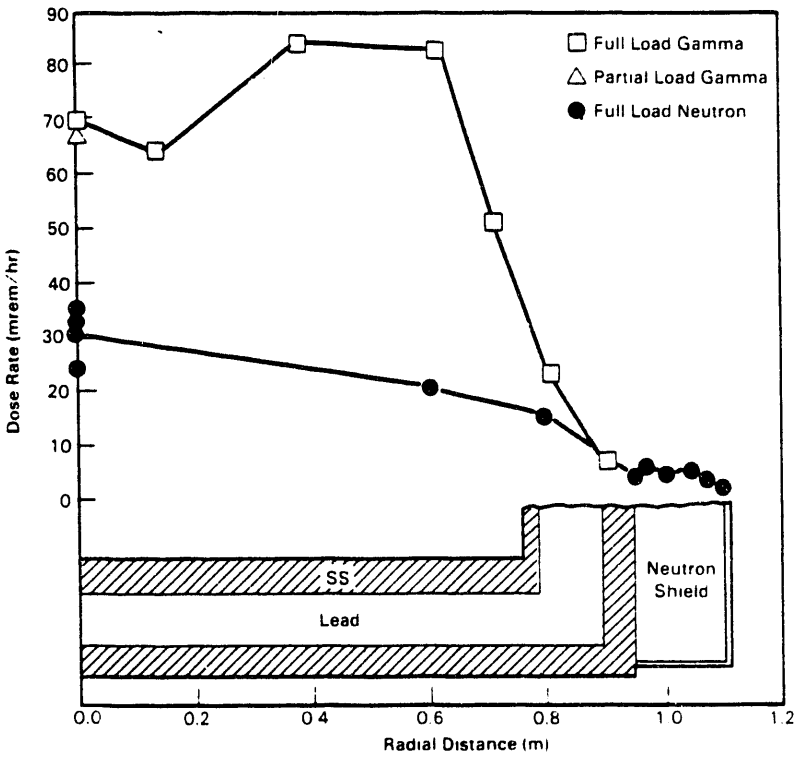

FIGURE C.3. Surface Dose Rate Profiles on the Bottom of the REA-2023 Cask Loaded with BWR Spent Fuel (McKinnon 1986: p. 5.53)

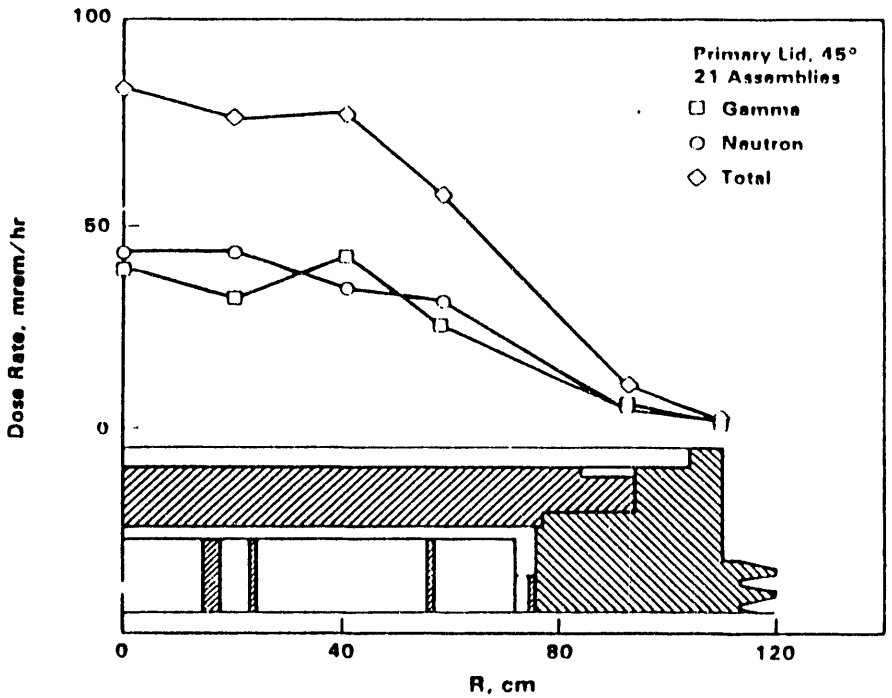

FIGURE C.4. Surface Dose Rate Profiles on the Primary Lid of the CASTOR-V/21 Cask Loaded with PWR Spent Fuel (Creer 1986: p. S-11). The secondary lid was absent.

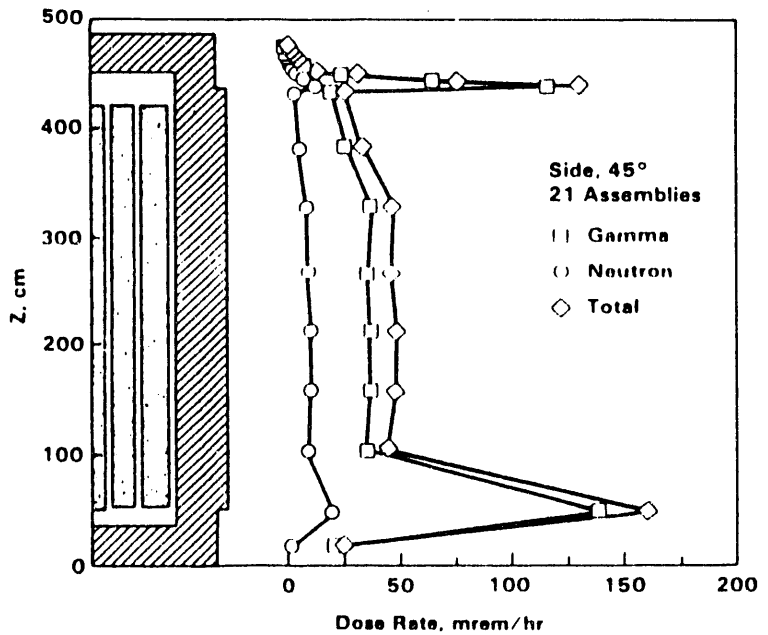

FIGURE C.5. Surface Dose Rate Profiles on the Side of the CASTOR-V/21 Cask Loaded with PWR Spent Fuel (Creer 1986: p. S-11)

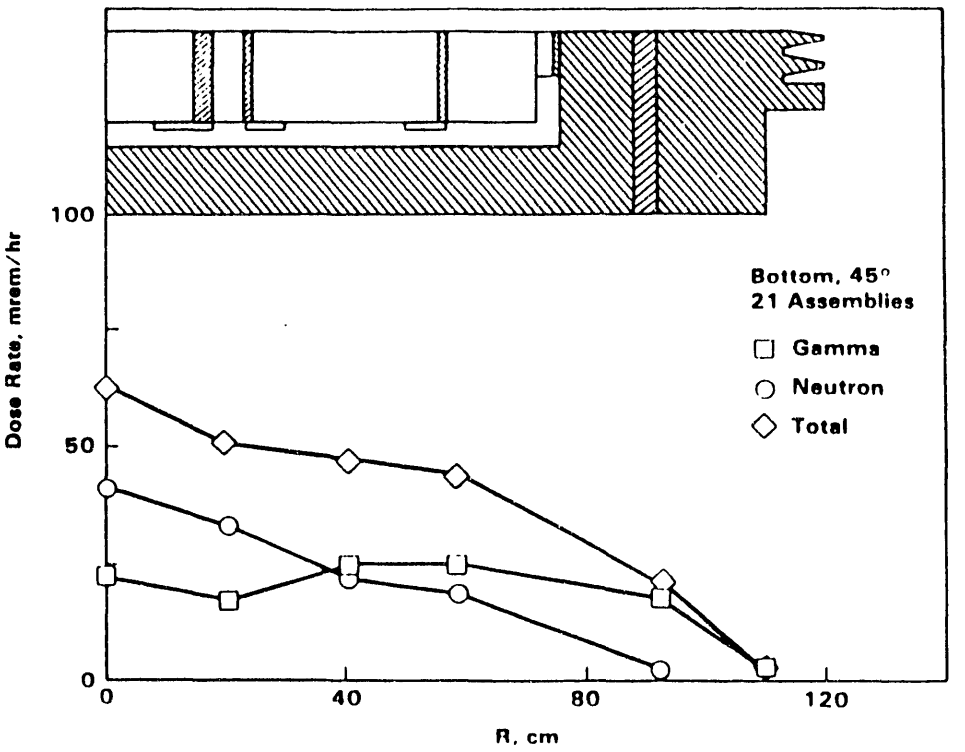

FIGURE C.6. Surface Dose Rate Profiles on the Bottom of the CASTOR-V/21 Cask Loaded with PWR Spent Fuel (Creer 1986: p. S-12)

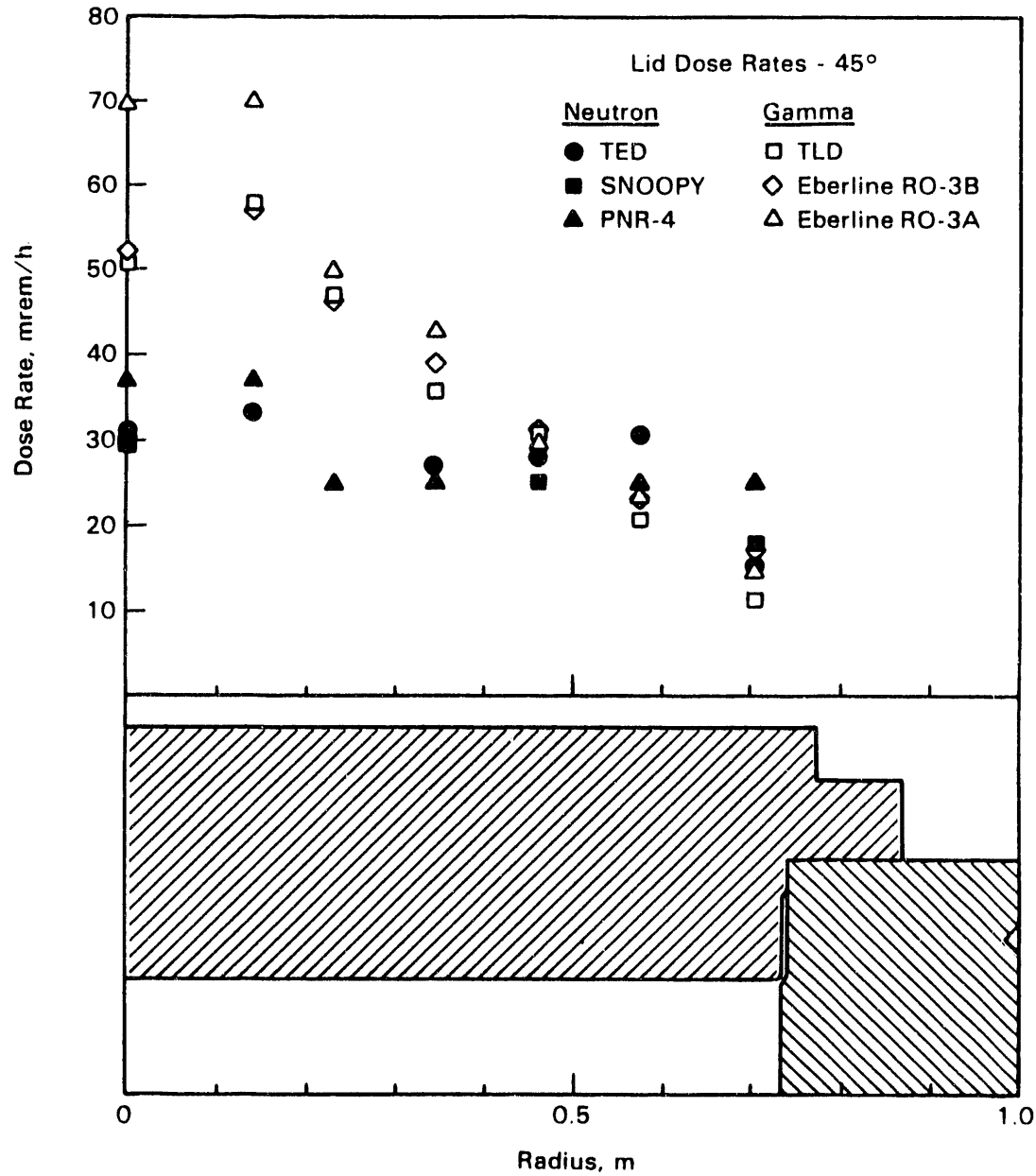

FIGURE C.7. Surface Dose Rate Profiles on the Primary Lid of the TN-24P Cask Loaded with PWR Spent Fuel (McKinnon 1987a: p. S-12)

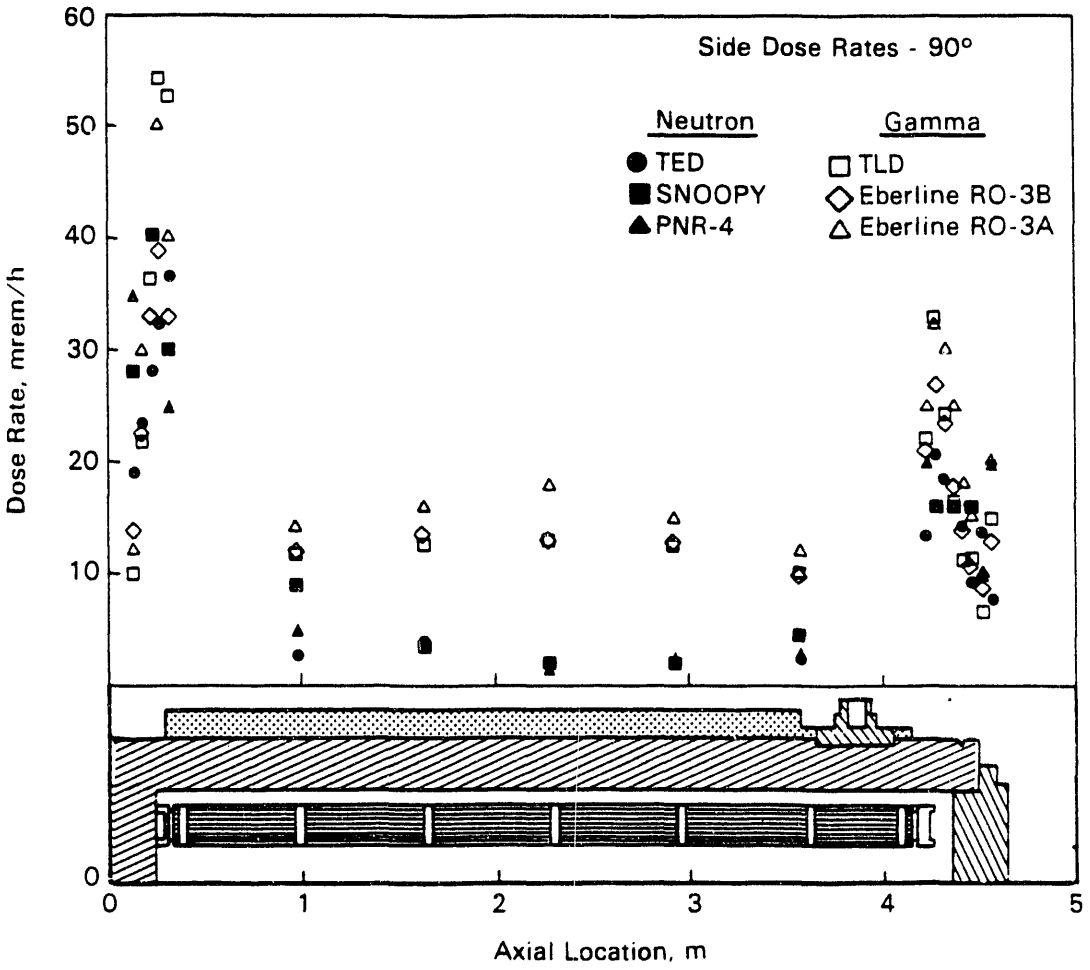

FIGURE C.8. Surface Dose Rate Profiles on the Side of the TN-24P Cask Loaded with PWR Spent Fuel (McKinnon 1987a: p. S-13)

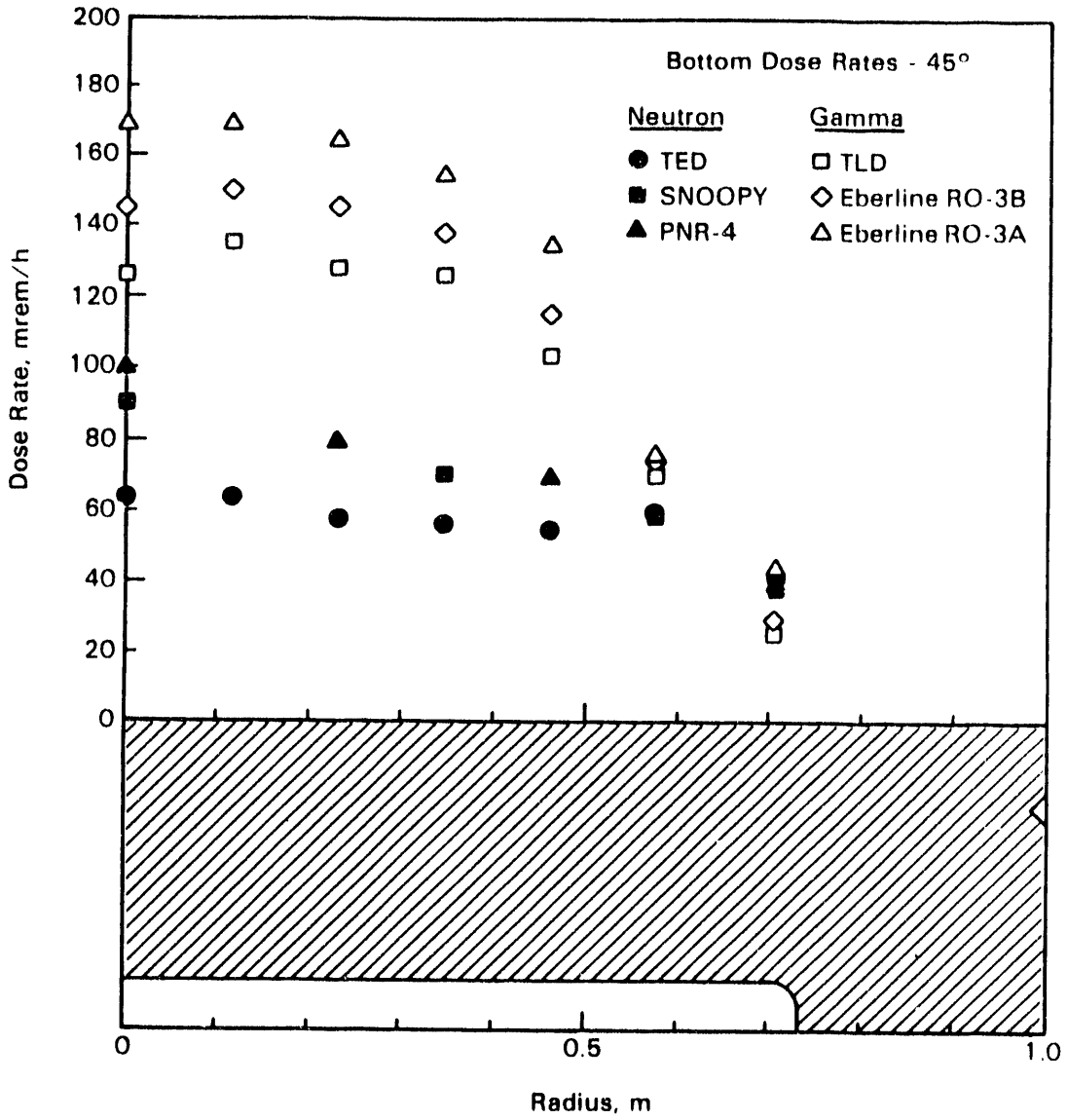

FIGURE C.9. Surface Dose Rate Profiles on the Bottom of the TN-24P Cask Loaded with PWR Spent Fuel (McKinnon 1987a: p. S-14)

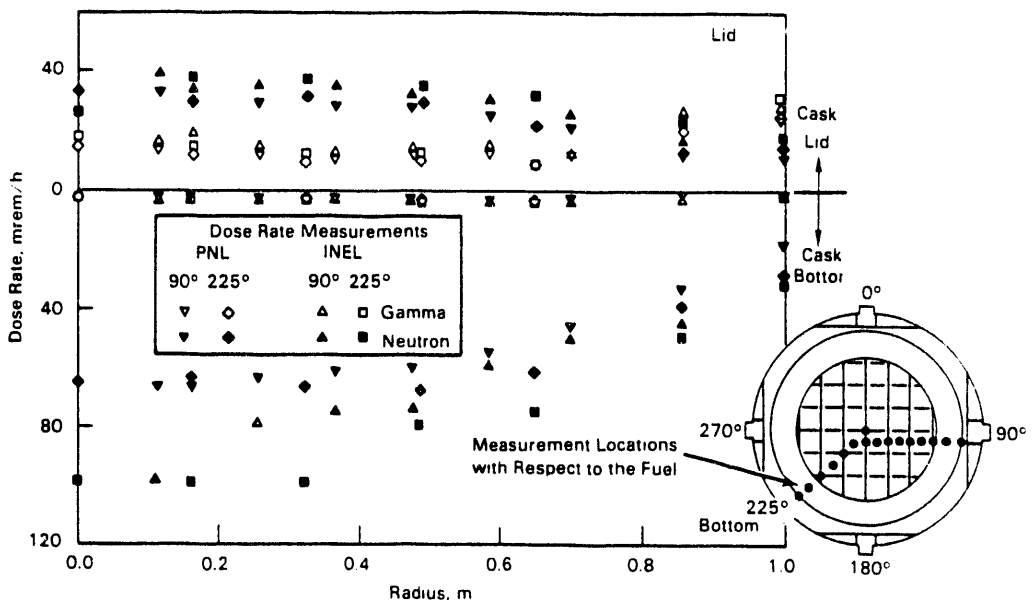

FIGURE C.10. Surface Dose Rate Profiles on the Lid and Bottom of the TN-24P Cask Loaded with Consolidated PWR Spent Fuel (McKinnon 1989: p. S-13)

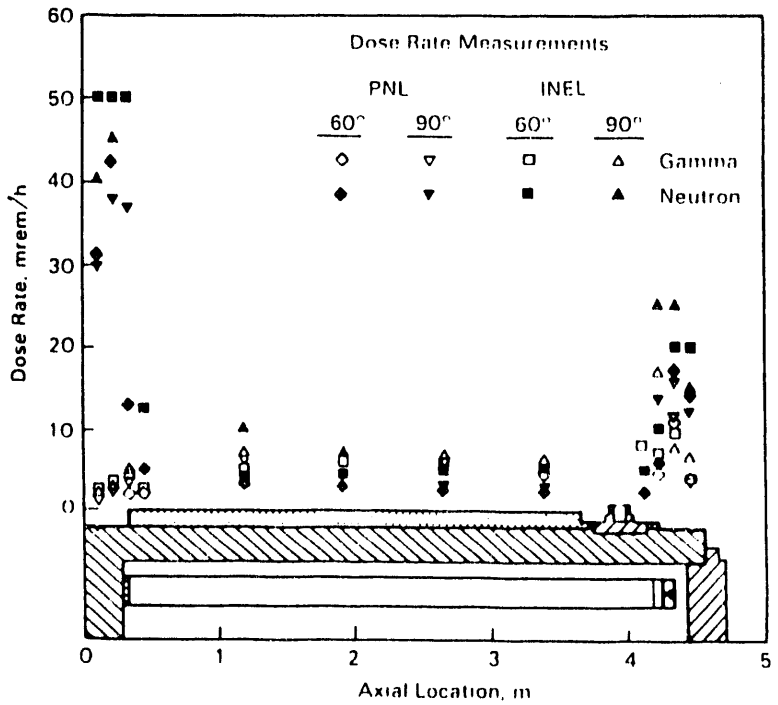

FIGURE C.11. Surface Dose Rate Profiles on the Side of the TN-24P Cask Loaded with Consolidated PWR Spent Fuel (McKinnon 1989: p. S-14)

Figure C.12 shows that the non-fuel bearing component of a fuel assembly are the primary contributor to the gamma source. Their removal during the consolidation process eliminates the gamma peak at the bottom of the cask, reduces the gamma dose along the side of the cask, and reduces the gamma peak at the top of the cask. The gamma peak at the upper end of the cask is associated with the stainless steel holddown springs in the fuel rods.

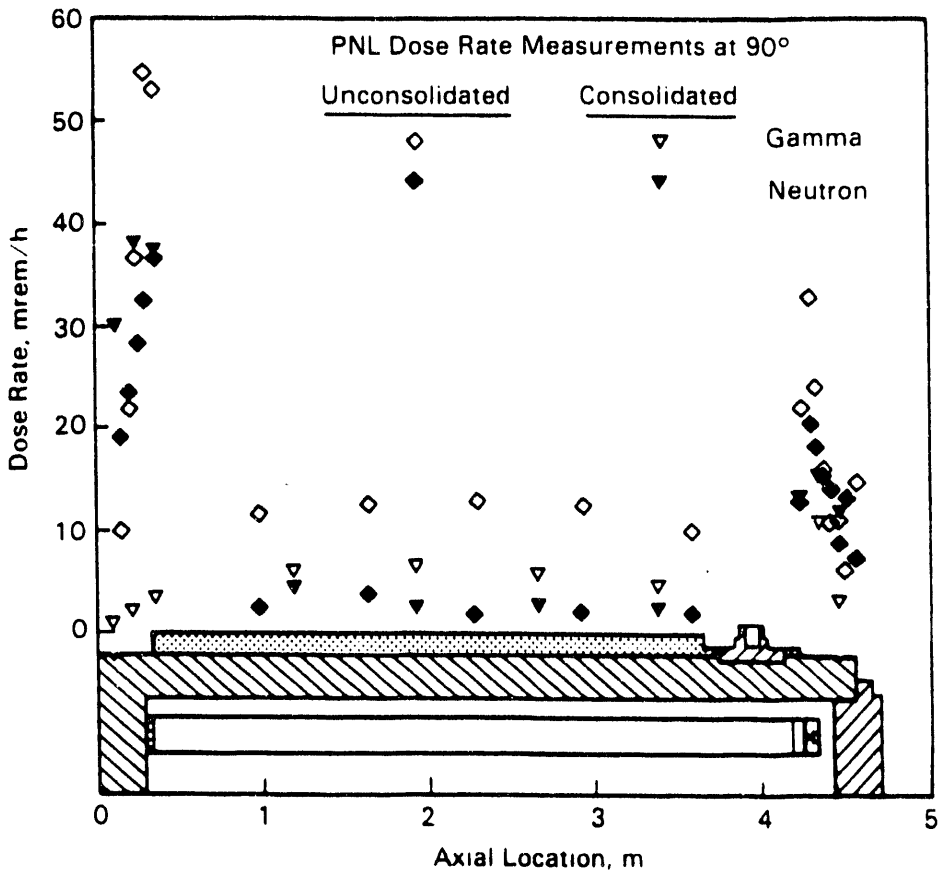

FIGURE C.12. Comparison of the Effect of Fuel Type (Unconsolidated PWR Versus Consolidated PWR Fuel) on the Surface Dose Rate Profiles on the Side of the TN-24P Cask (McKinnon 1989: p. 4-36)

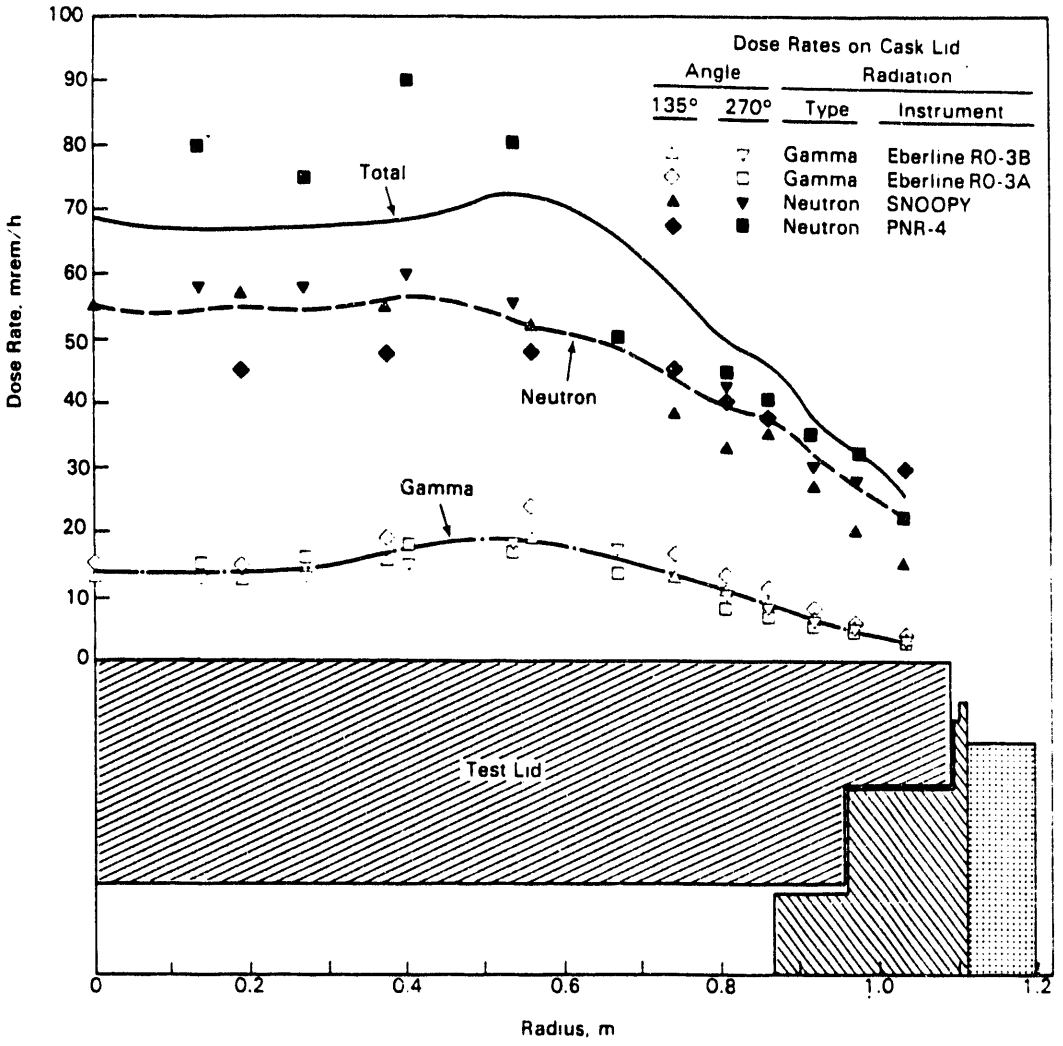

FIGURE C.13. Surface Dose Rate Profiles on the Test Lid of the MC-10 Cask Loaded with PWR Spent Fuel (McKinnon 1987b: p. 4-34)

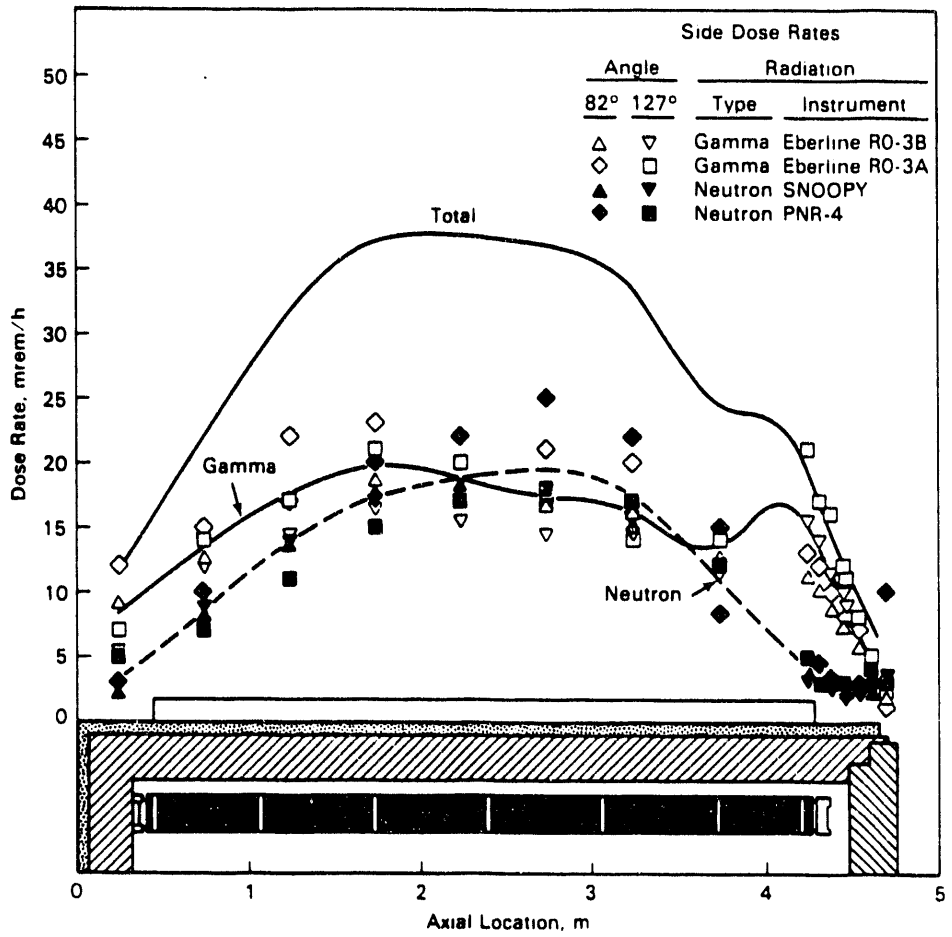

FIGURE C.14. Surface Dose Rate Profiles on the Side of the MC-10 Cask Loaded with PWR Spent Fuel (McKinnon 1987b: p. 4-36)

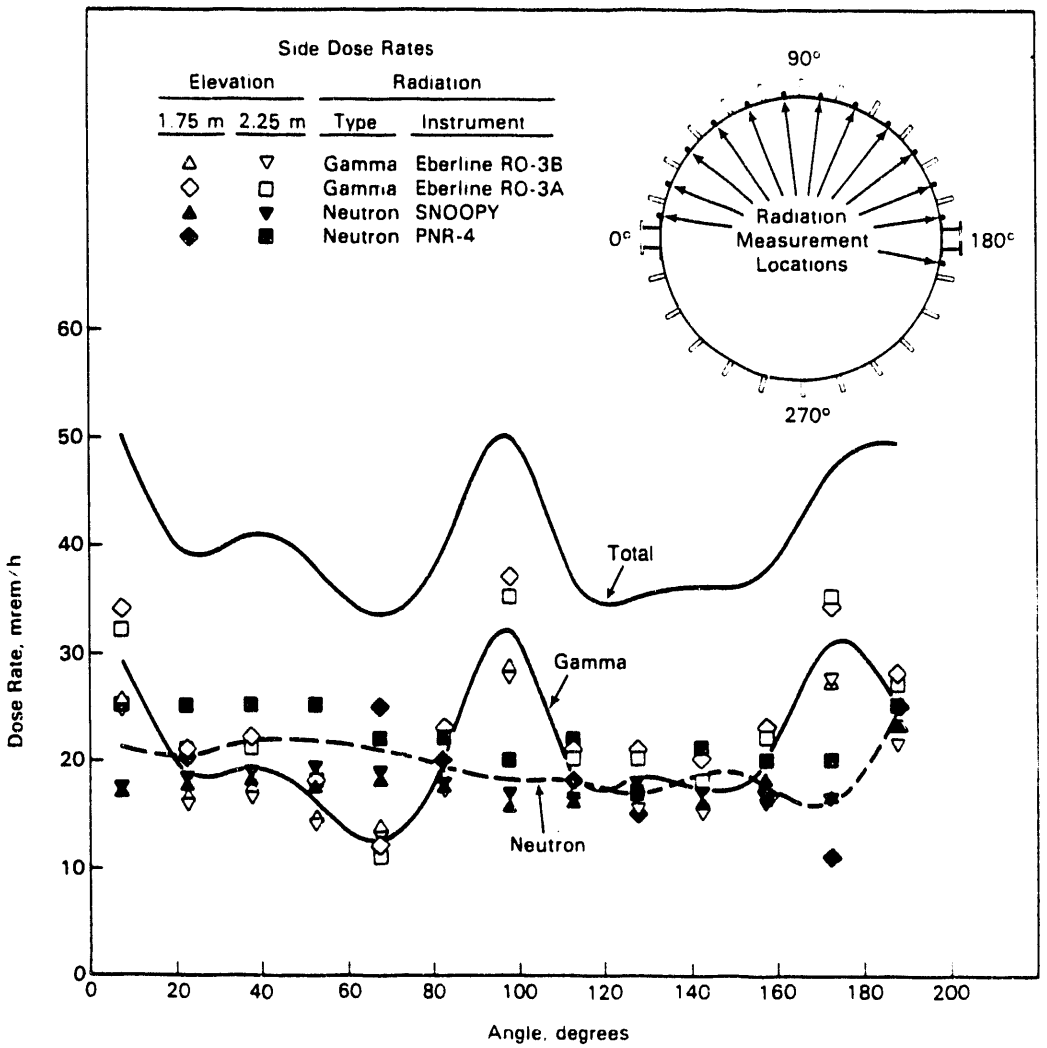

FIGURE C.15. Surface Dose Rate Profiles Around the Circumference of the MC-10 Cask Loaded with PWR Spent Fuel (McKinnon 1987b: p. 4-37). Dose Peaks and Valleys Correspond to Fuel Loading Pattern.

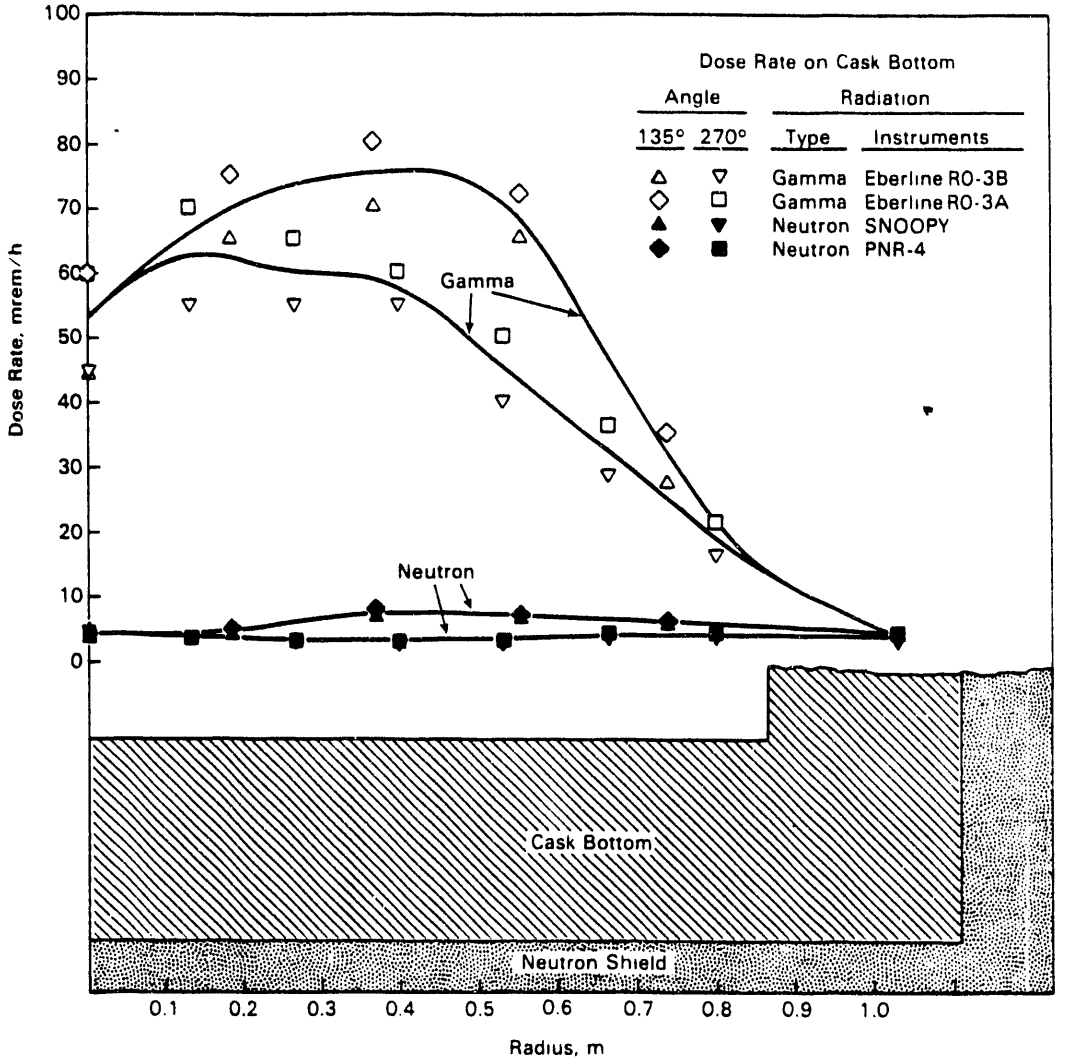

FIGURE C.16. Surface Dose Rate Profiles on the Bottom of the MC-10 Cask Loaded with PWR Spent Fuel (McKinnon 1987b: p. 4-38)

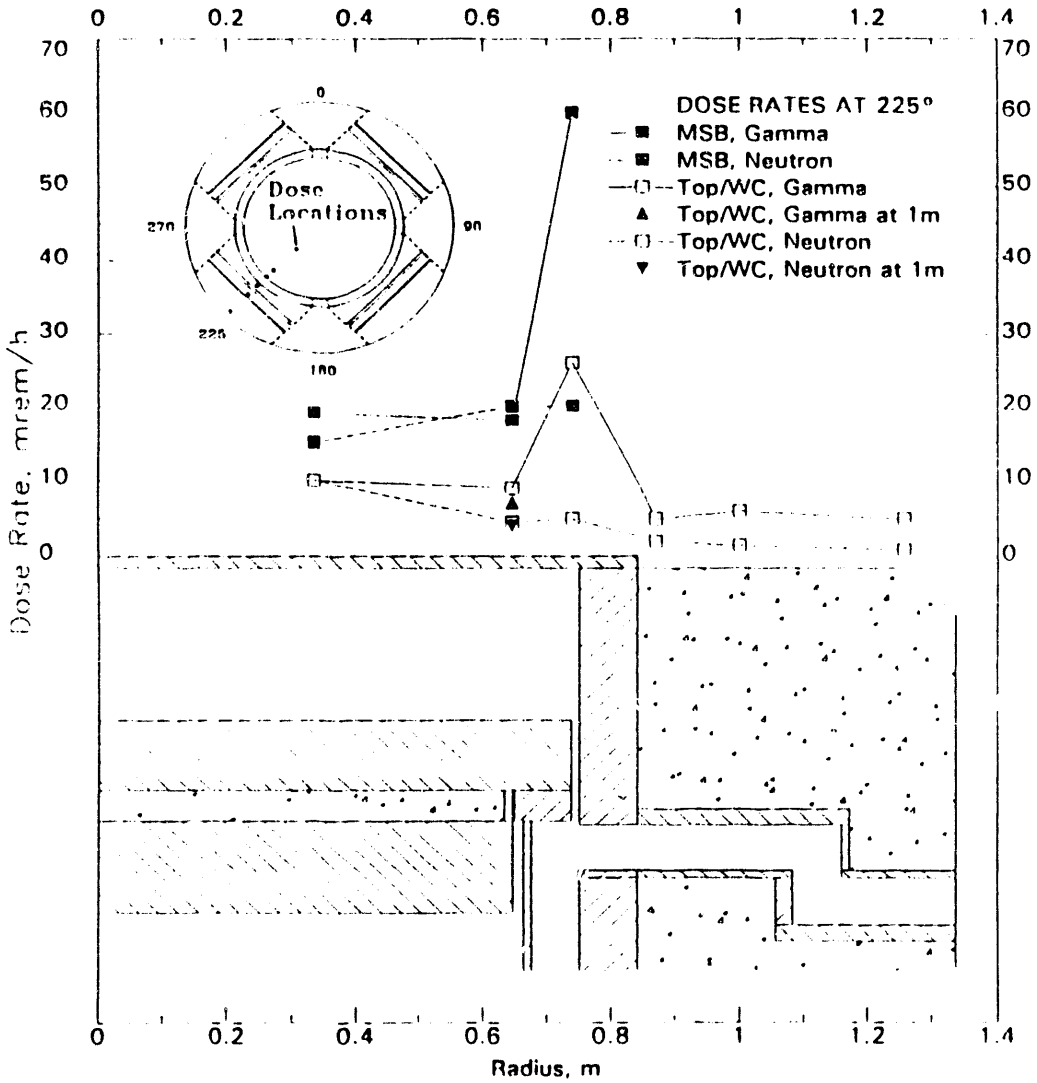

FIGURE C.17. Surface Dose Rate Profiles on the Lid of the VSC-17 Cask Loaded with Consolidated PWR Spent Fuel (McKinnon 1992: p. S-11)

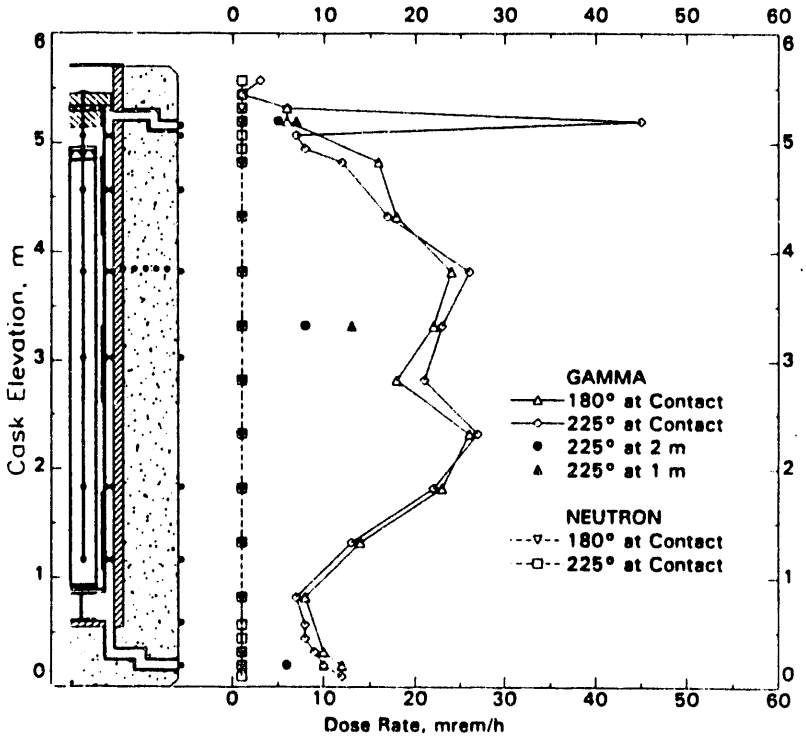

FIGURE C.18. Surface Dose Rate Profiles on the Side of the VSC-17 Cask Loaded with Consolidated PWR Spent Fuel (McKinnon 1992: p. S-12)

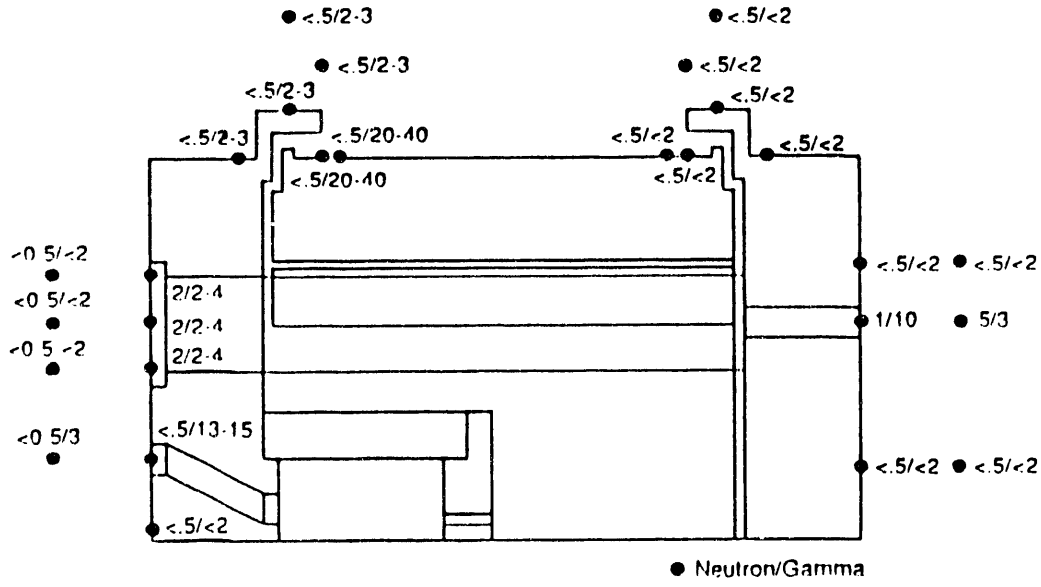

FIGURE C.19. Radiation Dose Rates at the Surface of the Modules and at 1 and 2 meters from the surface of the NUHOMS Horizontal Storage Module (Strope 1990: p. S-8)

DISTRIBUTION

No. of Copies

OFFSITE

80 DOE/Office of Scientific and Technical Information

C. W. Conner
Office of Civilian Radioactive Waste Management, RW-33
U.S. Department of Energy
Washington, DC 20585

W. J. Danker
Office of Civilian Radioactive Waste Management, RW-33
U.S. Department of Energy
Washington, DC 20585

R. A. Milner
Office of Civilian Radioactive Waste Management, RW-32
U.S. Department of Energy
Washington, DC 20585

L. Stewart
Office of Civilian Radioactive Waste Management, RW 321
U.S. Department of Energy
Washington, DC 20585

V. Trebules
Office of Civilian Radioactive Waste Management, RW-
U.S. Department of Energy
Washington, DC 20585

J. W. Williams
Office of Civilian Radioactive Waste Management, RW 321
U.S. Department of Energy
Washington, DC 20585

C. J. Daukowski
U.S. Department of Energy
Attention: Defense Programs
San Francisco Operations Office
1333 Broadway
Oakland, CA 94612

No. of Copies

A. Brownstein
U. S. Department of Energy
1000 Independence Ave.
Washington, DC 20585

2 U.S. Nuclear Regulatory Commission
Office of Nuclear Materials Safety and Safeguards
Mail Stop 6-H-3
Washington, DC 20555
ATTN: F. C. Sturz, M. B. Raddatz

W. R. Pearson
Regulatory Applications Division
U.S. Nuclear Regulatory Commission
Mail Stop NL-007
Washington, DC 20555

C. Feldman
U.S. Nuclear Regulatory Commission
Office of Nuclear Regulatory Research
Washington, DC 20555

C. Matthews
U.S. Department of Energy
Oak Ridge Operations Office
P.O. Box E
Oak Ridge, TN 37803

C. P. Gertz
U.S. Department of Energy
Waste Management Project Office
P.O. Box 98608
Las Vegas, NV 89193-8518

M. Fisher
U.S. Department of Energy
Idaho Operations Office
785 DOE Place
Idaho Falls, ID 83402

No. of
Copies

K. G. Golliher
U.S. Department of Energy
DOE Albuquerque Operations
Office
P.O. Box 5400
Albuquerque, NM 87115

R. W. Lambert
Electric Power Research
Institute
P.O. Box 10412
Palo Alto, CA 94303

R. F. Williams
Electric Power Research
Institute
P.O. Box 10412
Palo Alto, CA 94303

T. A. Mozhi
WESTON Technical Support Team
955 L'Enfant SW, 8th Floor
Washington, DC 20024

J. Richardson
WESTON Technical Support Team
955 L'Enfant SW
Washington, DC 20024

A. M. Segrest
Duke Engineering and
Services, Inc.
P.O. Box 1004
Charlotte, NC 28201-1004

J. B. Stringer
Duke Engineering and
Services, Inc.
P.O. Box 1004
Charlotte, NC 28201-1004

W. B. Andrews
Science Applications
International, Corp.
Valley Bank Center
101 Convention Center Drive,
Suite 407
Las Vegas, NV 89198

No. of
Copies

R. P. Morissette
Science Applications International
Corporation
Valley Bank Center
101 Convention Center Drive,
Suite 407
Las Vegas, NV 89198

J. H. Clark
EG&G Idaho Inc.
P.O. Box 1625 MS 1540
Idaho Falls, ID 83415

R. C. Schmitt
EG&G Idaho Inc.
P.O. Box 1625 MS 9109
Idaho Falls, ID 83415

H. E. Bliss
Nuclear Fuel Services
Commonwealth Edision
72 West Adams Street
P.O. Box 767
Chicago, IL 60690

C. K. Anderson
Combustion Engineering, Inc
1000 Prospect Hill Road
Windsor, CT 06095

Y. Hsii
Division of System Integration
Office of Nuclear Regulatory
U.S. Nuclear Regulatory
Commission
Washington, DC 20555

L. Phillips
Division of System Integration
Office of Nuclear Regulatory
U.S. Nuclear Regulatory
Commission
Washington, DC 20555

T. L. Sanders
Sandia National Laboratory
P.O. Box 5800
Albuquerque, NM 87185

No. of
Copies

G. Swinglehurst
Duke Power Company
P.O. Box 33189
422 South Church Street
Charlotte, NC 28242

R. Rassmussen
Duke Power Company
P.O. Box 33189
422 South Church Street
Charlotte, NC 28242

M. L. Smith
Virginia Power Company
5000 Dominion Blvd.
Glen Allen, VA 23060

D. L. Larkin
Washington Public Power
Supply System
P.O. Box 968
Richland, WA 99352

D.H. Nyman
Westinghouse Hanford Co.
P.O. Box 1970 G6-02
Richland, WA 99352

R. O. Anderson
Northern States Power Company
15 South Church Street
Minneapolis, MN 55401

R. Anderson
GNSI Chem-Nuclear Systems, Inc.
220 Stoneridge Drive
Columbia, SC 29210

D. Hamilton
Middle South Services, Inc.
Box 61000
New Orleans, LA 70161

P. Childress
B&W Fuel Company
P.O. Box 10935
Lynchburg, VA 24502

No. of
Copies

G. R. Bond
Manager, Nuclear Fuels
General Public Utilities, NUC
100 Interpace Parkway
Parsippany, NJ 07054

J. R. Ratliff
Tennessee Valley Authority
409 Krystal Building
Chattanooga, TN 37401

D. Zabransky
WEPCO
231 W. Michigan
Milwaukee, WI 53201

R. T. Harris
Northwest Utilities
Generating Company
P.O. Box 270
Hartford, CT 06101

J. V. Massey
Sierra Nuclear Corporation
5619 Scotts Valley Drive, #240
Scotts Valley, CA 95066

K. Miller
Sacramento Municipal Utility
District
14440 Twin Cities Rd.
Herald, CA 95638

J. H. Jones
Babcock and Wilcox
3315 Old Forest Road
P.O. Box 10935
Lynchburg, VA 24506-0935

C. E. Walter
Lawrence Livermore
National Laboratory
P.O. Box 808
Livermore, CA 94550

M. W. Schwartz
Nuclear Safety Engineering
2244 University Avenue
Sacramento, CA 95825

No. of
Copies

FLUOR Engineers
Advanced Technology Division
333 Michelson Drive
Irvine, CA 92730

B. Lehnert
Pacific Nuclear Fuel Services
145 Martinvale Lane
San Jose, CA 95116

W. J. McConagy
Pacific Nuclear Fuel Services
145 Martinvale Lane
San Jose, CA 95116

D. Woods
Ralph M. Parsons Company
100 West Walnut Street
Pasadena, CA 91124

R. Kunita
Carolina Power & Light Company
P.O. Box 1551
Raleigh, NC 27602

Technical Library
Battelle Memorial Institute
Office of Nuclear Waste
Isolation
505 King Avenue
Columbus, OH 43201

No. of
Copies

ONSITE

2 DOE Richland Field Office

D. K. Jones
D. C. Langstaff

25 Pacific Northwest Laboratory

G. H. Beeman
D. W. Bennett
D. M. Boyd
J. L. Ethridge
E. R. Gilbert
M. R. Kreiter
M. A. McKinnon (10)
R. I. Smith
L. A. Strope
G. L. Tingey
Technical Report Files (5)
Publishing Coordination

END

DATE FILMED

8/11/93